Aus dem Institut für Immunologie der Ludwig-Maximilians-Universität München
Vorstand: Prof. Dr. Thomas Brocker

The role of Rho-GTPases in dendritic cell functions

Dissertation
zum Erweb des Doktorgrades der Naturwissenschaften (Dr. rer. nat.)
an der Medizinischen Fakultät
der Ludwig-Maximilians-Universität München

vorgelegt von
Céline Leroy
aus Lannion (Frankreich)

2013

Aus dem Institut für Immunologie der Ludwig-Maximilians-Universität München
Vorstand: Prof. Dr. Thomas Brocker

The role of Rho-GTPases in dendritic cell functions

Dissertation
zum Erweb des Doktorgrades der Naturwissenschaften (Dr. rer. nat.)
an der Medizinischen Fakultät
der Ludwig-Maximilians-Universität München

vorgelegt von
Céline Leroy
aus Lannion (Frankreich)

München, den 05.02.2013

Gedruckt mit Genehmigung der Medizinischen Fakultät der Ludwig-Maximilians-Universität München

Betreuer:	Prof. Dr. Thomas Brocker
Zweitgutachter:	Priv. Doz. Dr. Anton Eberharter
Dekan:	Prof. Dr. med Dr.h.c. Maximilian Reiser, FACR, FRCR

Tag der mündlichen Prüfung: 15.10.2013

AUTHOR'S DECLARATION

Ich versichere hiermit ehrenwörtlich, daß die vorgelegte Dissertation "The role of Rho-GTPases in dendritic cell functions" von mir selbständig und ohne unerlaubte Hilfe angefertigt wurde. Ich habe mich dabei keiner anderen als der von mir ausdrücklich bezeichneten Hilfen und Quellen bedient.
Die Dissertation wurde in der jetzigen oder ähnlichen Form bei keiner anderen Hochschule eingereicht und hat auch noch keinen anderen Prüfungszwecken gedient.

Céline Leroy

ACKNOWLEDGEMENTS

I want to thank Prof. Dr. Thomas Brocker to give me the opportunity to perform my Ph.D. under his supervision and to participate to international meetings. I am also very grateful for the freedom that I had during my work.

For the help in the migration project, I would like to thank Melanie Laschinger and the SFB914.

I want to thank all the Brocker's girls and the late arrived men for the good mood and nice atmosphere in the lab. I am especially grateful to Nancy Luckashenak for her friendship and support in the first months of my PhD; to Stefanie Meier who has guided me during my first steps in the german administration as well as during the last steps by reviewing this manuscript, and whose organization talent permitted us to enjoy a lot of fun time; to Christine Ried for her constant help, without which the lab could not work properly; to Katharina Breit for her funny way to help improving my german; to Ksenija Jovanovic for her good mood and for reviewing this manuscript.

All this work could not have been done if Andrea Bol would not have taken care of the mice: Danke sehr, Andrea !!

I want to thank especially my partner Matthieu Muller for his love, his patience and tolerance in regard to my regular emotional peaks. To my mother and my grandmother for their permanent support, encouragement and affection. Merci, merci, merci à tous les trois pour votre amour, votre patience et pour le courage que vous avez su m'insuffler chaque jour. Sans vous, je n'en serais pas là aujourd'hui.

ABBREVIATIONS

ACK	Ammonium chloride potassium
AF	Alexa fluor
APC	Antigen presenting cell
APC	Allophycocyanin
APS	Ammonium persulfate
BATF3	Basic leucine zipper transcription factor, ATF-like 3
BMLC	Bone marrow derived Langerhans cells
bp	Base pair
CA	Constitutively active
CCL	C-C motif chemokine ligand
CCR	C-C motif chemokine receptor
CD	Cluster of differentiation
cDC	Conventional DC
Cdc42	Cell division control protein 42
CFSE	Carboxyfluorescein-diacetate-succinimidylester
CHS	Contact hypersensitivity
CP	Crossing point
CTL	Cytotoxic T lymphocyte
CXCL	C-X-C motif chemokine ligand
CXCR	C-X-C motif chemokine receptor
DC	Dendritic cell
dDC	Dermal DC
DEBM	Dermal-epidermal basement membrane
dLN	Draining lymph node
DN	Dominant negative
DNA	Desoxyribonucleic acid
dNTP	Desoxyribonucleotidtriphosphate
EDTA	Ethylenediaminetetraacetic acid
e.g.	*exempli gratia*, from Latin “for example”
ELISA	Enzyme-linked immunosorbent assay
FACS	Fluorescence activated cell sorter
FCS	Fetal calf serum
FITC	Fluoresceinisothiocyanate
Flt3L	FMS-like-tyrosine-kinase 3 ligand

GAP	GTPase activating protein
GDI	Guanine nucleotide dissociation inhibitor
GDP	Guanosine diphosphate
GEF	Guanine nucleotide exchange factor
GM-CSF	Granulocyte macrophage colony-stimulating factor
GTP	Guanosine triphosphate
HBSS	Hank's balanced salt solution
HPRT	Hypoxanthine phosphoribosyltransferase
i.e.	*id est*, from Latin "that is"
i.p. / i.v. / i.d.	Intraperitoneal / Intravenous / Intradermal
IFN-γ	Interferon gamma
IL	Interleukin
KO	Knockout
LC	Langerhans cell
LFA	leukocyte function-associated antigen
LN	Lymph node
M-CSF	Macrophage colony-stimulating factor
MACS	Magnetic cell sorting
mg, ml, mM, M	Milligram, Milliliter, Millimolar, Molar
MHC	Major histocompatibility complex
min	Minutes
MMP	Metalloproteinase
mRNA	Messenger RNA
MTOC	Microtubule organization center
ng, nm	Nanogram, Nanometer
OVA	Ovalbumin
PBS	Phosphate buffered saline
PCR	Polymerase chain reaction
pDC	Plasmacytoid DC
PE	Phycoerythrin
PerCP	Peridinin-Chlophyll
pH	Power of hydrogen
PMA	Phorbol 12-myristate 13-acetate
pmol	Picomolar
PRR	Pattern-recognition receptor
qPCR	Quantitative PCR
Rac1N17	Dominant negative form of Rac1

RNA	Ribonucleic acid
ROS	Reactive oxygen species
RT	Room temperature
SCF	Stem cell factor
sdLN	Skin draining lymph node
SDS	Sodium dodecyl sulfate
snd	Seconde
TAE	Tris-acetate-EDTA buffer
TCR	T cell receptor
TEMED	Tetramethylethylenediamine
Tg	Transgenic
TGF-β	Transforming growth factor beta
T_H cell	T helper cell
TLR	Toll-like receptor
TNF-α	Tumor necrosis factor alfa
V	Volt
VLA	Very Late Antigen
WP	Well-plate
WT	Wild type
µg, µl, µm	Microgram, Microliter, Micrometer

TABLE OF CONTENT

I SUMMARY

Dendritic cells (DCs) play a pivotal role in the induction of antigen-specific immune responses. One important function required to achieve this role is the capacity to present extracellular antigen on MHC class I to $CD8^+$ T cells (cross-presentation). We could previously show that the small Rho-GTPase Rac1 controls this function in spleen $CD8^+$ DCs (Kerksiek et al., 2005). However, different DC subsets that have different functions could require the same Rho-GTPase for different processes. For this reason, we compared the role of Rac1 in different DCs. Furthermore, the model used in the mentioned study was based on the expression of a dominant negative (DN) variant of Rac1 (Rac1N17), which may not be completely specific for Rac1, as it may inhibit pathways controlled by similar Rho-GTPases. Therefore, we engineered mice with DC-specific knockouts (KO) of Rac1, Cdc42 and RhoA to investigate their individual roles in DCs.

We found that Rac1 is neither required for uptake nor cross-presentation in Langerhans cells (LCs). Instead, Rac1 is required for the homeostasis and the migration of LCs. The comparison of Rac1N17 and Rac1-KO mice pointed out the unspecificity of DN proteins. Indeed, Rac1-KO mice have less LCs in the epidermis and no cross-presentation defect, unlike the Rac1N17 mice. The analysis of Rac1-, Cdc42- and RhoA-KO spleen DCs revealed a requirement of Rac1 and RhoA for $CD8^+$ DC homeostasis, a reduced T cell priming capacity in Cdc42- and RhoA-KO mice as well as a decreased phagocytosis in all KO mice. To investigate the role of LCs in skin immune responses, we generated bone marrow chimeras. We show a role of LCs in the $CD8^+$ T cell response but not in the $CD4^+$ T cell priming.

In this study, we showed that a DN form of Rac1 was not inhibiting only Rac1 specific pathways. We could demonstrate that the Rho-GTPases regulate various functions in different DCs. Finally we get evidence that LCs contribute to $CD8^+$ T cell response to particulate skin antigen.

II ZUSAMMENFASSUNG

Dendritische Zellen (DCs) spielen bei der Induktion von antigenspezifischen Immunantworten eine zentrale Rolle. Dafür müssen sie extrazelluläre Antigene aufnehmen und diese im Kontext von MHC Klasse I präsentieren (Kreuzpräsentation). Unsere Gruppe hat gezeigt, dass diese Funktion von der kleinen Rho-GTPase Rac1 gesteuert wird (Kerksiek et al., 2005). Es ist jedoch auch möglich, dass unterschiedliche Subtypen von DCs - wie z. B. Langerhans-Zellen (LCs) - die Rho-GTPase für verschiedene Vorgänge benötigen. Deswegen haben wir die Rolle von Rac1 für Milz-DCs und LCs verglichen. In früheren Arbeiten wurde eine dominant-negative (DN) Form von Rac1 (Rac1N17) verwendet. Diese Form könnte jedoch Prozesse ähnlicher Rho-GTPasen hemmen und wäre somit nicht spezifisch für Rac1. Aus diesem Grund haben wir Mausstämme mit jeweils einem für DCs spezifischen Knockout (KO) - Rac1, Cdc42 oder RhoA - generiert.

Wir konnten zeigen, dass Rac1 nicht für die Antigenaufnahme oder für die Kreuzpräsentation in LCs gebraucht wird, aber für Homöostase und Wanderung der LCs nötig ist. Der Vergleich von Rac1N17 und Rac1-KO Mäusen konnte demonstrieren, dass das DN Modell nicht Rac1-spezifisch ist. Rac1-KO-Mäuse haben weniger LCs in der Epidermis und keinen Kreuzpräsentation-Defekt im Gegensatz zu den Rac1N17-Mäusen. Mit der Auswertung von Rac1-, Cdc42- und RhoA-KO-Milz-DCs, konnten wir feststellen, dass Rac1 und RhoA für die Homöostase von $CD8^+$ Milz-DCs notwendig sind, dass die T-Zell-Antwort niedriger in Cdc42- und RhoA-Mäusen ist und dass Phagozytose abhängig von allen drei Rho-GTPasen ist. Um die Rolle von LCs bei der Immunantwort auf Hautantigene zu untersuchen, haben wir Knochenmarkschimären mit Rac1N17-LC und WT-DCs (und umgekehrt) generiert. Dabei konnten wir beobachten, dass LCs für die $CD8^+$ T-Zell-Antwort wichtig sind, aber dass sie keine Rolle bei der $CD4^+$ T-Zell-Antwort spielen.

In diesem Projekt haben wir somit den Nachweis erbracht, dass das dominant-negative Modell nicht spezifisch für Rac1 ist, dass die Rho-GTPasen unterschiedliche Funktionen in verschiedenen DC Subtypen regulieren und dass LCs zu der $CD8^+$ T-Zell-Antwort auf Hautantigene beitragen.

III INTRODUCTION

III.1 IMMUNE SYSTEM

The immune system is composed of cells and mechanisms, which protect an organism against diseases. The first line of defence is the innate immune system. It is composed of physical barriers (skin, respiratory and gastric epithelia), chemical defences (enzymes in tears, gastric acid, mucus), physiological systems (e.g. complement system) and immune cells. These cells are mainly phagocytes and natural killer cells. The immune response generated by the innate immune system is quick, robust yet short-term and non-specific.

Evolved organisms like vertebrates have in addition an adaptive immune system. It specifically recognizes pathogens, generates a specific immune response and develops memory against them. Depending on the microorganism, humoral immunity (production of specific antibodies by B cells) and/or cellular immunity (antigen-specific T cells) can be established. B cells recognize native antigen through their B cell receptor, whereas T cells recognize antigen via their T cell receptor (TCR) as a peptide bound to major histocompatibility complex (MHC) molecules on antigen presenting cells (APC). This is how the response is initiated.

III.2 DENDRITIC CELLS

Monocytes, macrophages and dendritic cells (DCs) are potent APCs. However, DCs are the most effective APCs involved in the establishment of an adaptive immune response. Since their first description in 1973 (Steinman and Cohn, 1973), knowledge about these cells keeps increasing. Because this study is performed on murine DCs, only mouse data and information about DCs will be presented.

DCs are located throughout the body, in direct contact with tissues and antigens. They have phagocytic capacities, engulfing particles and soluble molecules at high velocity almost constantly. This phagocytosed extracellular material is then degraded into peptides inside specialized intracellular compartments.

After sensing inflammatory signals through pattern recognition receptors (PRRs), DCs migrate from organs to the lymph nodes (LNs) draining the organs, or from spleen red pulp to spleen white pulp. On the way, they up-regulate several molecules necessary for

antigen presentation at their surface, such as MHC class I and class II (MHC-I and MHC-II), costimulatory molecules such as CD80/CD86 and CD40, as well as they produce cytokines.

Once in the T cell area of the neighboring lymphoid organ, DCs can present peptides of antigen they have engulfed on MHC-I and MHC-II (for $CD8^+$ and $CD4^+$ T cell recognition respectively). However, the maturation status of the DCs can determine whether the response will be either immunogenic or tolerogenic (Reis e Sousa, 2006; Villadangos and Schnorrer, 2007).

III.2.1 DC subsets

DCs are a heterogeneous group of cells that have been categorized in many different subsets. They have been classified depending on their precursor origin (classical DCs (cDCs) versus plasmacytoid DCs (pDCs)), their location (lymphoid versus non-lymphoid tissue DCs) and their migratory behaviour (resident versus migratory DCs). In 2010, Guilliams and colleagues have proposed a simplified classification based on both location and functional similarities (Guilliams et al., 2010). As shown in **Figure 1**, they distinguish Langerhans cells, pDCs, inflammatory monocyte-derived DCs and two types of cDCs ($CD11b^+$ and $CD8^+$ DCs). Further descriptions will focus on spleen and lymph node DCs for lymphoid tissues and on skin DCs for non-lymphoid tissues.

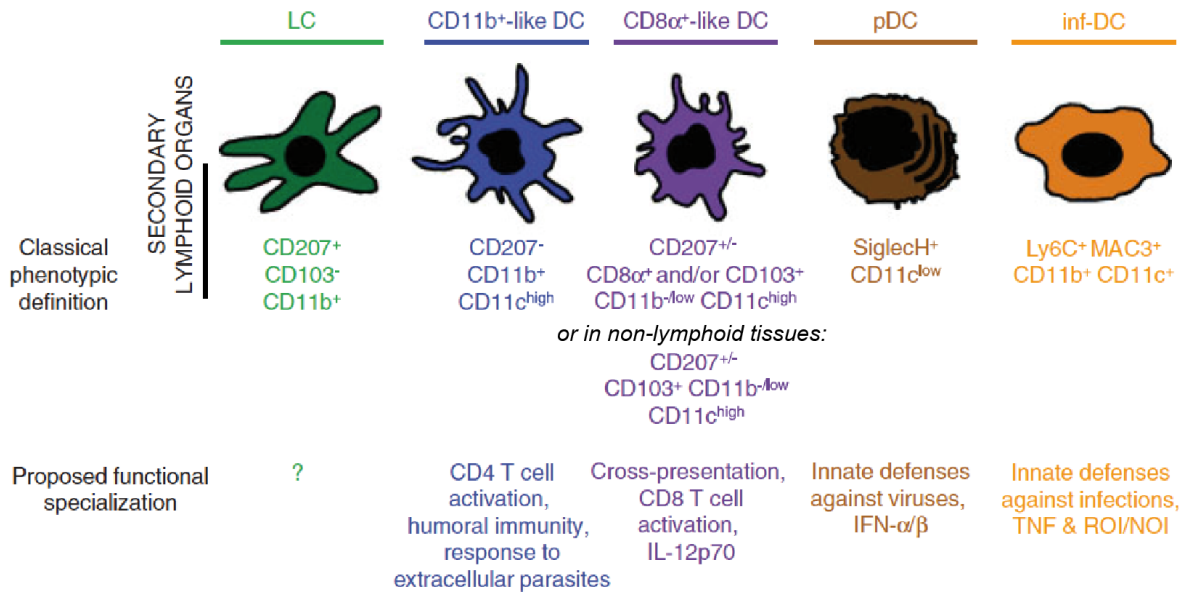

Figure 1: DC subsets in mice.
In non-lymphoid tissues, the same subsets as in lymphoid tissues are found, except for the $CD8^+$ DCs that have some differences in surface markers. Adapted from (Guilliams et al., 2010).

III.2.1.1 Lymphoid tissue DCs

The lymphoid tissues comprise spleen, lymph nodes, thymus and mucosa-associated lymphoid tissues. This study focuses on spleen and LNs, which contain pDCs and cDCs (**Figure 1**). Only cDCs will be investigated in more detail.

The cDCs can be subdivided into $CD8^+$ $CD11b^-$, $CD8^-$ $CD11b^+$ and $CD8^-$ $CD11b^-$ subsets. The $CD8^+$ $CD11b^-$ subset can present endogenous antigen on MHC-I and exogenous antigen on MHC-II (Pooley et al., 2001). Moreover, this subset is highly specialized in the presentation of exogenous antigen on MHC-I (den Haan et al., 2000), a process called cross-presentation. The $CD8^-$ $CD11b^+$ population is more potent at presenting exogenous antigen on MHC-II (Dudziak et al., 2007) than on MHC-I (Pooley et al., 2001). The $CD8^-$ $CD11b^-$ subset, also called merocytic DCs (Thacker and Janssen, 2012), is poorly described.

The lymph nodes also contain migratory DCs arriving from drained tissues. They are described in the next section.

III.2.1.2 Non-lymphoid tissue DCs

In non-lymphoid tissues, there are usually two cDC populations related to the spleen cDC subsets according to transcriptional (Robbins et al., 2008), developmental (Ginhoux et al., 2009) and functional data (Edelson et al., 2010). The spleen $CD11b^+$ DCs are related to tissue $CD11b^+$ DCs and spleen $CD8^+$ DCs correspond to the tissue $CD103^+$ DCs. The skin contains one additional subset that is the Langerhans cell (LC) subset.

The skin is composed of the superficial layer called epidermis and of the deeper dermis. The epidermis contains LCs whereas the dermis contains LCs leaving the epidermis, the classical $CD11b^+$ DCs and the $Langerin^+$ $CD103^+$ DCs (**Figure 2**).

$Langerin^+$ dermal DCs (dDCs) were recently identified as a subset distinct from LCs due to their radiosensitivity (Bursch et al., 2007; Ginhoux et al., 2007; Poulin et al., 2007), which helps to differentiate them from radioresistant LCs (Merad et al., 2002). Their development depends on the transcription factor BATF3 (Edelson et al., 2010) and on the cytokine Flt3L (Ginhoux et al., 2009) but not on TGF-β (Kel et al., 2010) or M-CSF (Ginhoux et al., 2009). $Langerin^+$ dDCs were identified as being responsible for most of the functions attributed so far to LCs (Bursch et al., 2007; Henri et al., 2010). They take part in contact hypersensitivity (CHS) reaction to topically applied haptens (Bursch et al., 2007;

Noordegraaf et al., 2010), induce $CD8^+$ T cell response to leishmaniasis (Brewig et al., 2009) and to herpes infection (Bedoui et al., 2009). Skin-derived antigens are cross-presented by $Langerin^+$ dDCs (Bedoui et al., 2009; Henri et al., 2010), but $CD4^+$ T cell activation seems to be dependent on another cell type (Bedoui et al., 2009; Brewig et al., 2009).

	Epidermal LCs	Dermal $Langerin^+$ DCs	Dermal $Langerin^-$ DCs	$CD8^+$ DCs
Tissue of residence	Skin, Epidermis	Skin, Dermis	Skin, Dermis	LN, Spleen, Thymus
Langerin	+++	+++	–	Strain dependent
CD8	–	–	–	+
CD103	–	+/Hetrogenous	-	
CD11b	+	–	Hetrogenous	
Ep-Cam	+	–	–	
Origin in chimeras	Host	Donor	Donor	Donor

Figure 2: DC subset markers.
From (Kaplan, 2010).

Langerhans cells were discovered in 1868 (Langerhans, 1868) and they are characterized by the expression of Langerin, which induces the formation of Birbeck granules, tennis racket-shaped organelles visible by electron microscopy (Birbeck et al., 1961). These granules are found exclusively in LCs and not in $Langerin^+$ dDCs. LCs are also positive for Epcam and negative for CD103 and CD11b (**Figure 2**).

LCs precursors arrive in the skin before birth and develop lifelong in the epidermis (Chorro et al., 2009). LCs are maintained at the steady state by self-renewal (Merad et al., 2002) thanks to an autocrine loop of TGF-β (Kaplan et al., 2007). M-CSF (Ginhoux et al., 2006) and IL-34 (Wang et al., 2012) but not Flt3L (Onai et al., 2007) are required for LCs development. The estimated half-life of LCs is about 53 to 78 days (Vishwanath et al., 2006). During inflammation, as LCs migrate out of the epidermis, they are replaced by blood-born monocyte-derived DCs that acquire LC markers (Nagao et al., 2012; Sere et al., 2012).

Although LCs are able to take up antigens and to prime naïve T cells (Schuler and Steinman, 1985; Holcmann et al., 2009), their function in immunity is not very clear. Indeed, until 2007 there was no distinction between $Langerin^+$ dDC and LCs (Bursch et al., 2007). LCs are not involved in either cross-presentation or graft versus host disease (GVHD) (Henri et al., 2010; Li et al., 2011). IL-17 producing T cells control fungal infection of the skin and LCs were recently shown to control this response (Igyarto et al., 2011; Haley et al., 2012). They can also promote T helper cell type 2 (T_H2) responses (Ding et al., 2008; Nagao et al., 2009). A role of LCs in tolerance induction and maintenance begins to emerge (Romani et al., 2012). Indeed, LCs negatively regulate the responses to

leishmaniasis (Kautz-Neu et al., 2011), skin graft (Obhrai et al., 2008), vaginal mucosa response (Hervouet et al., 2010), subcutaneous immunization (Shklovskaya et al., 2011) and self antigen (Holcmann et al., 2009; Seneschal et al., 2012). Whether LCs are required in CHS reactions is still a matter of debate (Kaplan, 2010).

III.2.2 DC migration

III.2.2.1 From the epidermis into the dermis

LCs are further away from lymph vessels than dDCs. They first have to leave the epidermis to reach the dermis. Keratinocytes are the main cells composing the epidermis. They are known to produce pro- and anti-inflammatory cytokines (Ansel et al., 1990). Notably, the production of IL1-α and TNF-α activates LCs that in turn produce IL1-β ((Heufler et al., 1992), **Figure 3** and **Figure 4.1**). Then LCs detach from keratinocytes, become responsive to chemokines that induce migration to skin draining LNs (sdLNs), unresponsive to skin-homing chemokines and they acquire the machinery to cross the dermal-epidermal basement membrane (DEBM) (Cumberbatch et al., 2000; Villablanca and Mora, 2008).

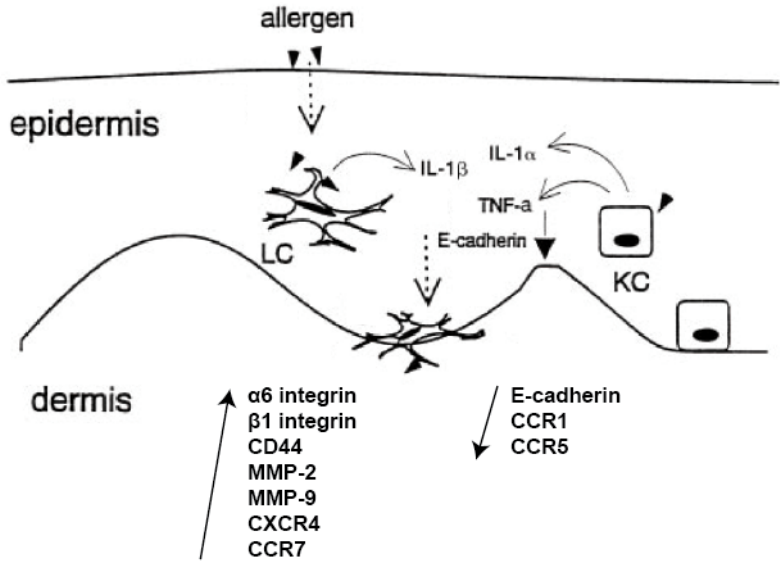

Figure 3: Signals and molecules required for LCs to exit the epidermis.
Adapted from (Wang et al., 1999).

To tear off surrounding keratinocytes, LCs down-regulate E-cadherin (**Figure 4.2**, (Schwarzenberger and Udey, 1996)). In order to adhere to matrix components, CD44 is up-regulated (Weiss et al., 1997).

The DEBM is composed of lamimins and nidogen in the upper regions, type IV collagen and heparin sulphate proteoglycan in the lamina densa, and type VII collagen in the sub-basal lamina densa (Burgeson and Christiano, 1997; Behrens et al., 2012). Therefore, the expression of α6- and β1-integrins that bind laminins is up-regulated on LCs (Price et al., 1997), as well as the production of MMP-9 and MMP-2 that degrade type IV collagen (**Figure 3** and **Figure 4.3**, (Ratzinger et al., 2002)). However, DEBM contains pre-existing pores where LCs can go through (Oakford et al., 2011), if they distort enough their cytoskeleton and nucleus.

Expression of CCR1 and CCR5, which control DC retention in the skin (Sallusto et al., 1998), is down-regulated whereas expression of CXCR4, which induces exit of the epidermis (Ouwehand et al., 2008), and expression of CCR7, which promotes migration to the sdLN, are up-regulated (Forster et al., 1999; Villablanca and Mora, 2008) (**Figure 3**).

III.2.2.2 From the dermis into skin draining lymph nodes

Once in the dermis, LCs and dDCs follow the same way and use the same molecular machinery. There is a continuous flow of DCs leaving the dermis to enter the lymph vessels and to migrate to the sdLN. Signals involved in DC emigration at the steady state are poorly understood, because of the difficulty of setting up a migration assay without inducing inflammation (Alvarez et al., 2008).

Sensing inflammatory signals induce DCs to mature. The maturation process is characterized by increased motility, rearrangement of chemokine receptors and up-regulation of the antigen presentation machinery (Granucci et al., 1999). Upon inflammation, similar to what happens for LCs, keratinocyte-produced cytokines promote dDC migration (**Figure 4.1,** (Mauviel et al., 1991; Cumberbatch et al., 1997)) and dDCs secrete metalloproteinases ((Ratzinger et al., 2002; Yen et al., 2008), **Figure 4.3**).

The dDCs switch their chemokine receptor repertoire to one that is responding to LN-homing chemokines (Sallusto et al., 1998). The most characterized are the chemokines CCL19 and CCL21 and their receptor CCR7 (**Figure 4.4** and **Figure 4.5**; (Schumann et al., 2010)). CXCL12 and CCL17 being sensed by CXCR4 and CCR4 respectively were also shown to be important for DC migration (Kabashima et al., 2007; Stutte et al., 2010). Additionally, even if its precise mechanism is not known, S1P receptor is also required (Maeda et al., 2007; Ocana-Morgner et al., 2011).

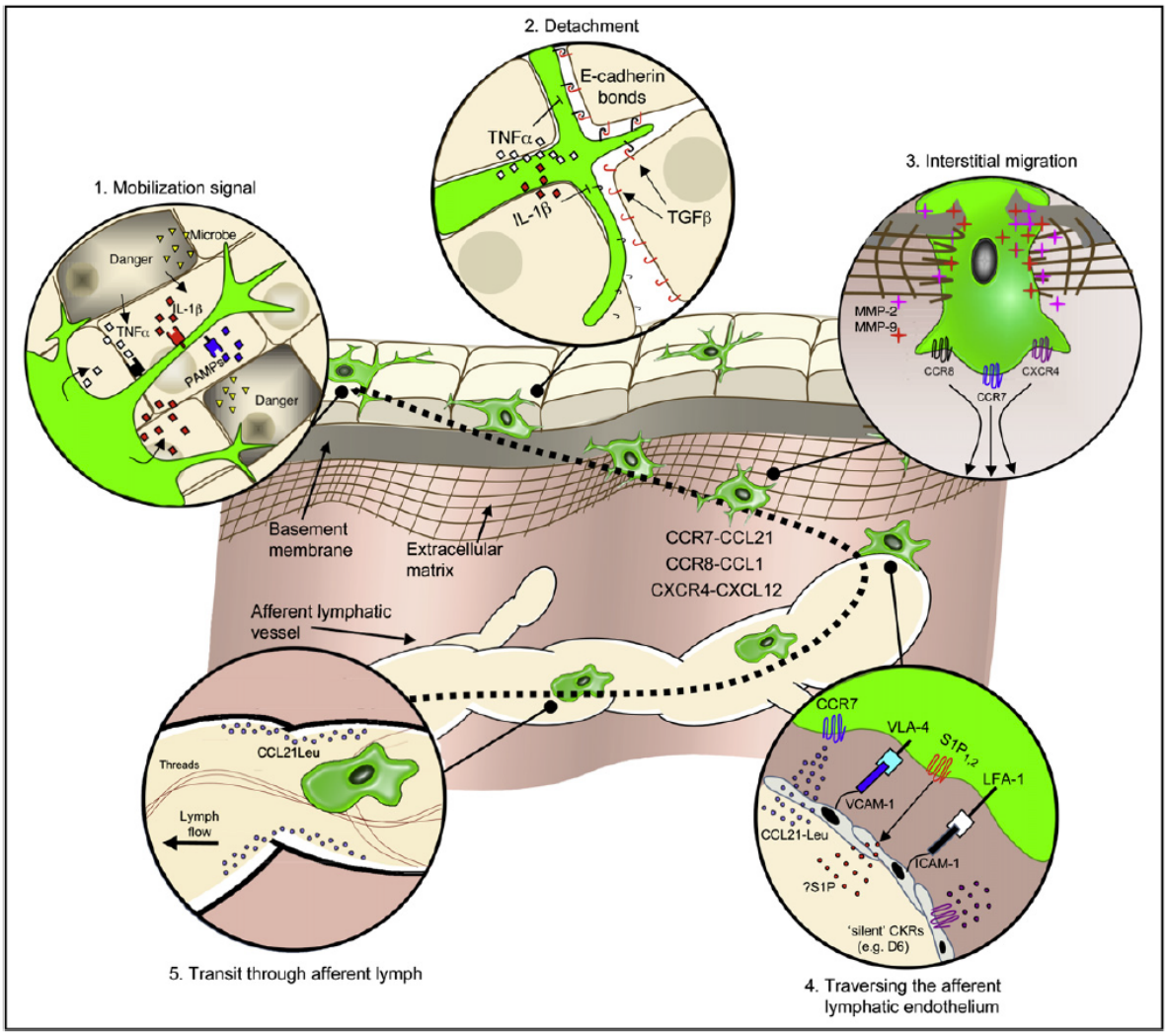

Figure 4: DC mobilization in the skin.
From (Alvarez et al., 2008).

Finally DCs use integrins such as VLA-4 and LFA-1 to bind to endothelial cells ((Joachim et al., 2008; Rouzaut et al., 2010), **Figure 4.4**) and to enter lymphatics, even if preformed pores exist to facilitate DC entry (Pflicke and Sixt, 2009). The travel from peripheral lymphatics to sdLNs is dependent on the CCL21 gradient (Tal et al., 2011).

Of note, the distinct skin DC subsets arrive in sdLN with different kinetics. Indeed, dDCs arrive in sdLN as early as one day after immunization and peak after two days. On the other hand, LCs peak 4 days after immunization (Kissenpfennig et al., 2005).

III.2.3 Induction of T cell response

As already described before, DCs mature when they sense inflammation signals through PRRs (Kawai and Akira, 2009). This process leads to a down-regulation of antigen

uptake, increased antigen processing and peptide loading of MHC molecules, stabilization of MHC molecules at the plasma membrane, up-regulation of co-stimulatory molecules and expression of adhesion molecules and chemokine receptors required for migration to lymphoid organs (Reis e Sousa, 2006).

Once in the lymphoid organ draining the tissue where the antigen was captured, DCs begin to sample T cells, until they encounter a T cell with a specific TCR recognizing the antigen they are presenting. $CD4^+$ T cells recognize peptides presented on MHC-II whereas $CD8^+$ T cells react to peptides on MHC-I ("signal 1"). Once $CD4^+$ T cells have recognized the MHC-peptide complex, they arrest on the presenting APC. Here they receive "signal 2", which consists in costimulatory signals provided by the binding of CD28 to CD80 or CD86 and of CD40L to CD40. Then, depending on the DC subset and the inflammatory signals sensed at the site of antigen uptake, $CD4^+$ T cells receive the "signal 3". This is a combination of cytokines that determine the fate of the T cell (**Figure 5**) (Reis e Sousa, 2006; Hirahara et al., 2011).

For instance, IL-12 secretion will promote T_H1 cell differentiation. These T cells produce IFNγ and provide help to $CD8^+$ T cells, (Oestreich and Weinmann, 2012). Production of a Notch ligand by DCs will lead to the differentiation into T_H2 cells, which secrete IL-4, IL-5 and IL-13 and which recruit eosinophils and B cells (Okoye and Wilson, 2011). The production of IL-6, IL-23 and TGF-β by DCs will induce the development of T_H17 cells. They are involved in protection against fungi and neutrophil recruitment, and they produce IL-17A, IL-17F and IL-22 (Bi and Yang, 2012). However, when DCs are not fully mature, e.g. at the steady state or in tumor environment, they produce TGF-β and IL10, promoting regulatory T cell differentiation to maintain tolerance against self-antigen (Luckashenak et al., 2008; Josefowicz et al., 2012).

The $CD8^+$ T cells need to be more tightly controlled to not over-react and cause auto-immunity. Indeed, after TCR engagement, they need to receive help from $CD4^+$ T cells recognizing the same antigen, which will induce further $CD8^+$ T cell differentiation into cytotoxic T lymphocyte (CTL) (Williams and Bevan, 2007; Zhang et al., 2009).

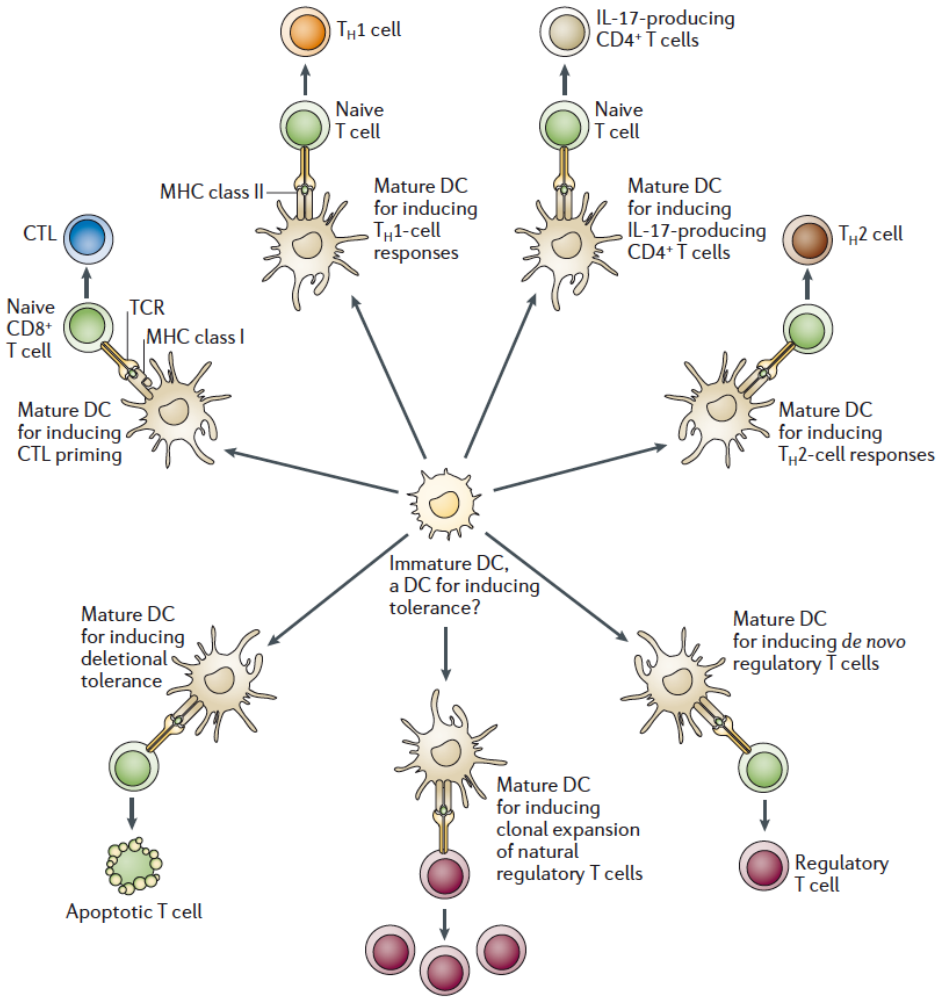

Figure 5: DC effector functions
Depending on the maturation state and the subset of the DC presenting the antigen, T cells will differentiate into different kind of T helper cells, cytotoxic T lymphocytes (CTL) or die. (Reis e Sousa, 2006).

III.3 SMALL Rho-GTPases

Small Rho-GTPases play a role in almost all actin-dependent processes (Jaffe and Hall, 2005; Heasman and Ridley, 2008). The sequences and functions of these proteins are well conserved in eukaryotes. They were first discovered in the marine gastropod genus *Aplysia* (Madaule and Axel, 1985) and because of their similarities with the Ras protein family, they were named Ras homolog proteins (i.e. Rho proteins). According to their sequence similarities, the small Rho-GTPase family is composed of 20 members subdivided into 8 subfamilies (van Helden and Hordijk, 2011). I will focus on three members of this family Rac1, Cdc42 and RhoA that are subject of this study.

III.3.1 Turn over

About 90 to 95 % of the small Rho-GTPases are confined in the cytosol by Rho-specific guanine nucleotide dissociation inhibitors (GDIs). At the C-terminal part of Rho-GTPases, there is a highly hydrophobic isoprenoid moiety, which impairs the proper folding of Rho-GTPases but which is necessary for their subcellular localization (**Figure 6.a**, (Cox and Der, 1992)). Therefore, GDIs stabilize the cytoplasmic pool of Rho-GTPases (**Figure 6.b**, (Boulter et al., 2010)). GDIs are present in limited amounts compared to newly synthetized Rho-GTPases. Therefore, Rho-GTPases compete for the binding of GDIs (**Figure 6.d**). The overexpression of one Rho-GTPase leads to displacement of the endogenous Rho-GTPase pool from GDIs and to their targeting to proteasomal degradation (**Figure 6.c**).

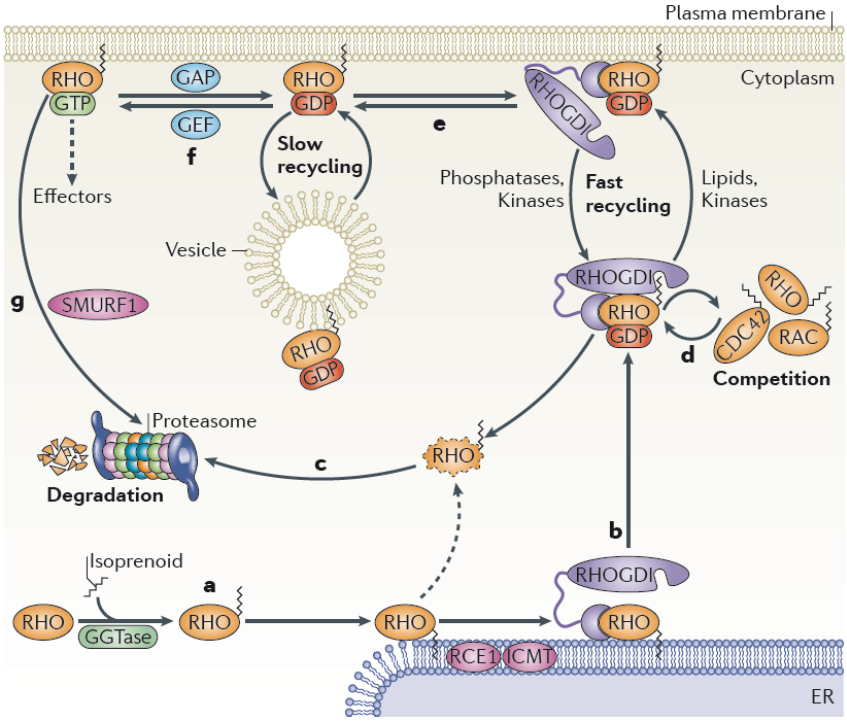

Figure 6: Classical small Rho-GTPase cycle.
From (Garcia-Mata et al., 2011).

Extracellular signals can activate Rho-specific guanine nucleotide exchange factors (GEFs), which will associate with phosphoinositides and lipid rafts in membranes. This proximity promotes the release of Rho-GTPase from GDIs, its association to membranes and its subsequent activation by GEFs (**Figure 6.f**, (Robbe et al., 2003; Ugolev et al., 2008)). Interactions with specific proteins and GDI phosphorylation can also release the Rho-GTPase (**Figure 6.e**, (Garcia-Mata et al., 2011)). GEFs catalyse the exchange of the

GDP molecule bound to the Rho-GTPase for a GTP molecule leading to Rho-GTPase activity. This activity can be turned off by the extraction of the Rho-GTPase from the membrane by GDIs, by Rho-GTPase-post-translational modifications or by GTP hydrolysis. This hydrolysis is catalysed by Rho-specific GTPase-activating proteins (GAPs), which stimulate the slow hydrolysis property of the Rho-GTPase (**Figure 6.f**, (Ligeti et al., 2012)). GTP-bound Rho-GTPase can also be ubiquitylated for proteasomal degradation (**Figure 6.g**, (Nethe and Hordijk, 2010)).

The GEFs and GAPs can bind several Rho-GTPases (**Figure 7**), the identity of which depends on the activation pathway followed and on the cell type (Schiller, 2006; Bos et al., 2007; Buchsbaum, 2007).

III.3.2 Function of the three main Rho-GTPases

Rho-GTPase functions were studied in many different cell types (Pedersen and Brakebusch, 2012). In this chapter, the state of knowledge about the role of Rho-GTPases in DC functions will be discussed. Most of the studies were performed *in vitro*, by transfection of cells with wild type (WT), dominant negative (DN) or constitutively active (CA) variants of the targeted protein. The DN form is the result of a substitution mutation of a threonine for an asparagine at position 17 (Rac1 numbering). This mutation leads to a higher affinity for GEFs, so endogenous Rho-GTPases can neither bind to GEFs, nor be activated nor induce downstream effectors (Feig, 1999). The CA form has a substitution mutation of a glycine or a glutamine for a valine or a leucine at position 12 or 61, respectively. They are unable to hydrolyse the GTP and remain bound to their effector molecules. The last past years, cell-specific knockouts (KOs) of Rho-GTPases were generated, based on the loxP system (Pedersen et al., 2012). These conditional KOs have become indispensable, as the complete KOs of Rac1, RhoA and Cdc42 are embryonically lethal (Sugihara et al., 1998; Chen et al., 2000; Pedersen and Brakebusch, 2012).

Cdc42	Rac1	RhoA	References
ECT2	ECT2	ECT2	(Tatsumoto et al., 1999)
Negf = Ephexin1	Negf = Ephexin1	Negf = Ephexin1	(Shamah et al., 2001)
VAV2	VAV2	VAV2	(Liu and Burridge, 2000)
DEF6 = SWAP70-like	DEF6 = SWAP70-like	DEF6 = SWAP70-like	(Mavrakis et al., 2004)
DBL = Mcf2	DBL = Mcf2	DBL = Mcf2	(Hart et al., 1994; Yaku et al., 1994)
DBS = Ost = Mcf2l	DBS = Ost = Mcf2l	DBS = Ost = Mcf2l	(Horii et al., 1994)
ARHGEF6 = alpha-Pix	ARHGEF6 = alpha-Pix		(Zheng, 2001; Rossman et al., 2005; Schiller, 2006)
Asef2 = Spata3	Asef2 = Spata3		(Kawasaki et al., 2007; Bristow et al., 2009)
DOCK6	DOCK6		(Miyamoto et al., 2007)
	VAV3	VAV3	(Movilla and Bustelo, 1999)
	ARHGEF2 = GEF-H1 = Lfc	ARHGEF2 = GEF-H1 = Lfc	(Ren et al., 1998; Glaven et al., 1999)
	SWAP70	SWAP70	(Shinohara et al., 2002; Ocana-Morgner et al., 2009)
	VAV1	VAV1	(Rossman et al., 2005; Spurrell et al., 2009)
	Kalirin = Duo	Kalirin = Duo	(Penzes et al., 2001; Zheng, 2001)
	SmgGDS = KAP3 = Kifap3	SmgGDS = KAP3 = Kifap3	(Lanning et al., 2003)
	ARHGEF18 = p114RhoGEF	ARHGEF18 = p114RhoGEF	(Zheng, 2001; Niu et al., 2003)
ARHGEF4 = Asef (1)	P-Rex1 = Setd6 (2)	Lbc = Brx = Akap3 (3)	(1) (Gotthardt and Ahmadian, 2007), (2) (Welch et al., 2002; Balamatsias et al., 2011), (3) (Glaven et al., 1996)
FGD4 = Frabin (1)	P-Rex2 = Depdc2 (2)	p190RhoGEF = Rgneg + Rasgrf1 (3)	(1) (Ono et al., 2000), (2) (Donald et al., 2004; Joseph and Norris, 2005) (3) (Jaiswal et al., 2011; Miller et al., 2012)
DOCK8 (1)	Tiam1 (2)	ARHGEF1 = p115RhoGEF = Lcs = Lbcl2 (3)	(1) (Ruusala and Aspenstrom, 2004), (2) (Habets et al., 1994; Rossman et al., 2005), (3) (Glaven et al., 1996; Mao et al., 1998; Jaiswal et al., 2011)
FGD2 = Tcd2 = Tcs2 (1)	Tiam2 = Stef (2)	ARHGEF3 = XPLN (3)	(1) (Huber et al., 2008), (2) (Zheng, 2001), (3) (Arthur et al., 2002)
DOCK9 = Zizimin1 (1)	DOCK2 (2)	ARHGEF8 = Net1 (3)	(1, 2) (Kulkarni et al., 2011), (3) (Alberts and Treisman, 1998; Dubash et al., 2011)
DOCK11 = Zizimin2 (1)	DOCK1 = DOCK180 (2)	ARHGEF12 = LARG (3)	(1) (Lin et al., 2006), (2) (Brugnera et al., 2002), (3) (Taya et al., 2001; Jaiswal et al., 2011)
ARHGEF9 = hPEM-2 (1)	ELMO/CDE-12 = Elmod3dc1 (2)	ARHGEF11 = KIAA0380 = PDZ-RhoGEF (3)	(1) (Zheng, 2001), (2) (Brugnera et al., 2002), (3) (Jaiswal et al., 2011)
Ese1 = Itsn1 = Intersectin1 (1)	TrioPH1 (2)	TrioPH2 (3)	(1) (Zheng, 2001), (2, 3) (Bellanger et al., 2003)
FGD1 = ZFYVE3 (1)	Sos1 (2)		(1) (Zheng et al., 1996; Hayakawa et al., 2005), (2) (Das et al., 2000; Furuta et al., 2002)
	ARHGEF7 = beta-Pix = Pix = Cool (2)		(2) (Feng et al., 2002)

Figure 7: Cdc42-, Rac1- and RhoA-GEF
GEFs common to Cdc42, Rac1 and RhoA (blue); to Cdc42 and Rac1 (orange); to Rac1 and RhoA (green); GEFs specific for Cdc42, Rac1 or RhoA (white).

III.3.2.1 Rac1

At the biochemical level (Jaffe and Hall, 2005), Rac1 interacts with effectors involved in actin-cytoskeleton reorganization. Therefore, disturbing Rac1 expression or activity leads to several phenotypes.

Spleen Rac1-DN DCs have no migration defects, but Rac1 controls apoptotic cell phagocytosis (Kerksiek et al., 2005) and macropinocytosis (West et al., 2000) in DCs. Rac1 also regulates the transport to plasma membrane of molecules required for immune response induction as well as cross-presentation in DCs (Benvenuti et al., 2004; Jaksits et al., 2004; Kerksiek et al., 2005; Shurin et al., 2005).

In other cell types Rac1 was reported to be involved in the control of gene expression (Coso et al., 1995; Minden et al., 1995) as it contains a nuclear localization sequence (Lanning et al., 2003), in the control of the cell cycle (Olson et al., 1995) and in the production of reactive oxygen species (ROS) (Sarfstein et al., 2004; Wu et al., 2009). Whether this is also the case in DCs has to be investigated.

III.3.2.2 Cdc42

Cdc42 activates several effectors, some of which being common with Rac1, therefore leading to a phenotype similar to the one describe above.

Cdc42 controls DC migration (Swetman et al., 2002; Lammermann et al., 2009; Luckashenak et al., 2013), adhesion (Shurin et al., 2005) and protrusion formation (Lammermann et al., 2009). Endocytosis (Shurin et al., 2005) but not pinocytosis (West et al., 2000) requires Cdc42 activity in DCs. Finally, Cdc42 regulates the reorganisation of the microtubule organisation center (MTOC) required for the formation of the immunological synapse (Pulecio et al., 2010) and it controls the transport to plasma membrane of molecules required for immune response induction (Jaksits et al., 2004). Antigen presentation is therefore dependant on Cdc42 (Shurin et al., 2005).

Similar to Rac1, the role of Cdc42 in the control of gene expression (Coso et al., 1995; Minden et al., 1995), of the cell cycle (Olson et al., 1995) and in ROS production was reported in other cell types but remains to be investigated in DCs.

III.3.2.3 RhoA

RhoA activates different effectors than Rac1 and CDC42, which mainly control myosin phosphorylation and microtubule dynamic.

In DCs, RhoA promotes the release of adhesion (Swetman et al., 2002) and the dissolution of podosomes (van Helden et al., 2008). At the organism level, depending on the type of migration, RhoA controls either positively or negatively DC migration (Quast et al., 2009; Ocana-Morgner et al., 2011). RhoA seems to counteract the events controlled by Rac1 and Cdc42. For instance, receptor-mediated endocytosis in DCs is inhibited by RhoA activity (Leverrier and Ridley, 2001; Nakaya et al., 2006; Ocana-Morgner et al., 2011), but RhoA is not involved in pinocytosis (West et al., 2000). There are no data on the importance of RhoA in DCs for the initiation of immune responses.

III.4 AIM OF THE PROJECT

This project is composed of three distinct parts investigating the role of Rho-GTPases in dendritic cell functions.

The laboratory of Thomas Brocker has developed a mouse model where a dominant negative variant of Rac1 is expressed in $CD11c^+$ cells (Rac1N17 mouse, (Kerksiek et al., 2005; Neuenhahn et al., 2006; Luckashenak et al., 2008; Luckashenak et al., 2013)). It has been published that spleen DCs from these mice fail to take up soluble molecules, apoptotic cells and bacteria. These cells have a cross-presentation defect but a normal migration capacity. In the first part of this study, we were interested in the effects of Rac1N17-expression in skin DCs and particularly in Langerhans cells.

As explained in the previous pages (**Figure 7**, (Feig, 1999; Guilluy et al., 2011)), the utilisation of a dominant negative variant is not very specific. We compared dominant negative transgenic mice with DC-specific conditional Rac1-KO mice, to find out what the real functions of the Rho-GTPase Rac1 in skin DCs are.

Finally, in the last part of this work, we investigated which protein functions were actually inhibited in Rac1N17 spleen DCs, by comparing them to spleen DCs deficient for Rac1, Cdc42 and RhoA.

IV MATERIALS AND METHODS

IV.1 MATERIAL

IV.1.1 Antibodies for flow cytometry

Specificity (anti-mouse)	Conjugate	Clone	Supplier
CD103	PE	M290	BD Pharmingen
	Biotin	2E7	eBioscience
CD11c	FITC	HL3	BD Pharmingen
	PE-Cy7	HL3	BD Pharmingen
CD16/32 (FC-block)	None	2.4G2	BD Pharmingen
CD184 (CXCR4)	AF-647	TG12/CXCR4	Biolegend
CD195 (CCR5)	AF-488	HM-CCR5	Biolegend
CD197 (CCR7)	APC	4B12	eBioscience
CD207 (Langerin)	AF-647	929F3.01	Dendritics
CD324 (E-cadherin)	AF-647	DECMA-1	eBioscience
CD326 (Epcam)	PerCP-Cy5.5	G8.8	Biolegend
CD4	PE-Cy7	L3T4	eBioscience
CD40	APC	HM40-3	eBioscience
CD45	APC-eF780	30-F11	eBioscience
CD45.1	FITC	A20	BD Pharmingen
	APC	A20	eBioscience
CD45.2	APC	104	eBioscience
CD49f (a6-integrin)	AF-488	GoH3	Biolegend
CD8	FITC	53-6.7	eBioscience
	PerCP	53-6.7	BD Pharmingen
	APC-Cy7	53-6.7	eBioscience
CD80	Biotin	16-10A1	eBioscience
CD86	Biotin	GL1	BD Pharmingen
CD90.1	PerCP	OX-7	BD Pharmingen
F4/80	PE	BM8	eBioscience
H-2D^b	FITC	KH95	BD Pharmingen
I-A^b	FITC	AF6-120.1	BD Pharmingen
	PE	AF6-120.1	BD Pharmingen
	PE-Cy5	M5/114.15.2	eBioscience

	biotin	AF6-120.1	BD Pharmingen
IFNγ	APC	XMG1.2	eBioscience
Streptavidin	PerCP		BD Pharmingen
	Pacific Blue		Invitrogen
TFNα	APC	MP6-XT22	eBioscience
Vα2-TCR	PE	B20.1	eBioscience
Vβ5.1/5.2-TCR	FITC	MR9-4	BD Pharmingen

IV.1.2 Antibodies for western blot

Specificity	Host	Dilution	Time	Solution	Supplier
β-Actin	rabbit	1/1000	1h	PBST	Cell Signaling
Rac1	mouse	1/500	1h30	PBST	Cytoskeleton
Mouse		1/2000	1h30	PBST + 1 % milk powder	Jackson Lab
Rabbit	donkey	1/2500	1h30	PBST + 5 % milk powder	Jackson Lab

IV.1.3 Chemicals

If not stated differently, chemicals were purchased from Merck (Darmstadt, Germany), Roth (Karlsruhe, Germany) or Sigma-Aldrich (St. Louis, MO, USA). All buffers and solutions were prepared using double distilled water.

IV.1.4 Consumables

Mesh filter 41 µm	Reichelt Chemietechnik, Heidelberg, Germany
injection needles 26 G x 1/2	Terumo Medical Corporation, Tokyo, Japan
disposable syringes (1 ml)	Braun, Melsungen, Germany
tubes 1.5 ml und 2 ml	Eppendorf, Hamburg, Germany
tubes 5 ml	SARSTEDT, Nümbrecht, Germany

Other materials and plastic wares were purchased from BD, Nunc (Wiesbaden, Germany) and Greiner (Frickenhausen, Germany).

IV.1.5 Devices

Analytic scale (Adventurer, Ohaus Corp., Pine Brooks, NJ, USA), automatic pipettors (Integra Biosciences, Baar, Switzerland), bench centrifuge (Centrifuge 5415 D, Eppendorf, Hamburg, Germany), cell counter (Coulter Counter Z2, Beckman Coulter, Krefeld, Germany), centrifuge (Rotixa RP, Hettich, Tuttlingen, Germany), chemical scale (Kern, Albstadt, Germany), flow cytometer (FACSCalibur, FACSCantoII, FACSAria BD), incubator (Hera cell, Heraeus Kendro Laboratory Products, Hanau, Germany), laminar airflow cabinet (Heraeus), magnetic stirrer (Ika Labortechnik, Staufen, Germany), PCR-machine (Biometra, Goettingen, Germany), pH-meter (Inolab, Weilheim, Germany), pipettes (Greine, Frickenhausen, Germany), power supply (Amersham Pharmacia, Piscataway, NJ, USA), vacuum pump (KNF Neuberger, Munzingen, Germany), water bath (Grant Instruments Ltd., Barrington Cambridge, UK).

All other devices are mentioned in the methods section.

IV.1.6 Medium and buffers

PBS (Phosphate buffered saline)	150 mM NaCl 10 mM Na_2HPO_4 2 mM KH_2PO_4 pH 7.4 or Dulbecco's PBS without Ca^{2+}/Mg^{2+} (Gibco, Invitrogen, Carlsbad, CA, USA)
Culture medium	RPMI 1640 (PAA, Pasching, Austria) 10 % FCS (Gibco) 0.05 mM (1%) βmercaptoethanol (PAN biotech GmbH) 100 U/ml Penicillin (PAN biotech GmbH) 100 μg/ml Streptomycin (PAN biotech GmbH) 10 mM Hepes (Gibco)

MACS buffer	PBS
	0.5 % FCS
	8 μM EDTA
FACS buffer	PBS
	2 % FCS
	0.01 % NaN_3
Anesthetic	PBS
	2 % Rompun (Bayer)
	10 mg/ml Ketavet (Pfistzer)
ACK buffer	1 L H_2O
	8.29 g NH_4Cl
	1 g $KHCO_3$
	37.2 mg Na_2EDTA
	pH 7.3
50x TAE buffer	1 L H_2O
	242 g Tris
	57.1 ml 100 % acetic acid
	100 ml 0.5 M EDTA
	pH 8.0
Borate buffer	H_2O
	0,1 M boric acid
	pH 8.5
Storage buffer	PBS
	10 mg/ml BSA sterile filtrated
	0.1 % NaN_3
	5 % glycerol
	pH 7.4

10X Gitocher buffer	670 mM Tris pH 8.8
	166 mM $(NH_4)_2SO_3$
	65 mM $MgCl_2$
	0.1 % Gelatin
Digestion mix for genotyping	H_2O
	1X Gitocher buffer
	0.5 % Triton-X
	1 % βmercaptoethanol
	0.4 mg/ml Proteinase K

Western blot solutions:

Lysis buffer	50 mM Tris/HCl pH 8.8
	150 mM NaCl
	1 % NP40
	1/100 protease inhibitor cocktail
	1 mM PMSF
Resolving gel 12%	H_2O
	30 % Acrylamid/Bisacrylamid-mix
	1.5 mM Tris/HCl pH 8.8
	1 % SDS
	1 % APS
	0.04 % TEMED
Stacking gel 5%	H_2O
	30 % Acrylamid/Bisacrylamid-mix
	1 M Tris/HCl pH 6.8
	1 % SDS
	1 % APS
	0.1 % TEMED
Running buffer	25 mM Tris Base
	192 mM Glycin
	0.1 % SDS

Blotting buffer	25 mM Tris-Base 192 mM Glycin 20 % Methanol 0.002 % SDS
PBST	PBS 0.05 % Tween-20
Blocking buffer	PBST Milk powder 5 %
Stripping buffer	62.5 mM Tris HCl pH 6.7 2 % SDS, warm 15 min at 55°C 100 mM βmercaptoethanol at the last moment in warm solution

IV.1.7 Protein, peptide and oligonucleotides

Ovalbumin (albumin from chicken egg, OVA, Grade VII) was purchased from Sigma-Aldrich (St. Louis, MO, USA). The peptide $OVA_{257-264}$ SIINFEKL was purchased from PolyPeptide Group (Strasbourg, France). The following oligonucleotides were purchased from MWG-Biotech AG (Edersberg, Germany)

For qPCR

IL1-α 5′	GAGCGCTCACGAACAGTTG	Probe 52
IL1-α 3′	TTGGTTAAATGACCTGCAACA	
IL1-β 5′	TCTTCTTTGGGTATTGCTTGG	Probe 78
IL1-β 3′	TGTAATGAAAGACGGCACACC	
TNF-α 5′	GGTTGTCTTTGAGATCCATGC	Probe 79
TNF-α 3′	CTGTAGCCCACGTCGTAGC	
TGF-β 5′	CAGCAGCCGGTTACCAAG	Probe 72
TGF-β 3′	TGGAGCAACATGTGGAACTC	
HPRT 5′	CCTGGTTCATCATCGCTAATC	Probe 95
HPRT 3′	TCCTCCTCAGACCGCTTTT	

For PCR:

Rac1-flox 5´	GTCTTGAGTTACATCTCTGG
Rac1-flox 3´	CTGACGCCAACAACTATGC
Rac1N17 5´	AACCAATGCATTTCCTGGAG
Rac1N17 3´ (Rac reverse)	AGGGTACCACTTTGCTCGAA
Rac left 5´	CTGATCAGTTACACAACCAATGC
Cre 5´	GGACATGTTCAGGGATCGCCAGGCG
Cre 3´	GCATAACCAGTGAAACAGCATTGCTG

IV.1.8 Mice

All mice were bred and maintained at the animal facility of the Institute for Immunology (LMU, Munich).

IV.1.8.1 C57BL/6 and BALB/cJ

The MHC-haplotype of C57BL/6 strain is H-2^b. Mice from this strain express the congenic markers CD45.2 and CD90.2 on all leukocytes. A congenic strain expressing CD45.1 was also used. The MHC-haplotype of BALB/cJ strain is H-2^d.

IV.1.8.2 OT-I and OT-II

$CD8^+$ T cells from OT-I mice express a transgenic Vα2/Vβ5 TCR, which recognizes the ovalbumin peptide $OVA_{257–264}$, in the context of MHC-I H2-K^b (Hogquist et al., 1994). These mice express the congenic marker CD90.1 on the C57BL/6 background.

$CD4^+$ T cells from OT-II mice express a transgenic Vα2/Vβ5 TCR, which recognizes the ovalbumin peptide $OVA_{323-339}$ in the context of MHC-II I-A^b (Robertson et al., 2000). These mice express the congenic marker CD90.1 on the C57BL/6 background.

IV.1.8.3 Rac1N17 mice

Rac1N17 mice express the transgenic dominant negative form of the small Rho-GTPase Rac1 in $CD11c^+$ cells (abbreviated Rac1N17 mice (Kerksiek et al., 2005)).

These mice are on the C57BL/6 background.

IV.1.8.4 Rac1-flox in CD11c-Cre and Langerin-Cre

To generate mice with DCs deficient for the small Rho-GTPase Rac1 (**Figure 8**), $Rac1^{fl/fl}$ mice (Benninger et al., 2007) provided by Cord Brakebusch (University of Copenhagen, Copenhagen, Denmark) were crossed with either CD11c-Cre mice (Caton et al., 2007) provided by Boris Reizis (Columbia University, New York, NY, USA) or Langerin-Cre mice (Zahner et al., 2011) provided by Bjorn Clausen (Erasmus University Medical Center, Rotterdam, The Nederland). These mice are abbreviated CD11c-$Rac1^{-/-}$ and Lang-$Rac1^{-/-}$ mice respectively. These mice were backcrossed on the C57BL/6 background.

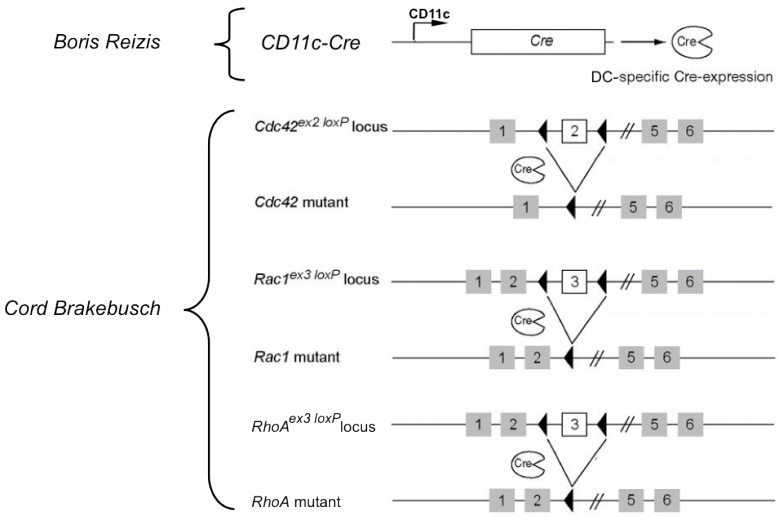

Figure 8: Generation of mice deleted of Rac1, Cdc42 and RhoA in DCs
Adapted from (Caton et al., 2007) and from (Benninger et al., 2007).

IV.1.8.5 Cdc42-flox in CD11c-Cre and RhoA-flox in CD11c-Cre

To generate mice with DCs deficient for the small Rho-GTPases Cdc42 or RhoA (**Figure 8**), $Cdc42^{fl/fl}$ or $RhoA^{fl/fl}$ mice (Wu et al., 2006) provided by Cord Brakebusch (University of Copenhagen, Copenhagen, Denmark) were crossed with CD11c-Cre mice (Caton et al., 2007) provided by Boris Reizis (Columbia University, New York, NY, USA). These mice were abbreviated $Cdc42^{-/-}$ and $RhoA^{-/-}$ mice respectively. Nancy Luckashenak, Anna Wähe and Shuai Li provided genotyped mice. These mice are on the C57BL/6 background.

IV.2 METHODS

IV.2.1 Cellular and immunological methods

IV.2.1.1 *In vivo* assays and immunization

IV.2.1.1.a Adoptive transfer

This method consists in the transfer of T cells from a donor mouse into a recipient mouse. T cells were isolated from spleens and lymph nodes of donor mice using magnetic CD8 or CD4 negative selection (MACS®, IV.2.1.2.b) and CFSE-labeled (IV.2.1.2.c). Cell purity was determined by flow cytometry (IV.2.1.2.e). Either 10^6 $CD8^+$ T cells or $2x10^6$ $CD4^+$ T cells were injected i.v. into syngenic recipients of the same sex. The congenic marker CD90.1 allows subsequent detection of transferred T cells in the recipient.

IV.2.1.1.b Intradermal immunization

Mice were anesthetized with intraperitoneal injection of 150 µl of the anesthetic (IV.1.6). They were shaved on the left flank and 5 µg of OVA-coated polystyrene beads (IV.2.2.6) were injected intradermally in a maximum volume of 30 µl. As an irritant, 15 µl acetone were added on the skin at the injection site. Proliferation of T cells was assessed 5 days later.

IV.2.1.1.c Uptake of apoptotic cells

Splenic B cells were isolated from BALB/cJ mice using CD19 positive selection (MACS®, IV.2.1.2.b). Cells were labeled with 5 µM of CFSE (IV.2.1.2.c) and 10^7 cells were injected i.v. in the recipient mice. The MHC mismatch between the injected cells and the recipient mouse leads to opsonization of the foreign cells and their subsequent phagocytosis by recipient APCs. Uptake was investigated 14 hours later.

IV.2.1.1.d FITC painting

A 10 mg/ml solution (1 %) of FITC was prepared in a mix 1:1 of acetone and dibutylphthalate. Mice were anesthetized, shaved on the abdomen and painted with 200 µl

of the FITC solution (2 mg). Four days later, mice were sacrificed and inguinal and axillary lymph nodes were removed to assess the presence of $FITC^+$ cells.

IV.2.1.1.e Bone marrow chimeras

The recipient mice (minimum 10 weeks old) were irradiated a first time with 550 rad from a 137-Cesium source (Model G.C. 40; Type B(4); Atomic Energy of Canada Limited, Ontario, Canada) and 48 hours later they were irradiated a second time with 550 rad. From the first irradiation until 6 weeks after reconstitution, recipient mice received water with 1.2 g/l of Neomycin. Four hours after the second irradiation, recipient mice were reconstituted with intravenous injection of 10^7 cells from the desired bone marrow depleted of erythrocytes. Bone marrow cells from leg bones of the donor mice (minimum 8 weeks old) were prepared as described in IV.2.1.3.a and IV.2.1.3.b. Six weeks after reconstitution, antibiotic was stopped and chimerism in blood was analyzed on T and B cells. Experiments were performed between 8 and 10 weeks after reconstitution. When the mice were sacrificed, the ears were removed and skin DC chimerism was analyzed.

IV.2.1.2 *Ex vivo* manipulations common to the different organs or cell types

IV.2.1.2.a Determination of cell numbers

Cell count and size are measured by the change of electrical resistance that a cell causes by passing through the hole of the electrode. For analysis, cell suspensions were diluted in a conductive solution (Isoton II, Beckman Coulter) and 2 drops of a lytic reagent (ZAP-OGLOBIN II, Beckman Coulter) were added to remove residual erythrocytes.

IV.2.1.2.b Magnetic cell separation (MACS®)

Magnetic cell sorting (MACS®, Miltenyi Biotec, Bergisch-Gladbach, Germany) is a technique that allows the isolation of different cell-subpopulations based on their expression of different antigens on the cell surface. This can be achieved by positive or negative selection. Targeted cells are bound to MACS® colloidal super-magnetic MicroBeads. Passing the cell suspension through a column, which is maintained in a magnetic field, separates the positive fraction from the negative one. For some positive selection

procedures, positive cells were passed through a second column to increase purity.

MACS® separation was applied to purify spleen DCs (CD11c Microbeads, positive selection; $CD8^+$ DCs isolation kit, negative and positive selections), B cells (CD19 Micro Beads, positive selection), $CD8^+$ T and $CD4^+$ T cells ($CD8^+$ T cell Isolation Kit and $CD4^+$ T cell Isolation Kit, negative selections) and epidermal LCs (Epidermal Langerhans Cells MicroBeads Kit, positive selection). The instructions of the manufacturer were followed for all the procedures. To isolate LCs from bone marrow derived LC (BMLC) cultures, we used anti-biotin beads in combination with I-A^b-biotin antibody (IV.1.1).

IV.2.1.2.c CFSE labelling

CFSE (carboxyfluorescein-diacetate-succinimidylester*)* staining is used to track cell divisions both *in vitro* and *in vivo*. CSFE binds to amino groups of intra- and extra-cellular proteins. When cleaved by intracellular esterases, CFSE becomes a fluorescent dye. After each cell division, the amount of dye is equally divided between the daughter cells and the intensity of the fluorescence is reduced about 50 %. The number of cell divisions can be identified by the number of times the fluorescence intensity is reduced by the half.

The cells were resuspended in pre-warmed PBS with 0.03 % FCS (1 ml per 1 to $50x10^6$ cells) and CSFE was added at 5 µM or 0.5 µM for *in vivo* or *in vitro* experiments, respectively. The cells were incubated for 10 minutes at 37°C in a water bath and protected from light. The reaction was stopped by addition of an equal amount of pure FCS. The cells were washed twice with PBS and resuspended at the desired concentration in PBS or culture medium.

IV.2.1.2.d *Ex vivo* antigen uptake

Epidermal cell suspensions or MACS® purified $CD8^+$ DCs were resuspended at $5x10^5$ cells per ml of culture medium (IV.1.6) with 5 µg/ml of OVA-AF647, 250 µg/ml of FITC-dextran or 500 µg/ml of luciferase-yellow (all from Molecular Probes) in 96 well-plate (WP) with U-bottom. Cell suspensions were then incubated for 40 min at 37°C or 4°C. The cells were intensively washed to stop the reaction. During the staining procedure, plates were kept on ice until fixation to avoid any further uptake or processing of residual antigen.

IV.2.1.2.e FACS

In flow cytometry, various cell characteristics such as size, granularity and marker expression can be detected. Cells are stained with fluorochrome-coupled antibodies against surface or intracellular antigens. In a fluid stream, cells pass a laser beam and several detectors. The resulting information is acquired and can be used to identify distinct cell populations within a heterogeneous mixture of cells.

In a 96 WP, 100 µl of a single cell suspension (1 to $5x10^6$ cells) were washed in FACS buffer (IV.1.6). Cells were incubated for 20 min in the dark at 4°C with 100 µl of antibody solution (IV.1.1) at the appropriate dilution; antibodies were titrated before use. The cells were then washed with FACS buffer to remove the excess of unbound antibodies. If biotinylated antibodies were used, a second staining step with fluorochrome-conjugated streptavidin followed. The CCR7 antibody requires an staining step at 37°C prior to the classical surface staining for the other markers at 4°C.

Intracellular staining was performed according to the manufacturer's protocol with the Cytofix/Cytoperm kit (BD Bioscience). To analyze cytokine production, $10x10^6$ sdLN cells were restimulated 4 hours in 2 ml of culture medium (IV.1.6) plus 20 ng/ml of GM-CSF, which was produced in our laboratory, and 2 µl of GolgiStop (BD Bioscience), which blocks protein secretion, with either 2 µg of SIINFEKL peptide or 40 ng/ml of PMA and 2 µg/ml of Ionomycine.

Prior to acquisition, all samples were filtered to remove cell aggregates (41 µm mesh; Reichelt Chemietechnik). Data were acquired on a FACSCalibur flow cytometer (BD Bioscience) with two lasers (488 and 633 nm) or on a FACSCanto II flow cytometer (BD Bioscience) with three lasers (488, 633 and 405 nm) and analyzed with FlowJo software (TreeStar, Ashland, OR, USA). For some experiments, LCs and spleen DCs were sorted on the FACSAria flow cytometer (BD Bioscience) after MACS® purification.

IV.2.1.3 *Ex vivo* manipulations of spleen, lymph node and bone marrow cells

IV.2.1.3.a Organ preparation

Mice were sacrificed by cervical dislocation or CO_2 asphyxia, fixed with needles on a styrofoam pad, disinfected with 70 % ethanol and cut open. Lymph nodes, spleens and leg bones were harvested with fine tweezers and kept on ice in RPMI medium.

Lymph nodes and spleens were placed on a cell strainer (100 µm, BD) on a 50 ml tube and mashed with a 1 ml syringe plunger. For optimal recovery of DCs, organs were first enzymatically digested: the mashed organ was incubated for 20 min at 37°C in a solution containing 0.1 mg/ml of Liberase DL and 0.2 mg/ml of DNase I (both from Roche), followed by a second mechanical dispersion using a cell strainer.

For bone marrow cell preparation, the hind legs were removed. The bones were cleaned from muscles, separated into tibia and femur and disinfected with 70 % ethanol. Terminal parts of bones were cut and the bone marrow was flushed out with needle and syringe. For large-scale isolation, bones in medium were carefully fragmented with a mortar and pestle. The cell suspension was then filtered through a cell strainer.

IV.2.1.3.b Erythrocyte lysis

Erythrocytes from peripheral blood were lyzed using Pharm Lyse reagent (BD) according to the manufacturer's instructions.

Cell pellets from spleens were incubated in 1 ml of ACK buffer (IV.1.6) for 5 min at room temperature (RT). Afterwards, 15 ml PBS was added, the cells were centrifuged and resuspended in the appropriate buffer or medium for the following use of the cells.

Bone marrow erythrocytes were lysed with the Mouse Erythrocyte Lysing Kit from R&D System, according to the manufacturer's instructions.

IV.2.1.3.c *Ex vivo* T cell proliferation induced by spleen $CD8^+$ DCs

Cells purified with the $CD8^+$ DCs isolation kit of Miltenyi Biotec were incubated with OVA-AF647 as described in IV.2.1.2.d. After intensive wash, cells were stained to know the amount of $CD8^+$ DCs among the isolated cells. $7x10^3$ $CD8^+$ DCs were co-cultured with CFSE labeled OT-I or OT-II cells at a 1 to 10 ratio of DCs to T cells in culture medium plus 20 ng/ml of GM-SCF in 96 WP with U-bottom. Proliferation was analyzed by CFSE dilution after 3 or 4 days respectively.

IV.2.1.3.d BMLC culture

Bone marrow cells were seeded at 10^5 cells per ml of culture medium with 7.5 ng/ml of GM-CSF, 2.5 ng/ml of TGF-β and 5 ng/ml of SCF. After 3 and 7 days, medium was

changed and cells were split for further expansion in the same cocktail as the first day. After 13 days, cells were matured in culture medium with 10 ng/ml of GM-CSF, 10 ng/ml of TNF-α and 10 ng/ml of IL-4. At day 17, more than 90 % of the cells were LC-like cells. Except GM-SCF, all these molecules were purchased by Peprotech.

IV.2.1.4 *Ex vivo* manipulations of skin cells

IV.2.1.4.a Isolation of epidermal cells

Ears were removed. The dorsal and ventral layers were separated with fine forceps and incubated dermal face down in 2 U/ml of Dispase II (Roche) in HBSS in 24 WP for 90 min at 37°C. Skin sheets were separated into dermis and epidermis with fine forceps in cold PBS. Epidermal sheets were further incubated for 2 hours at 37°C in HBSS with 157 U/ml of collagenase IV (Worthington) and 10 % FCS in 24 WP. Dermal sheets were digested for 2 hours at 37°C in a solution containing 0.5 mg/ml of DNase I, 2.7 mg/ml of Collagenase XI, 27 µg/ml of Hylaronase VI and 10 mM of Hepes in RPMI.

The suspensions were passed through a cell strainer and the sheets were mashed on the cell strainer to obtain a homogenous cell suspension. The cells were washed and counted. They were then either directly stained, used for experiments or further cultured.

IV.2.1.4.b *Ex vivo* maturation

Epidermal cell suspensions were incubated overnight in culture medium with 20 ng/ml of GM-SCF with or without 20 µg/ml of peptidoglycan (InvivoGen) in 24 WP. At the indicated time points, cells were stained for flow cytometry analysis or used to isolate mRNA (IV.2.2.4).

IV.2.1.4.c Crawl out assay

Ears were removed, ventral and dorsal layers were separated and incubated in 500 µl of complete medium with 100 ng/ml of CCL21 (R&D Systems) in 24 WP. Every day, migrated cells were collected and epidermal sheets were placed in fresh complete medium with CCL21, for a total of 3 days.

IV.2.1.4.d *Ex vivo* T cells proliferation induced by Langerhans cells

Epidermal sheets were incubated overnight in 2 ml of culture medium with 500 µg/ml of OVA grade VII in 24 WP. On the next day, migrated cells and epidermal sheets were intensively washed and placed in culture medium with 20 ng/ml of GM-CSF for two other days to crawl out. Migrated cells were collected and counted. Some cells were stained to assess LCs purity and concentration.

Cells were resuspended in 200 µl of culture medium with 20 ng/ml of GM-SCF in U-bottom 96 WP with CFSE-labeled OT-I or OT-II cells at a ratio of 1:20 of LCs to T cells. Proliferation was analyzed by CFSE dilution 3 and 4 days later respectively.

IV.2.1.4.e Histology of ear sheets

Ears were cut, dorsal and ventral layers were incubated with dermal side down in 0.5 M of PBS-NH_4SCN for 20 min at 37°C. Epidermis was carefully separated from dermis and fixed on glass slides in acetone at RT for 5 min. Epidermis was washed in PBS and incubated in 100 µl of blocking solution (PBS with 0.25 % BSA and 10 % FCS) for 30 min in a humidified box. Sheets were then incubated for 30 min in 100 µl of blocking solution with FC-block and biotinylated anti-I-A^b. After three washes in PBS, sheets were incubated 30 min in blocking solution with streptavidin-AF555 and 1 µg/ml of DAPI. Slides were washed in PBS. Finally, 100 µl of fluoromount G (Biozol) were added and the coverslip was mounted. Slides were kept at 4°C.

IV.2.2 Molecular biology methods

IV.2.2.1 Agarose gel electrophoresis

This technique was used to separate DNA fragments according to their length. The different fragments were identified by comparison to a 100 bp ladder (New England Biolabs, Ipswich, MA, USA). Separation was carried out by application of constant voltage (80 V) to an electrophoresis chamber containing conductive buffer (TAE, IV.1.6). A 1 % agarose gel was used. DNA was visualized by addition of ethidium bromide to the gel (0.5 µg/ml) and subsequent examination under UV light (312 nm, Intas, Goettingen, Germany).

IV.2.2.2 Polymerase chain reaction

The polymerase chain reaction (PCR) is a method used to amplify a piece of DNA across several orders of magnitude, generating thousands to millions of copies of a particular DNA sequence.

The DNA polymerase synthesizes new strands of DNA complementary to the offered template strand. Primers (IV.1.7) specific for the 5′ and 3′ ends of the DNA target were used. The DNA is first denaturized at a high temperature to separate the two strands of DNA, then the temperature goes down to allow both primers to hybridize with the target sequence as well as the DNA polymerase to synthesize the supplementary strand. Each step is repeated several times to expend exponentially the targeted DNA sequence.

Digestion of tail pieces for genotyping:
50 µl digestion mix (IV.1.6), 2 millimeters tail
6 hours at 55°C, 5 minutes 95°C, resting at 4°C

PCR mix:
0.2 µl Primer 5′ (100 pmol/µl) and 0.2 µl Primer 3′ (100 pmol/µl)
12.5 µl ReadyMix PCR Mastermix (Thermo Fisher scientific)
2.0 µl DNA
H_2O to reach 25 µl

PCR	Rac1N17	Rac1-flox	CD11c- and Langerin-Cre	Reverse Transcriptase-PCR
Step1	5 min at 95°C	5 min at 95°C	5 min at 95°C	10 min at 95°C
Step2	30 snd at 95°C	30 snd at 94°C	30 snd at 95°C	10 snd at 95°C
Step3	45 snd at 55°C	30 snd at 63°C	30 snd at 55°C	30 snd at 60°C
Step4	30 snd at 72°C	30 snd at 72°C	45 snd at 72°C	cycling 90 times from Step2
Step5	cycling x29 from Step2	cycling x10 from Step2, at each cycle -1°C for Step3	cycling x35 from Step2	30 snd at 40°C
Step6	10 min at 72°C	30 snd at 94°C	5 min at 72°C	resting at 4°C
Step7	resting at 4°C	30 snd at 53°C	resting at 4°C	
Step8		30 snd at 72°C		
Step9		cycling x35		
Step10		Resting at 4°C		

IV.2.2.3 Western blot

Approximately 10^6 $CD11c^+$ MACS-sorted splenocytes were lysed for 15 min in lysis buffer on ice with constant vortexing. Protein concentration was determined with the Quant-iT^{TM} protein assay kit (Invitrogen). Then 15 µg of protein were reduced in a 5 % SDS solution for 10 min at 95°C. Protein samples were loaded on a 5–12% gradient gel (Bio-Rad) (IV.1.6) and let run for 2 hours at 80 V. Transfer on nitrocellulose membrane was performed for 90 min at 70 V. Membranes were blocked overnight in blocking solution (IV.1.6 and IV.1.2). For the detection of several proteins of the same size, the membrane was stripped 30 min in stripping buffer (IV.1.6) and then blocked again. Proteins were detected with the antibodies described in section IV.1.2. To control for cell loading, blots were subsequently stained with anti–β-actin antibody. Signal intensities were quantified with ImageJ software (National Institutes of Health, Bethesda, MD).

IV.2.2.4 mRNA isolation and cDNA generation

The RNeasy Micro Kit (Qiagen, Hilden, Germany) was used according to the manufacturer's instructions. During RNA isolation, residual amounts of DNA were removed by on-column DNase I treatment.

Nucleic acid concentrations were determined by UV absorbance measurement at 260 nm with a NanoDrop device (Thermo Fisher Scientific, Waltham, MA, USA). The 260/280 ratio is an indicator for nucleic acid purity: values between 1.8 and 2 are desirable, because it represents a low protein contamination. The mRNA was either frozen at -80°C or directly reverse transcribed into cDNA.

The mRNA was reverse transcribed using SuperScript III First-StrandSynthesis System using random hexamers (Invitrogen). To standardize the qPCR, 200 ng mRNA was used. The cDNA was either frozen at -20°C or directly used for quantitative PCR (qPCR).

IV.2.2.5 Quantitative PCR

Quantitative PCR is used to determine the concentration of a particular cDNA sequence within a sample. The TaqMan method of cDNA detection is based on probe use. These probes are oligonucleotides labeled with fluorescent dyes, which give a signal only when the probes are bound to their specific DNA sequences. The initial amount of the

targeted DNA is correlated with the number of cycles (crossing point, CP value) that is reached when fluorescence intensity exceeds a certain threshold.

The TaqMan assay was performed with the LightCycler TaqMan Master Kit (Roche) and the Universal ProbeLibrary Set mouse (Roche) according to the manufacturer's instructions, on a CFX96 Real Time System (BIO-RAD). Primers and probes are listed in IV.1.7. Expression levels were normalized to HPRT and relative quantification was calculated using the ΔΔCT-method (Livak and Schmittgen, 2001).

IV.2.2.6 Generation of ovalbumin-coated polystyrene beads

The polystyrene microparticles of 2 µm of diameter from Polysciences, Inc were coated with OVA as indicated in their technical datasheet. This is not a covalent coating. The beads have a slight anionic charge because of sulfate ester groups, allowing adsorbtion of proteins.

Briefly, 0.5 ml of a 2.5 % beads suspension were washed and incubated overnight with 500 µg of OVA grade VII in borate buffer (IV.1.6). The supernatant was harvested to determine the concentration of uncoupled protein. It allows the determination of OVA concentration on the beads. Free spaces on the beads were blocked 3 times in 10 mg/ml of BSA in borate buffer for 30 min. The pellet was resuspended in 1 ml of storage buffer (IV.1.6) and stored at 4°C. Before use, the appropriate volume of beads was washed 3 times in PBS and resuspended in the appropriate volume of PBS (5 µg of OVA-coated beads in 30 µl).

IV.2.2.7 MMP-9 ELISA on BMLC culture supernatant

BMLC culture supernatants were concentrated with Centricon®Plus-70 (Millipore). The concentration efficiency is the ratio between the initial volume and the final concentrated volume of supernatant. Samples were used in an ELISA (R&D Systems) to determine the concentration of total MMP-9. MMP-9 concentration in undiluted supernatants corresponds to the concentration in concentrated supernatants determined according to manufacturer's instruction divided by the concentration efficiency.

IV.3 STATISTICAL ANALYSIS

Data were analyzed using the Student's *t* test (GraphPad Prism 5.0b; GraphPad Software). P-values were defined as: ***: $p<0.001$, **: $p=0.001$ to 0.01, *: $p=0.01$ to 0.05. Error bars represent standard deviations. All experiments were repeated at least three times, with at least 3 mice per group, unless otherwise stated.

V RESULTS

V.1 CHARACTERIZATION OF LCs IN Rac1N17 MICE

V.1.1 Characterization of epidermis, dermis and sdLNs

Spleen DCs expressing a dominant negative form of the Rho-GTPase Rac1 (Rac1N17) are known to have uptake and cross-presentation defects (Kerksiek et al., 2005; Neuenhahn et al., 2006; Luckashenak et al., 2008). We were wondering if this was also the case for epidermal LCs, and if so, we could use these mice to investigate the controversial role of LCs in skin immune responses.

First, we verified that Rac1N17 LCs express the dominant negative variant of Rac1. The Rac1N17 cDNA is from canine origin (Chavrier et al., 1990; Dutartre et al., 1996; Guillemot et al., 1997; Franco et al., 1999) and it has 90 % similarity with the murine sequence at the mRNA level and 100 % at the protein level. The use of primers specific for the canine sequence of Rac1 revealed the presence of Rac1N17 mRNA in Rac1N17 spleen DCs and Rac1N17 LCs (**Figure 9**). This means that the dominant negative variant of Rac1 is expressed in Rac1N17 but not in WT LCs.

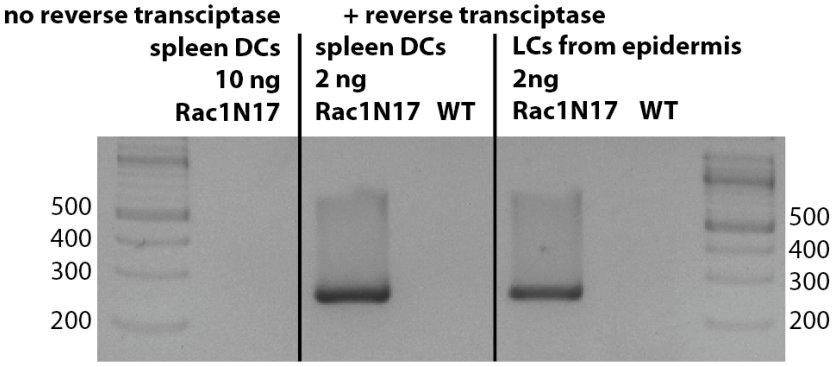

Figure 9: Rac1N17 mRNA is expressed in Rac1N17 LCs
WT and Rac1N17 spleen DCs (as positive control) and LCs were sorted by flow cytometry, mRNA was isolated and reverse transcribed. Rac1N17 cDNA was amplified with primers specific for canine Rac1 (Rac1N17 3' and Rac left 5', see IV.1.7). The absence of genomic DNA contamination was assessed by a control sample that was not reverse transcribed. The markers show DNA size in bp, the expected product has 240 nucleotides.

Next, in order to determine the frequency of LCs in the skin, we analyzed Rac1N17 and WT epidermis by histology and flow cytometry. Rac1N17 and WT LCs were present in comparable amounts in the epidermis, as detected by both methods (**Figure 10.A**). The dermal sheets were enzymatically digested and dermal cells were stained for flow cytometry analysis. Here, LCs (defined in the dermis as $CD45^+$ $CD11c^+$ $MHC\text{-}II^+$ $Langerin^+$

CD103$^-$ (Bursch et al., 2007)) were found reduced by half in Rac1N17 dermis as compared to WT (**Figure 10.B**).

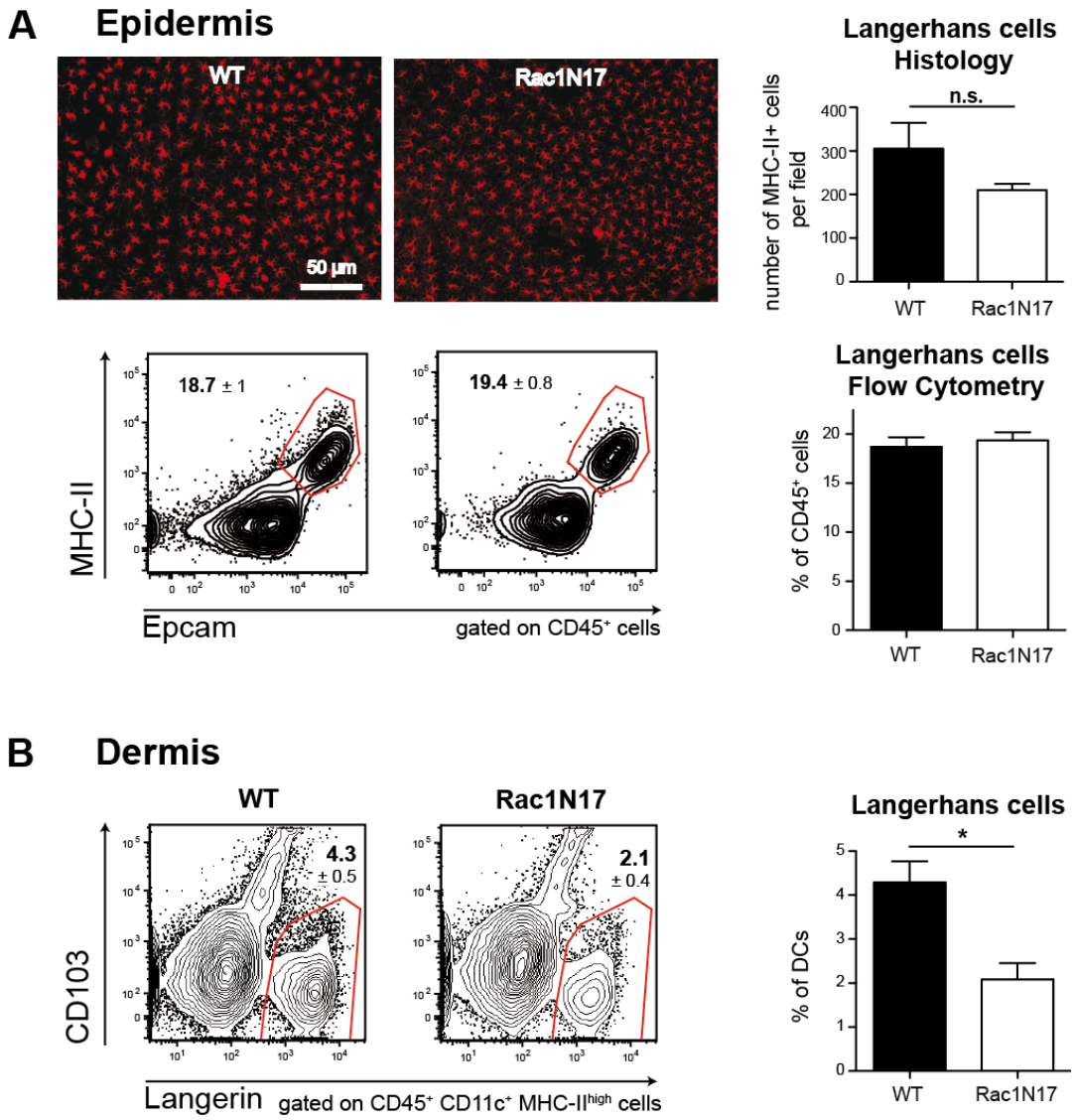

Figure 10: Rac1N17 LCs in steady state skin
A, *Upper panel*: epidermis was stained with anti-MHC-II antibody and positive cells were counted. Images were acquired at original magnification x200. Scale bar, 50 µm. *Lower panel*: epidermis and dermis were separated, epidermis was further enzymatically digested and LCs were analyzed by flow cytometry (identified as CD45$^+$ CD11c$^+$ MHC-II$^+$ Epcam$^+$ cells, red gate). **B**, Epidermis and dermis were separated, dermis was further enzymatically digested and LCs were analyzed by flow cytometry (red gate). Statistics represent the frequency of LCs inside the DC population. Data are representative of 3 independent experiments. Groups were compared by unpaired *t* test: not significant p>0.05; * 0.01>p>0.05.

Finally, we investigated the number of LCs in sdLNs. The global migratory DC population (CD11c$^+$ MHC-II^{high} cells, (Salomon et al., 1998; Henri et al., 2001)) was significantly reduced in Rac1N17 mice (**Figure 11**, upper panels). Within this population, Rac1N17 LCs were even more reduced in proportions (8.6 % ± 1.5 of migrating DCs in Rac1N17 mice as compared to 28.1 % ± 2.7 in WT mice, **Figure 11**, lower panels), leading to an overall 2.5 fold decrease of migratory LC numbers in the Rac1N17 sdLNs. Langerin$^+$

dDCs (Langerin^{+} CD103^{+}) were even more decreased in sdLNs of Rac1N17 mice (for more details see V.2.1).

From these data, we conclude that Rac1N17 LCs develop normally but have a defect in migration at the steady state.

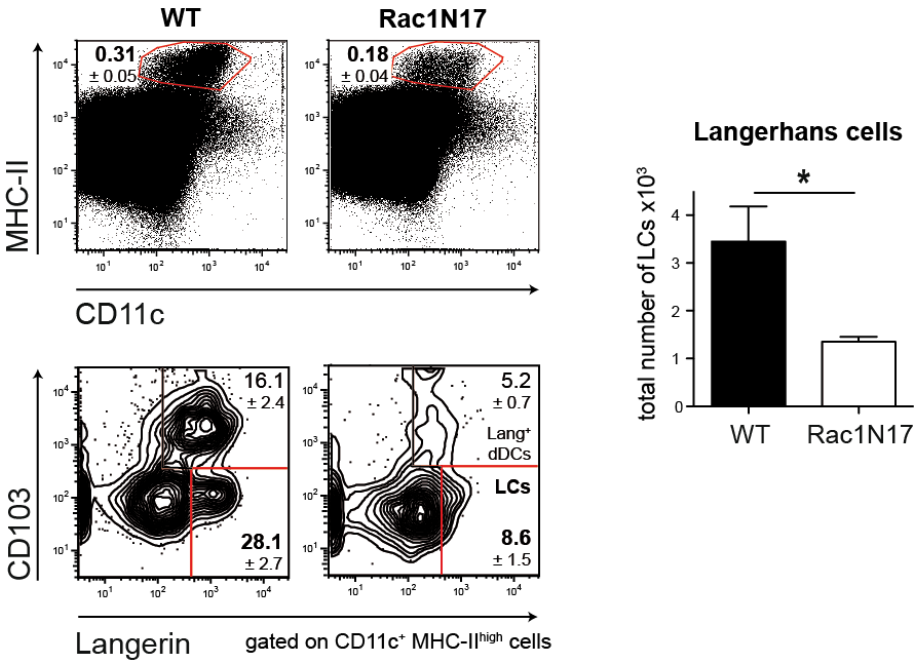

Figure 11: Rac1N17 LCs in steady state skin draining lymph nodes
Inguinal and axillary LNs were enzymatically digested. Cells were then stained and analyzed by flow cytometry. *Upper panels* represent migratory DCs (CD11c^{+} MHC-II^{high}, red gate) among total LN cells. Dermal and epidermal DCs were identified in the *lower panels* according to their expression of CD103 and Langerin. Statistics represent the number of LCs in sdLNs. Data are representative of 3 different experiments; groups were compared by unpaired *t* test: not significant $p>0.05$; * $0.01>p>0.05$.

V.1.2 Functional analysis of Rac1N17 LCs

Next we investigated whether Rac1N17 LCs could be activated. Epidermal cells were activated overnight in the presence of GM-CSF and up-regulation of MHC-I, MHC-II, CD40, CD80 and CD86 was analyzed. We could not detect differences between Rac1N17 and WT LC activation state (**Figure 12.A**).

Then, we tested if Rac1N17 LCs have the same uptake defect as detected in Rac1N17 spleen DCs (Kerksiek et al., 2005). Non-activated epidermal cells were incubated for 40 minutes with either FITC-dextran (mannose-receptor mediated endocytosis), luciferase yellow (fluid phase endocytosis: pinocytosis) or OVA-AF647 (both mannose-receptor mediated endocytosis and pinocytosis, pH insensitive fluorochrome). Rac1N17 LCs did not display any uptake defect at the concentrations and time points used in this study (**Figure 12.B**).

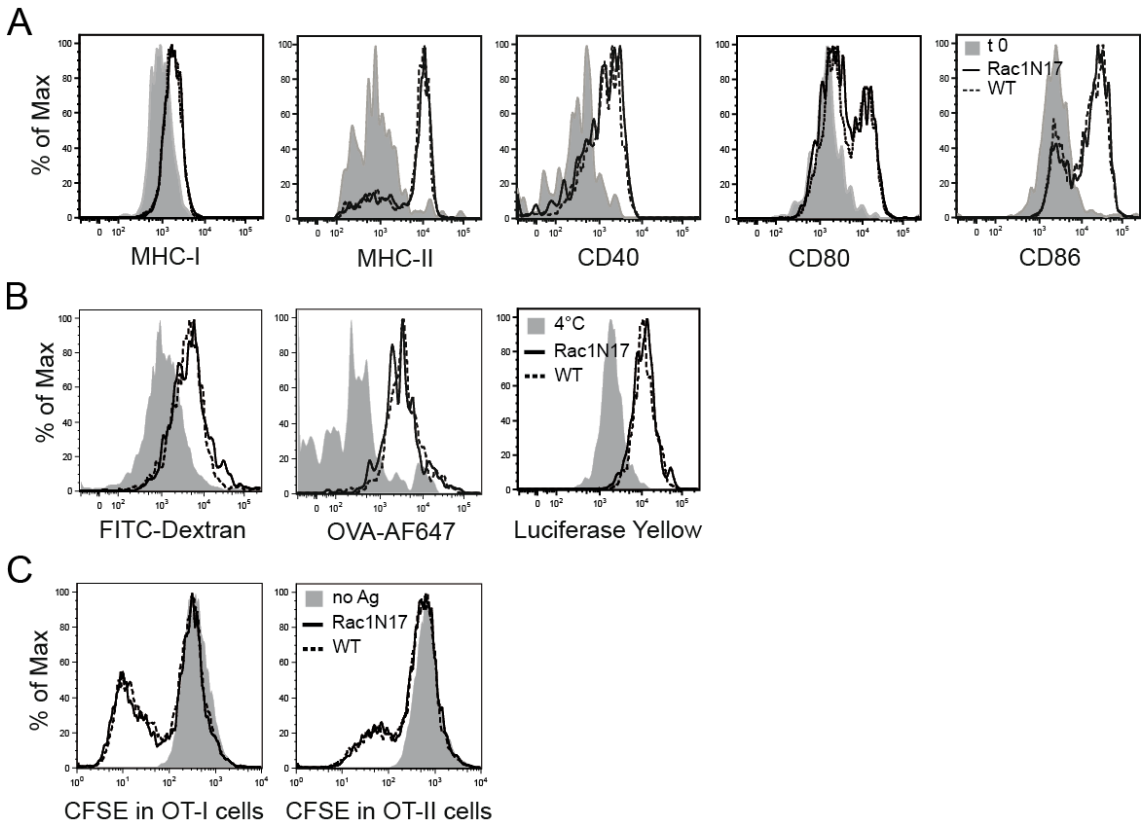

Figure 12: Activation, uptake of soluble molecules and T cell priming are normal in Rac1N17 LCs
A, Epidermal cells were incubated overnight with GM-SCF. Up-regulation of MHC-I, MHC-II, CD40, CD80 and CD86 was assessed directly after cell isolation (gray filled histogram) and after 12 hours of GM-CSF-induced maturation. Rac1N17: full line; WT: dotted line. LCs were identified as $CD45^+$ $CD11c^+$ $MHC\text{-}II^+$ $Epcam^+$ cells. **B**, Epidermal cells were incubated for 40 minutes with either 250 µg/ml FITC-dextran, 500 µg/ml luciferase yellow or 5 µg/ml OVA-AF647. Rac1N17: full line; WT: dotted line; gray filled histogram: 4°C control. LCs were identified as $CD45^+$ $CD11c^+$ $MHC\text{-}II^+$ $Epcam^+$ cells. **C**, Epidermal sheets were incubated for 12 hours with peptide free OVA, washed intensively the next day and put in culture medium with GM-SCF for 2 other days of crawl out. After crawl out, migrated LCs were co-cultured with CFSE-labeled OT-I or OT-II cells. T cell proliferation was assessed by measuring CFSE dilution 3 and 4 days later, respectively. Rac1N17: full line; WT: dotted line; gray filled histogram: no antigen control. OT-II and OT-I T cells were identified as $CD90.1^+$ $CD4^+$ and $CD90.1^+$ $CD8^+$ cells respectively. Data are representative of 5 (**A**), 3 (**B**) and 6 (**C**) independent experiments.

Finally, we examined whether Rac1N17 LCs were able to perform *in vitro* direct MHC-II presentation or MHC-I cross-presentation. Epidermal sheets were incubated with peptide free Ovalbumin (OVA) and after crawl out (Stoitzner et al., 2006), migrated LCs were co-cultured with either CFSE-labeled OT-I or OT-II cells ($CD8^+$ and $CD4^+$ T cells recognizing the OVA peptides presented on MHC-I and MHC-II in C57BL/6 mice respectively). Both $CD4^+$ and $CD8^+$ T cell proliferations were similarly induced by Rac1N17 and WT LCs (**Figure 12.C**). From this assay, we concluded that Rac1N17 LCs have no defect in MHC-II presentation and cross-presentation.

Although transgenic canine Rac1N17 is expressed in the Rac1N17 LCs, Rac1N17 LCs are present in normal numbers in Rac1N17 skin, can be activated, take up antigen normally and can initiate both $CD4^+$ and $CD8^+$ T cell responses. Rac1-dependent functions in spleen DCs appear to be Rac1-independent in LCs.

V.1.3 Migratory behaviour

Rac1 is responsible for a wide range of functions depending on the cell type (Vega and Ridley, 2008). It controls uptake, processing (Heasman and Ridley, 2008) and migration (Swetman et al., 2002) in phagocytes. We have already showed that Rac1N17 LCs perform normal antigen uptake and presentation, and have a migration defect at the steady state. Therefore, we next investigated the migratory behaviour of these cells in inflammatory conditions.

We first performed an *in vivo* FITC painting assay (Macatonia et al., 1986). Briefly, FITC was painted on the abdomen of mice and sdLNs were harvested four days later. The global MHC-II^{high} (migratory DCs) FITC^{+} population represented 0.15 % ± 0.04 of sdLN cells in Rac1N17 mice, whereas WT sdLNs contained 0.33 % ± 0.1 of these migratory cells (**Figure 13.A**, upper panel). Within this population, Rac1N17 LCs were even more reduced proportionally (56.2 % ± 3.4 of FITC^{+} DCs in Rac1N17 mice as compared to 75.7 % ± 5 in WT mice), leading to an overall 3.5 fold decrease in migrating LC numbers in the Rac1N17 sdLNs (**Figure 13.A**, lower panel and bar graph). Furthermore, CD103^{+} Langerin^{+} dDCs also had a migratory defect (**Figure 13.A,** and more detailed in **Figure 23**). We conclude that Rac1 is required for LC and Langerin^{+} dDC migration.

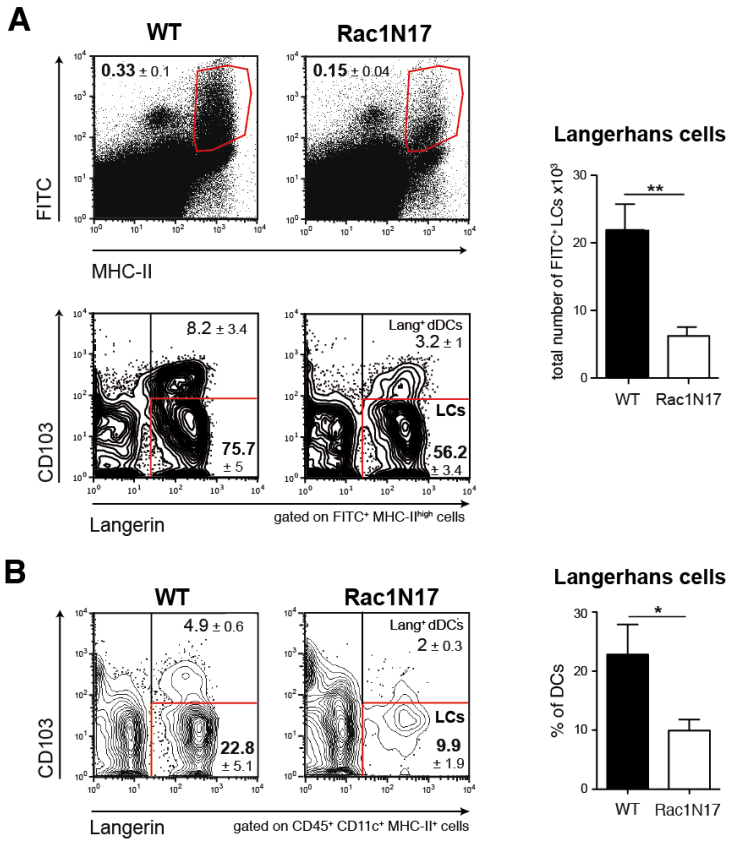

Figure 13: Impaired LC migration under inflammatory conditions (*Figure legend continues*)

A, *In vivo* FITC painting: A solution of 2 mg FITC in a 1:1 mix of acetone : dibutylphthalate was applied on the shaved abdomen of the mice. Four days later, the inguinal and axillary LNs were analyzed by flow cytometry. The red gates from *upper panels* indicate $FITC^+$ $MHC\text{-}II^+$ cells according to the unpainted control. The red gates from *lower panels* indicate $FITC^+$ LCs ($Langerin^+$ $CD103^-$ from $FITC^+$ $MHC\text{-}II^{high}$ cells). Statistics represent the number of $FITC^+$ LCs. **B**, *In vitro* crawl out assay: Total skin explants were floated on medium in the presence of CCL21. After three days, the migrated DCs were stained and analyzed by flow cytometry (gated on $CD45^+$ $CD11c^+$ $MHC\text{-}II^+$ cells). Red gates from representative flow cytometry plots and statistics indicate the frequency of LCs inside the DC population. Data are representative of 3 (A) and 4 (B) independent experiments; groups were compared by unpaired *t* test: not significant $p>0.05$; * $0.01>p>0.05$; ** $0.001>p>0.01$.

Second, we performed an *in vitro* crawl out assay (Stoitzner et al., 2003), where total skin (dermis and epidermis) floats for three days on culture medium in the presence of CCL21. Migrated cells were counted and analyzed by flow cytometry. As shown in **Figure 13.B**, there were almost two times less LCs migrating out from Rac1N17 skin in response to chemoattractant as compared to WT. Similarly, $Langerin^+$ dDCs did also have a migration defect (**Figure 13.B** and **Figure 22**). These results suggest that LCs require Rac1 for migration, which results in reduced numbers of Rac1N17 LCs in sdLNs in the steady state (**Figure 11**) as well as upon activation (**Figure 13**).

Finally, we further investigated the migratory defect of Rac1N17 LCs. We isolated Rac1N17 and WT epidermis and placed it in culture medium in the presence of CCL21 for three days, in order to assess the ability of LCs to leave the epidermis. As shown in **Figure 14**, the amount of harvested LCs was comparable between Rac1N17 and WT epidermis.

Therefore, we concluded that Rac1N17 LCs can migrate out of the epidermis, when the dermis is absent, but not of total skin.

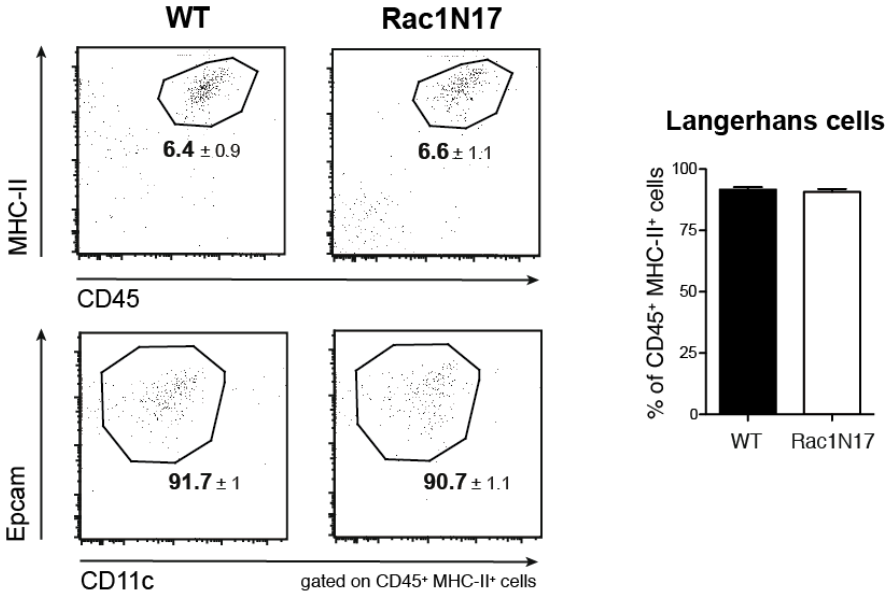

Figure 14: Rac1N17 LCs migrate normally from epidermis
In vitro epidermis crawl out assay: epidermis was floated on medium in the presence of CCL21. After three days, the migrated cells were stained and analyzed by flow cytometry (first gated on $CD45^+$ $MHC\text{-}II^+$ cells on *upper graph*, then on $CD11c^+$ $Epcam^+$ cell on *lower graph*). Statistics represent (*Figure legend continues*)

frequency of LCs inside the $CD45^+$ $MHC\text{-}II^+$ population. Data are representative of 6 independent experiments; groups were compared by unpaired *t* test: not significant $p>0.05$.

V.1.4 Molecules required to exit the epidermis

When the dermis is separated from the epidermis through Dispase II digestion, the DEBM remains attached to the dermis (Oakford et al., 2011). Therefore, we have hypothesized that LCs cannot migrate through the DEBM, which would explain the different outcomes obtained from the two crawl out assays (total skin in **Figure 13** versus epidermis in **Figure 14**).

When LCs get activated, they down-regulate the surface expression of several markers, first to detach from the keratinocytes and then to become insensitive to skin homing (Sallusto et al., 1998). For this reason, we investigated the down-regulation of E-cadherin and CCR5 on LCs upon maturation. As shown in **Figure 15.A**, Rac1N17 and WT LCs modulated to the same extent the surface level of these molecules. To leave the epidermis, LCs also need to up-regulate integrins that bind DEBM, chemokine receptors for LN homing and other molecules important for the interaction with matrix substrates. Therefore, we tested the up-regulation of α6-integrin, CCR7, CXCR4 and CD44 by activated LCs, but we could not detect differences between the surface levels of these markers on Rac1N17 or WT LCs both before or after maturation (**Figure 15.A**).

The absence of TGF-β induces LCs to exit the epidermis (Kaplan et al., 2007). Upon activation, LCs produce pro-inflammatory IL1-β, which in turn induces the release of the proinflammatory cytokines TNF-α and IL1-α by keratinocytes. TNF-α and IL1-α are produced only by keratinocytes whereas TGF-β and IL1-β are exclusively produced by LCs. Therefore, we investigated the expression level of these cytokines in the epidermis before and during activation. As expected, IL1-β expression was increasing upon activation, but there was no difference between the IL1-β level of Rac1N17 and WT epidermis (**Figure 15.B**, lower graph). TGF-β expression did not change over time (**Figure 15.B**, upper graph), meaning that its absence is sufficient (Kaplan et al., 2007), but not nessecary for LCs to exit from the epidermis. Rac1N17 LCs produced as much IL1-β and TGF-β as WT LCs upon activation.

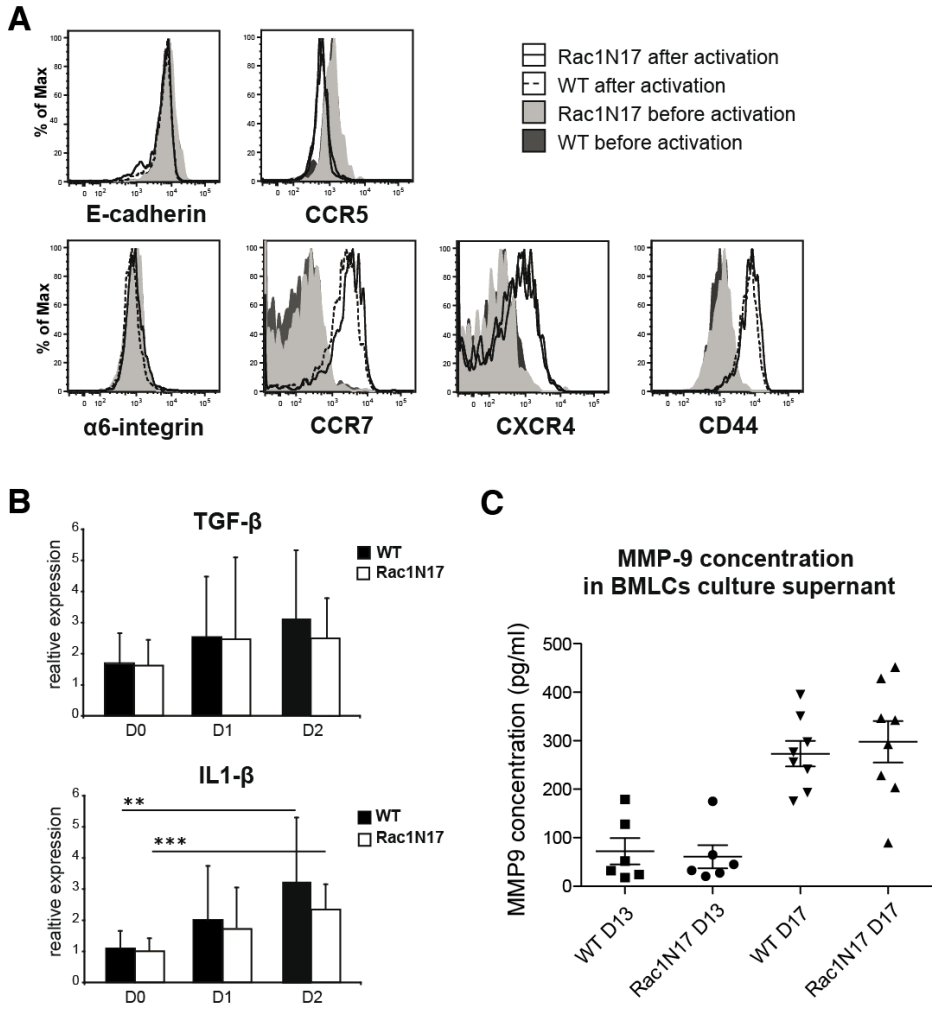

Figure 15: The molecular machinery required for Rac1N17 LC migration is normally regulated
A, Epidermal cells were activated in culture medium with GM-CSF and peptidoglycan (TLR2 ligand) for 18 hours (CCR7, CD44) or 66 hours (CXCR4, CCR5, E-cadherin, α6 integrin). These incubation times were determined after a time course experiment. Rac1N17: full line; WT: dotted line; gray filled histogram: before activation. LCs were identified as $CD45^+$ $CD11c^+$ $MHC\text{-}II^+$ $Epcam^+$ cells. **B**, Epidermal cells were activated in culture medium with GM-CSF and peptidoglycan. At the indicated time, a third of the culture was harvested (D0: before activation). mRNA was isolated and reverse transcribed. Quantitative PCR was performed for TGF-β and IL1-β. Expression levels are relative to HPRT mRNA level. **C**, Bone marrow cells were cultured and differentiated into LCs. Supernatants were harvested after 13 days (after expansion) and 17 days (after terminal differentiation) of culture. Supernatants were concentrated and total MMP-9 ELISA was performed. Data are representative of 4 independent experiments. Groups were compared by unpaired *t* test: not significant $p>0.05$; * $0.01>p>0.05$; ** $0.001>p>0.01$; *** $p<0.001$.

Matrix metalloproteinases (MMPs) are important to digest the extracellular matrix and MMP-9 was identified as one of the key MMPs required to digest the DEBM (Ratzinger et al., 2002). In the epidermis, LCs are not the only cells producing MMPs. Given the small number of LCs in mouse epidermis and the necessity to FACS-sort these cells in order to study MMP production, it would require a high amount of mice to isolate enough LCs. Therefore, we decided to generate bone marrow derived Langerhans cells (BMLCs, (Merad et al., 2000)). The cells proliferated for 13 days in a cocktail of GM-CSF, TGF-β and SCF. On day 13 of culture, they received differentiation cytokines (GM-SCF, TNF-α and IL-4) to become LC-like cells (more than 90 % of the cells at day 17 express LC

markers, data not shown). MMP-9 concentation in supernatants of day 13 (as negative control) and day 17 was determined. As shown in **Figure 15.C**, Rac1N17 BMLCs produced the same proportion of MMP-9 as WT BMLCs.

In summary, none of the molecules required for LC migration we have tested was differentially regulated in Rac1N17 LCs.

V.1.5 Role of LCs in skin immune responses

Skin dLNs of Rac1N17 mice have the following phenotype: migratory skin derived DCs and particularly LCs show an impaired migration capacity; resident DCs (related to spleen DCs, (Guilliams et al., 2010)) have uptake and cross-presentation defects. Therefore, we expected an impaired T cell priming to skin immunization.

In order to investigate the role of LCs in T cell priming, we generated bone marrow chimeras, as LCs resist irradiation (Merad et al., 2002). CD45.1 WT or CD45.2 Rac1N17 mice were irradiated and reconstituted with either CD45.1 WT or CD45.2 Rac1N17 bone marrow. Nine weeks after reconstitution, more than 97 % of LCs remained from recipient origin in both epidermis and dermis, whereas more than 96 % of dDCs were from donor origin (**Figure 16**, according to CD45 expression that is a hematopoietic cell marker).

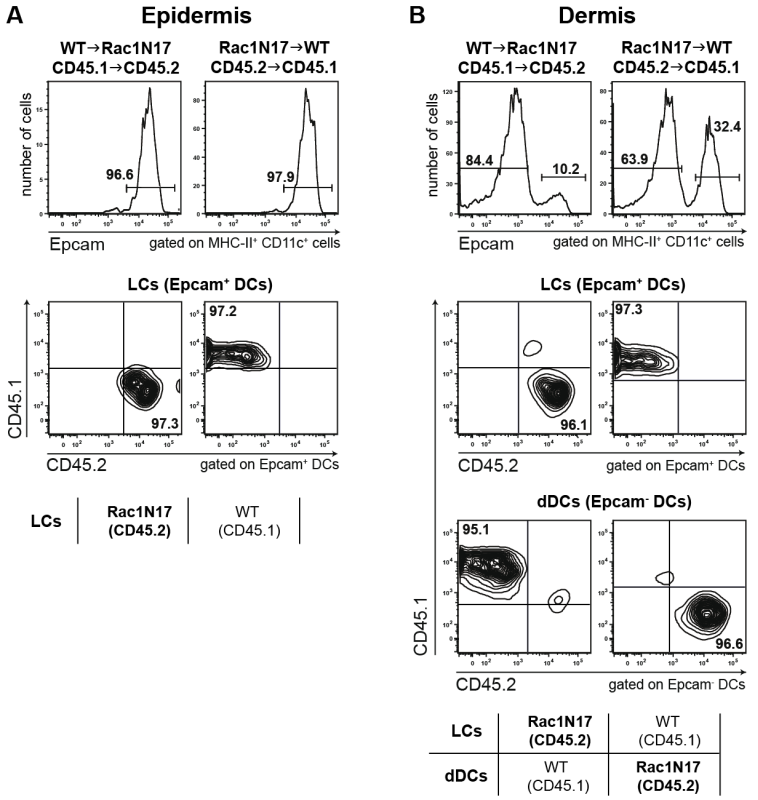

Figure 16: Skin chimerism of bone marrow chimeric mice (*Figure legend continues*)

A, Epidermis from chimeric mice (WT→Rac1N17 and Rac1N17→WT) was enzymatically digested and LCs ($CD11c^+$ $MHC\text{-}II^+$ $Epcam^+$) were analyzed for CD45 expression. **B**, Dermis from chimeric mice was enzymatically digested and DCs ($CD11c^+$ $MHC\text{-}II^+$) were identified as either LCs or dermal DCs according to Epcam expression. These cells were further analyzed for CD45 expression. Data are representative of 8 independent experiments.

The difference between the first two combinations (Rac1N17→Rac1N17 and Rac1N17→WT, **Figure 17.A**) was that LCs were WT only in the last combination, whereas in both cases all other DC subsets were Rac1N17. Eight weeks after reconstitution, mice received CFSE-labeled OT-I cells. The following day, they were immunized intradermally with 5 µg of OVA-coated polystyrene beads and 15 µl of acetone were applied on the injection site to activate DCs. Five days later, T cell proliferation was assessed by measuring CFSE dilution. In the presence of WT LCs, the $CD8^+$ T cells expanded twice more than in presence of Rac1N17 LCs (**Figure 17.A**), both in terms of cell number and proliferation. The CFSE dilution profiles of the chimeras were different, but because the proportions of non-divided cells ($CFSE^{high}$) were similar, we focus our analysis on cells that underwent more than 5 divisions (**Figure 17.A**, lower dot plots and bar graph, $CFSE^{low}$). To investigate effector functions, we examined the intracellular production of IFN-γ and TNF-α, but could not detect any differences (**Figure 17.B**).

In the reverse chimeras (WT→WT and WT→Rac1N17, **Figure 17.C**), all DC subsets were WT, with either WT LCs or migration-defective LCs. We performed the same immunization strategy as described above. The decreased number of LCs in WT→Rac1N17 sdLNs did neither significantly impair $CD8^+$ T cell priming (**Figure 17.C**) nor $CD8^+$ T cell effector functions (**Figure 17.D**).

Together, these data showed that migratory LCs contribute to $CD8^+$ T cell priming upon intradermal immunization when the other DC subsets express Rac1N17, but that this contribution does not have a significant impact when the other DCs are derived from WT bone marrow. This demonstrates a role of LCs in $CD8^+$ T cell priming. It also shows that the presence of WT dDCs is sufficient to overcome the defect of Rac1N17 LCs. So in the case of intradermally injected antigen, LCs contribute to $CD8^+$ T cell response but this contribution is undetectable when the other DC subsets are functional to take part to the response. However, even if LCs play a role in $CD8^+$ T cell priming, they do not influence the differentiation of $CD8^+$ T cells.

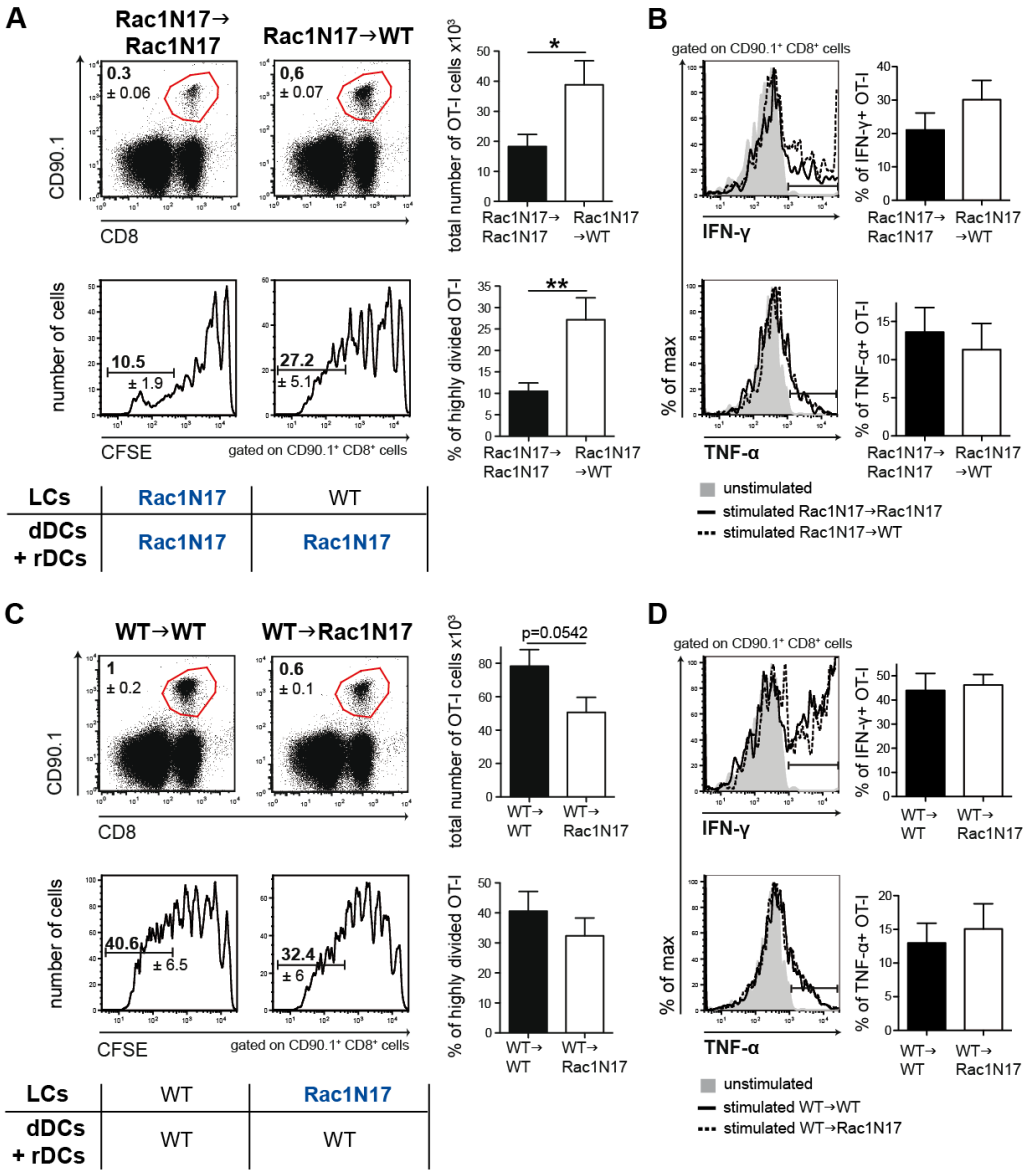

Figure 17: LCs contribute to CD8$^+$ T cell priming
A and **B**, only LCs are derived from WT bone marrow; **C** and **D**, only LCs express Rac1N17: CD45.2 Rac1N17 and CD45.1 WT mice were lethally irradiated and received either CD45.2 Rac1N17 or CD45.1 WT bone marrow. Eight weeks later, chimeric mice received 1x10^6 CFSE-labeled OT-I T cells via i.v. injection. On the next day, 5 µg of OVA-coated beads were injected i.d. on the flank and 15 µl of acetone were applied on the site of immunization. Five days later, inguinal and axillary LNs were harvested and stained. **A** and **C**, OT-I cells among the LN cells (CD90.1$^+$ CD8$^+$, *upper panels*, red gate); proliferation was assessed by CFSE dilution (*lower panels*). Statistics show absolute numbers of OT-I T cells and proportions of OT-I cells that underwent more than 5 divisions. **B** and **D** represent intracellular cytokine stainings of IFN-γ and TNF-α in OT-I cells, performed after 4 hours of *in vitro* restimulation with SIINFEKL peptide. Data are representative of 3 independent experiments; groups were compared by unpaired *t* test: not significant p>0.05; * 0.01>p>0.05; ** 0.001>p>0.01.

Next, we investigated the role of LCs in CD4$^+$ T cell priming. We generated bone marrow chimeras using the same combinations as described above. Eight weeks after reconstitution, mice received CFSE-labeled OT-II cells. The following day, they were immunized intradermally with 5 µg of OVA-coated polystyrene beads and 15 µl of acetone were applied on the injection site to activate DCs. Five days later, T cell proliferation was assessed by measuring CFSE dilution. As shown in **Figure 18.A** and **Figure 18.C**, CD4$^+$ T

cell responses in Rac1N17→Rac1N17 and WT→WT mice were similar to that observed in Rac1N17→WT and WT→Rac1N17 mice, respectively. Examination of IFN-γ and TNF-α production by $CD4^+$ T cells revealed identical effector functions in the mixed chimeras and their controls (**Figure 18.B** and **Figure 18.D**). Therefore, we concluded that in our settings LCs do not play a role in $CD4^+$ T cell priming.

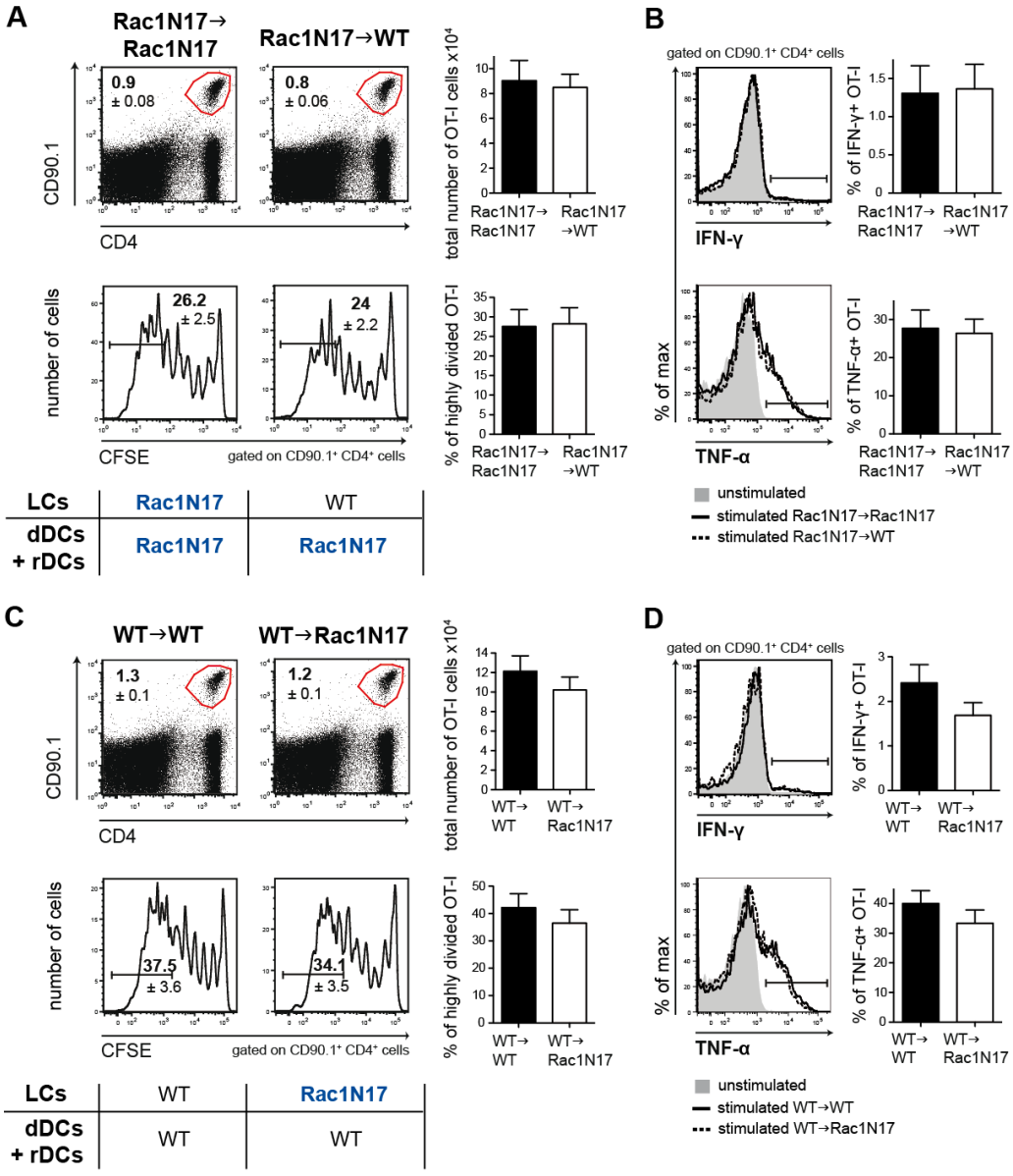

Figure 18: $CD4^+$ T cell priming is not controlled by LCs
A and **B**, only LCs are derived from WT bone marrow; **C** and **D**, only LCs express Rac1N17: CD45.2 Rac1N17 and CD45.1 WT mice were lethally irradiated and received either CD45.2 Rac1N17 or CD45.1 WT bone marrow. Eight weeks later, chimeric mice received $2x10^6$ CFSE-labeled OT-II T cells via i.v. injection. On the next day, 5 µg of OVA-coated beads were injected i.d. on the flank and 15 µl of acetone were applied on the site of immunization. Five days later, inguinal and axillary LNs were harvested and stained. **A** and **C**, OT-II cells among LN cells ($CD90.1^+$ $CD4^+$, *upper panels*, red gate); proliferation was assessed by CFSE dilution (*lower panels*). Statistics show absolute numbers of OT-II T cells and proportions of OT-II cells that underwent more than 5 divisions. **B** and **D** represent intracellular cytokine stainings of IFN-γ and TNF-α in OT-II cells, performed after 4 hours of *in vitro* restimulation with PMA and ionomycin. Data are representative of 6 independent experiments; groups were compared by unpaired *t* test: not significant $p>0.05$.

V.2 ADDITIONAL MOUSE MODELS TO STUDY THE ROLE OF Rac1 IN LC FUNCTIONS

V.2.1 Characterization of epidermis, dermis and sdLNs

The dominant negative protein Rac1N17 blocks GEFs of Rac1, but some of these GEFs are also required for the activation of other Rho-GTPases (**Figure 7**). Therefore, the phenotype of spleen and skin Rac1N17 DCs may be the result of the blockade of Rac1 pathway plus of some pathways controlled by other Rho-GTPases (Feig, 1999). In order to focus exclusively on Rac1 in LCs, we bred conditional Rac1-KO mice with mice expressing the Cre recombinase under the control of either the CD11c promotor (CD11c-Cre x Rac1-flox, abbreviated CD11c-Rac1$^{-/-}$) or the murine Langerin promotor (Langerin-Cre x Rac1-flox, abbreviated Lang-Rac1$^{-/-}$). Because we used the murine Langerin promotor in the Lang-Rac$^{-/-}$ mice, Rac1 should be deleted in both LCs and Langerin^{+} dDCs.

Mice bearing the conditional KO were compared to mice expressing the Cre recombinase only (CD11c-Rac1$^{-/-}$ and Lang-Rac1$^{-/-}$ mice were compared to CD11c-Cre and Langerin-Cre mice respectively). Because WT mice serve as control for transgenic mice, Rac1N17 mice were compared to C57BL/6 mice.

We first characterized the epidermis of these mice. As shown in **Figure 19**, LC proportions were reduced in both KO mice, which was not the case in Rac1N17 mice. It shows the requirement of Rac1 for LC homeostasis.

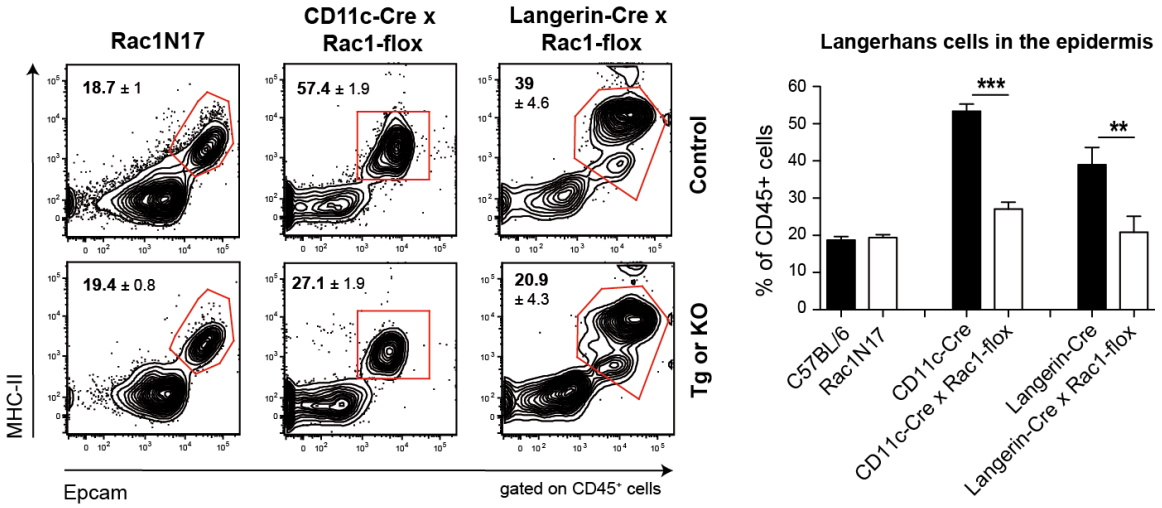

Figure 19: Characterization of CD11c-Rac$^{-/-}$ and Lang-Rac$^{-/-}$ epidermis, compared to Rac1N17 epidermis

Epidermis and dermis were separated, epidermis was further enzymatically digested and LCs were analyzed by flow cytometry (gated on CD45^{+} cells, red gate). Statistics represent proportions of LCs in the CD45^{+} population. Data are representative of 3 independent experiments; groups were compared by unpaired *t* test: not significant $p>0.05$; * $0.01>p>0.05$; ** $0.001>p>0.01$, *** $p<0.001$. Tg: transgenic Rac1N17; KO: Knockout Rac1$^{-/-}$.

Surprisingly, LCs from Rac1N17 mice and its control were present in lower amounts in the epidermis than LCs from the other strains. This suggests that the different strains have specific differences, even if they are all on the C56BL/6 background.

We then characterized the dermis of these mice. LCs were reduced in both KO strains and Rac1N17 mice (**Figure 20**, panels and upper bar graph), whereas there were no differences in Langerin$^+$ dDC proportions (**Figure 20**, panels and lower bar graph). This suggests that Rac1 is not required for Langerin$^+$ dDC homeostasis.

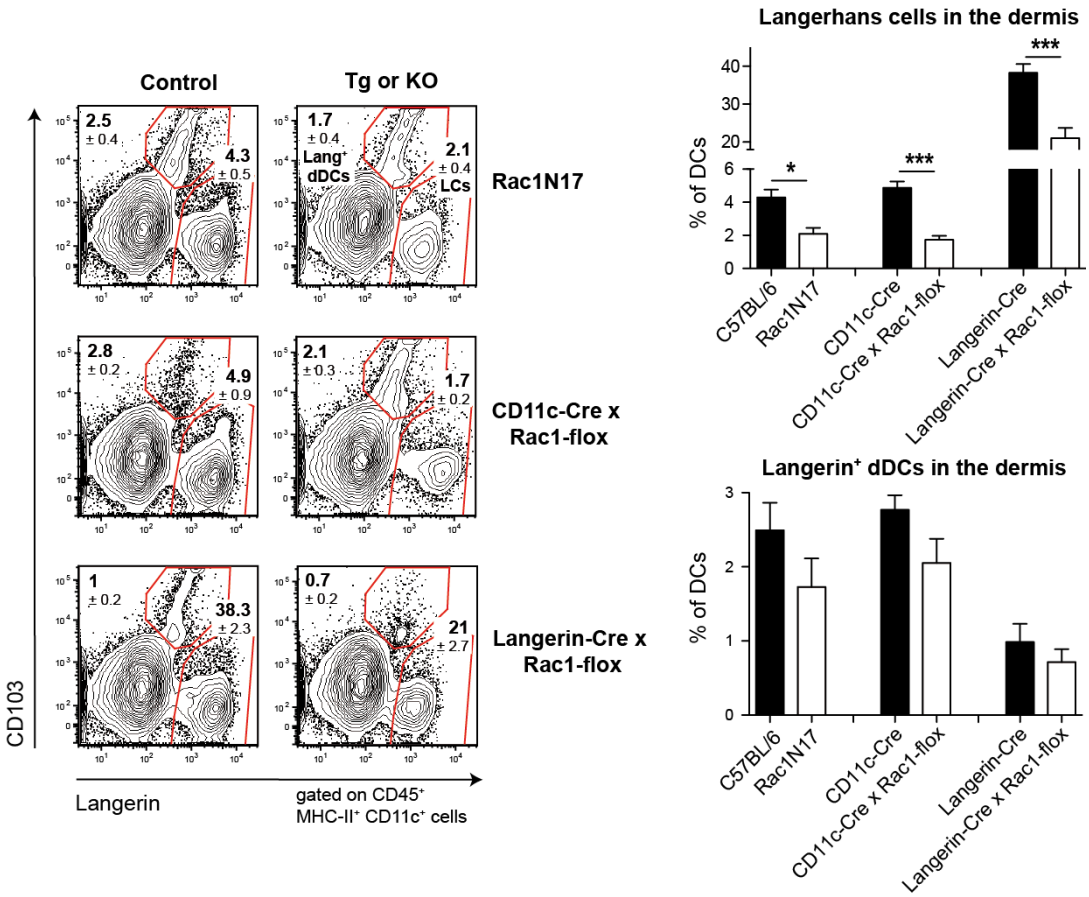

Figure 20: Characterization of CD11c-Rac$^{-/-}$ and Lang-Rac$^{-/-}$ dermis, compared to Rac1N17 dermis
Epidermis and dermis were separated, dermis was further enzymatically digested and LCs and Langerin$^+$ dDCs were analyzed by flow cytometry (gated on CD45$^+$ CD11c$^+$ MHC-II$^+$ cells, red gates). Statistics represent the frequency of LCs (*upper bar graph*) and of Langerin$^+$ dDCs (*lower bar graph*) inside the DC population. Data are representative of 3 independent experiments; groups were compared by unpaired *t* test: not significant p>0.05; * 0.01>p>0.05; ** 0.001>p>0.01, *** p<0.001. Tg: transgenic Rac1N17; KO: Knockout Rac1$^{-/-}$.

We were expecting a decrease of both, LCs and Langerin$^+$ dDCs in the sdLNs of KO mice, similar to what was observed in Rac1N17 mice (**Figure 11**). Indeed, we saw an overall 40 % decrease of migratory DCs in both KO strains and Rac1N17 mice as compared to control mice (**Figure 21**, upper panels). Within this population, KO LCs were reduced compared to controls (**Figure 21**, lower panels and upper bar graph). Langerin$^+$ dDCs from

CD11c-Rac1$^{-/-}$ and Lang-Rac1$^{-/-}$ mice were decreased compared to controls but lacked significance (**Figure 21**, lower panels and bar graphs).

Taken together, these data indicate that Rac1 is required for the homeostasis and the steady state migration of LCs but not of Langerin^{+} dDCs.

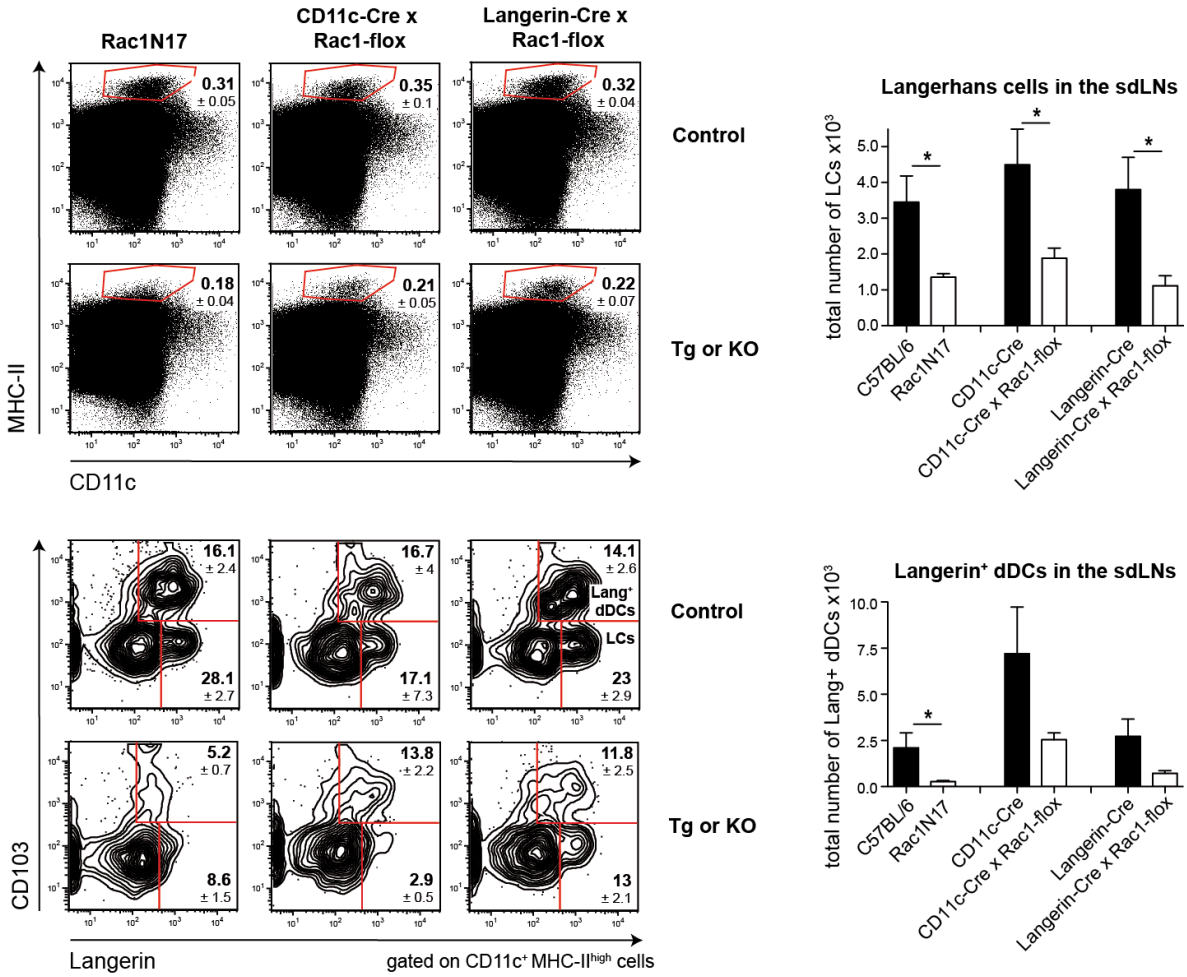

Figure 21: Characterization of CD11c-Rac$^{-/-}$ and Lang-Rac$^{-/-}$ sdLNs, compared to Rac1N17 sdLNs
Inguinal and axillary LNs were enzymatically digested. Cells were then stained and analyzed by flow cytometry. *Upper panels* represent migratory DCs (CD11c^{+} MHC-II^{high}, red gate) among total LN cells. Dermal and epidermal cells were identified in the *lower panels* according to their expression of CD103 and Langerin (red gates). Statistics represent the number of LCs and Langerin^{+} dDCs in sdLNs. Data are representative of 3 independent experiments; groups were compared by unpaired *t* test: not significant p>0.05; * 0.01>p>0.05. Tg: transgenic Rac1N17; KO: Knockout Rac1$^{-/-}$.

V.2.2 Migratory behaviour

Because analysis of steady state sdLNs of CD11c-Rac1$^{-/-}$ and Lang-Rac1$^{-/-}$ mice showed reduced LC numbers (**Figure 21**) and because we previously showed that Rac1N17 LCs have a migratory defect also in inflammatory conditions, we assumed a similar phenotype in CD11c-Rac1$^{-/-}$ and Lang-Rac1$^{-/-}$ mice.

Therefore, we first tested DC emigration from total skin with an *in vitro* crawl out assay. As expected, LCs and Langerin^{+} dDCs from both KO and Rac1N17 mice were unable to migrate out of the skin (**Figure 22**).

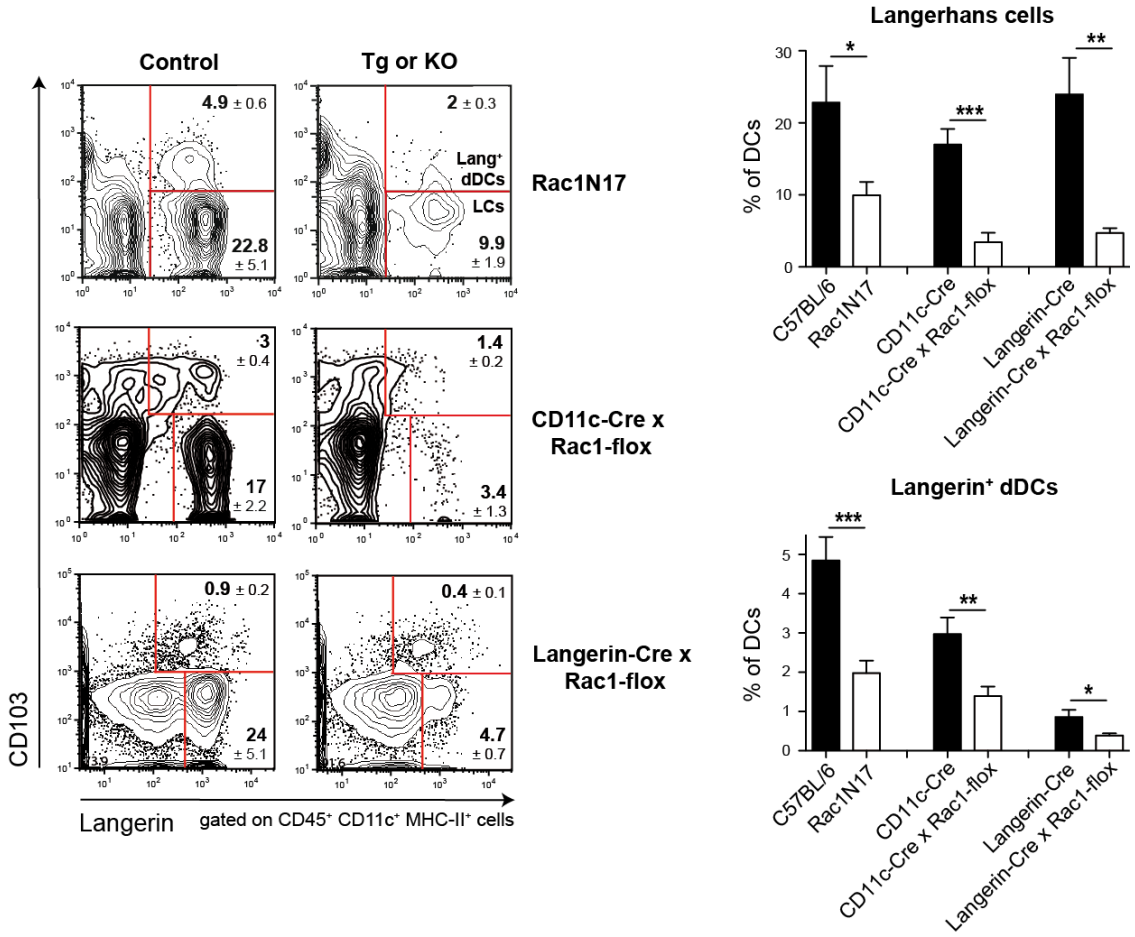

Figure 22: *In vitro* migration of CD11c-Rac$^{-/-}$ and Lang-Rac$^{-/-}$ skin DCs, compared to Rac1N17 skin DCs
Total skin explants were floated on medium in the presence of CCL21. After three days, the migrated cells were stained and analyzed by flow cytometry (gated on CD45^{+} CD11c^{+} MHC-II^{+} cells). Representative flow cytometry plots and statistics represent proportions of dermal and epidermal cells inside the DC population. Data are representative of 3 independent experiments; groups were compared by unpaired *t* test: not significant p>0.05; * 0.01>p>0.05; ** 0.001>p>0.01; *** p<0.001. Tg: transgenic Rac1N17; KO: Knockout Rac1$^{-/-}$.

Next, we investigated the *in vivo* migratory behaviour of LCs and Langerin^{+} dDCs of the KO mice by performing a FITC painting assay. Again we observed an overall decrease in the proportions of FITC^{+} MHC-II^{high} cells in all groups (**Figure 23**, upper panel). Within this FITC^{+} DC population, the numbers of migratory LCs from all mice were reduced compared to controls (**Figure 23**, lower panel and upper bar graphs). While CD11c-Rac1$^{-/-}$ Langerin^{+} dDCs numbers were also diminished, Lang-Rac1$^{-/-}$ sdLNs contained as many migratory Langerin^{+} dDCs as control sdLNs (**Figure 23**, lower panel and upper bar graphs).

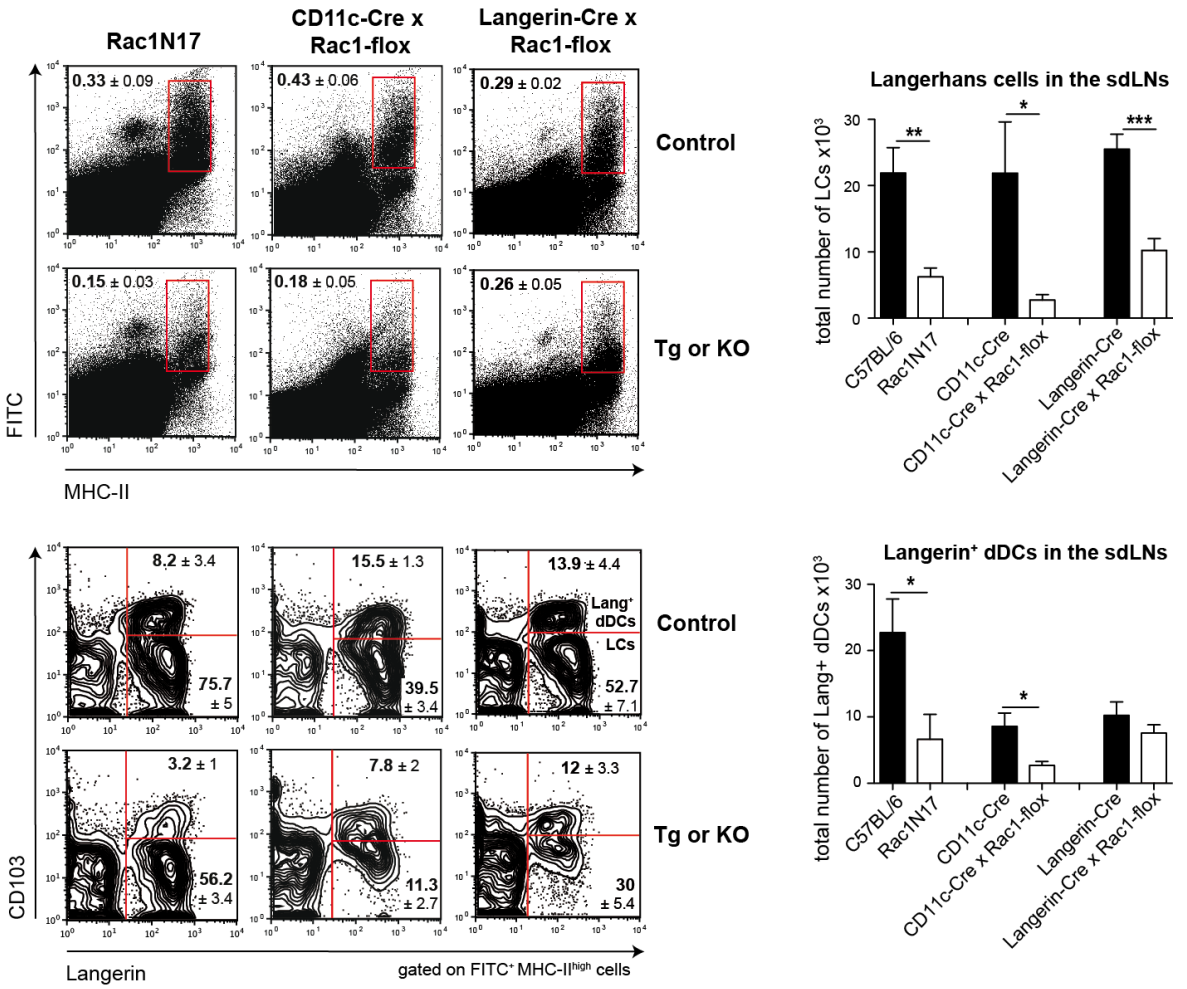

Figure 23: *In vivo* migration of CD11c-Rac$^{-/-}$ and Lang-Rac$^{-/-}$ skin DCs, compared to Rac1N17 skin DCs
A solution of 2 mg FITC in a 1:1 mix of acetone : dibutylphthalate was applied on the shaved abdomen of the mice. Four days later, the inguinal and axillary LNs were analyzed by flow cytometry. *Upper panels* represent FITC$^+$ migratory DCs (FITC$^+$ MHC-II^{high}, red gate) among total LN cells, according to unpainted controls. Dermal and epidermal cells were identified in the *lower panels* according to their expression of CD103 and Langerin. Statistics represent the number of FITC$^+$ LCs and FITC$^+$ Langerin$^+$ dDCs in sdLNs. Data are representative of 3 independent experiments; groups were compared by unpaired *t* test: not significant p>0.05; * 0.01>p>0.05; ** 0.001>p>0.01; *** p<0.001. Tg: transgenic Rac1N17; KO: Knockout Rac1$^{-/-}$.

In summary, the three different models used to study the role of Rac1 in LCs showed the same migratory defect both *in vivo* and *in vitro*. The Langerin$^+$ dDCs of the three strains, present in the dermis in similar amounts as compared to control mice, displayed an *in vivo* migration defect in CD11c-Rac1$^{-/-}$ and Rac1N17 mice, but not in Lang-Rac1$^{-/-}$ mice.

V.2.3 T cell response to skin immunization

Having detected this migration defect in Langerin$^+$ APCs, we next wanted to test the impact of migration defective LCs and Langerin$^+$ dDCs on T cell priming. CFSE-labeled OT-I cells were injected i.v. into mice. One day later, 5 µg of OVA-coated polystyrene

beads were injected intradermally and 15 µl of acetone were applied on the injection site to activate DCs. T cell proliferation was assessed by measuring CFSE dilution five days later.

As expected from previous experiments (**Figure 17**, (Kerksiek et al., 2005; Neuenhahn et al., 2006)), $CD8^+$ T cell priming was impaired in Rac1N17 mice (**Figure 24**). It can be explained by the migration defect of LCs and $Langerin^+$ dDCs, as well as by the cross-presentation defect in lymph node resident $CD8^+$ DCs (Luckashenak et al., 2008).

In CD11c-$Rac1^{-/-}$ mice, T cell proliferation was not significantly decreased, despite the migration defect of LCs and $Langerin^+$ dDCs. Therefore, Rac1 deletion affects LC and $Langerin^+$ dDC migration without decreasing skin $CD8^+$ T cell response.

Additionally, we did not detect any defect in $CD8^+$ T cell priming in Lang-$Rac1^{-/-}$ mice. Therefore, we concluded that the migration defect of Lang-$Rac1^{-/-}$ LCs is not sufficient to influence $CD8^+$ T cell response to intradermally injected particulate antigen.

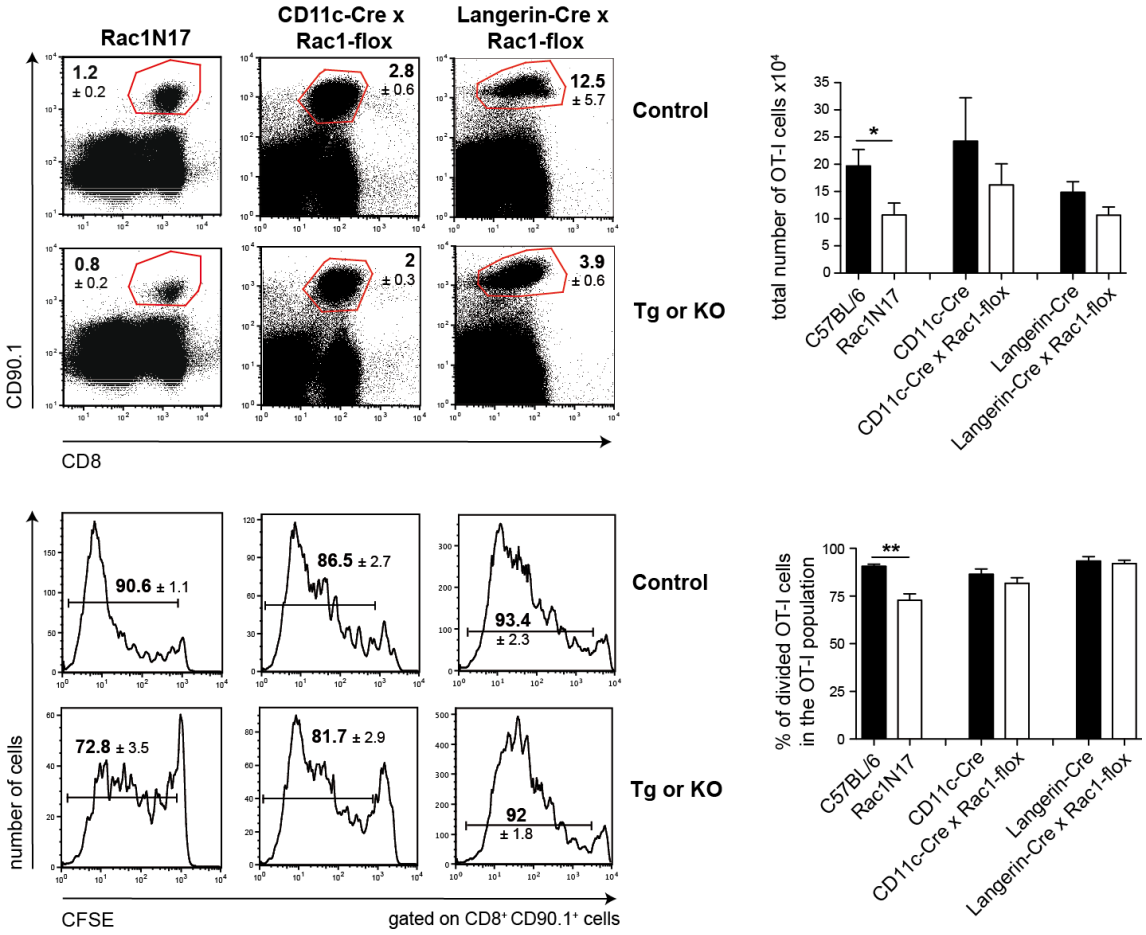

Figure 24: $CD8^+$ T cell priming in skin of CD11c-$Rac^{-/-}$ and Lang-$Rac^{-/-}$ mice, compared to Rac1N17 mice

Mice received $1x10^6$ CFSE-labeled OT-I T cells via i.v. injection. On the next day, 5 µg of pure OVA-coated beads were injected i.d. on the flank and 15 µl of acetone were applied on the site of immunization. Five days later, inguinal and axillary LNs were harvested and stained to identify OT-I cells ($CD90.1^+$ $CD8^+$, *upper panels*, red gate); proliferation was assessed by CFSE dilution (*lower panels*). Statistics represent absolute numbers of OT-I T cells and proportions of divided OT-I cells. Data are (*Figure legend continues*)

representative of 3 independent experiments; groups were compared by unpaired *t* test: not significant p>0.05; * 0.01>p>0.05; ** 0.001>p>0.01. Tg: transgenic Rac1N17; KO: Knockout Rac1$^{-/-}$.

Next, we investigated the CD4^{+} T cell priming in these mice. CFSE labeled OT-II cells were injected i.v. into mice. One day later, the same immunization procedure as explained above was followed. T cell response was assessed five days later.

In no type of mouse, we could detect defects in CD4^{+} T cells responses (**Figure 25**). For Lang-Rac1$^{-/-}$ mice, this means that LCs do not influence CD4^{+} T cells response to intradermal particulate antigen. For CD11c-Rac1$^{-/-}$ and Rac1N17 mice, this indicates that migrating LCs and Langerin^{+} dDCs as well as sdLN resident CD8^{+} DCs are not involved in the development of a CD4^{+} T cell response to intradermal immunization.

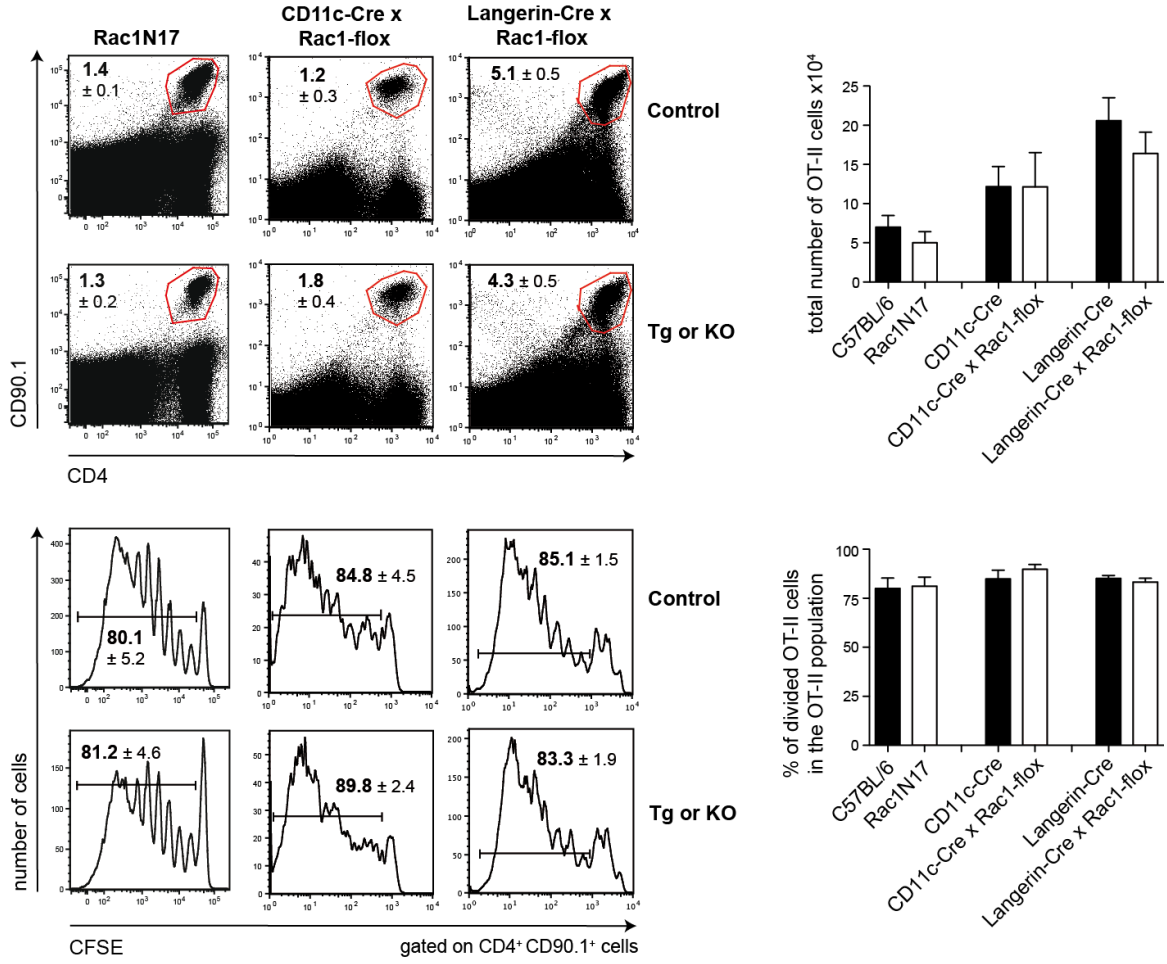

Figure 25: CD4^{+} T cell priming in skin of CD11c-Rac$^{-/-}$ and Lang-Rac$^{-/-}$ mice, compared to Rac1N17 mice

Mice received 2x10^{6} CFSE-labeled OT-II T cells via i.v. injection. On the next day, 5 µg of pure OVA-coated beads were injected i.d. on the flank and 15 µl of acetone were applied on the site of immunization. Five days later, inguinal and axillary LNs were harvested and stained to identify OT-II cells (CD90.1^{+} CD4^{+}, *upper panels*, red gate); proliferation was assessed by CFSE dilution (*lower panels*). Statistics represent absolute numbers of OT-II T cells and proportions of divided OT-II cells. Data are representative of 3 independent experiments; groups were compared by unpaired *t* test: not significant p>0.05. Tg: transgenic Rac1N17; KO: Knockout Rac1$^{-/-}$.

In brief, the homeostasis and the steady state migration of LCs but not of Langerin$^+$ dDCs requires Rac1 expression. Rac1 is also important for the migration under inflammatory conditions of both, LCs and Langerin$^+$ dDCs. In our settings, T cell responses to intradermal immunization appeared independent of LCs and Langerin$^+$ dDCs. The expression of Rac1N17 and the absence of Rac1 in CD11c$^+$ cells result in different phenotypes. Similarly, different results are obtained when different promotors are used to study the effect of Rac1 deletion in Langerin$^+$ cells.

V.3 ROLE OF Rac1, Cdc42 AND RhoA IN SPLEEN DC FUNCTIONS

V.3.1 Efficiency of the different knock-out strains

As explained before, the use of a dominant negative mutant may not be completely specific. For this reason, we decided to test which protein functions were actually inhibited in Rac1N17 spleen DCs. To achieve this, we compared the phenotype of Rac1N17 spleen DCs with the phenotype of spleen DCs deficient for Rac1, Cdc42 or RhoA (Rac1$^{-/-}$, Cdc42$^{-/-}$ and RhoA$^{-/-}$).

We first verified that the KOs were complete. Western blot analysis of spleen CD11c$^+$ cells from Rac1$^{-/-}$, RhoA$^{-/-}$ and Cdc42$^{-/-}$ mice confirm the absence of Rac1 (**Figure 26**), RhoA (data from Nancy Luckashenak) and Cdc42 (Luckashenak et al., 2013), respectively.

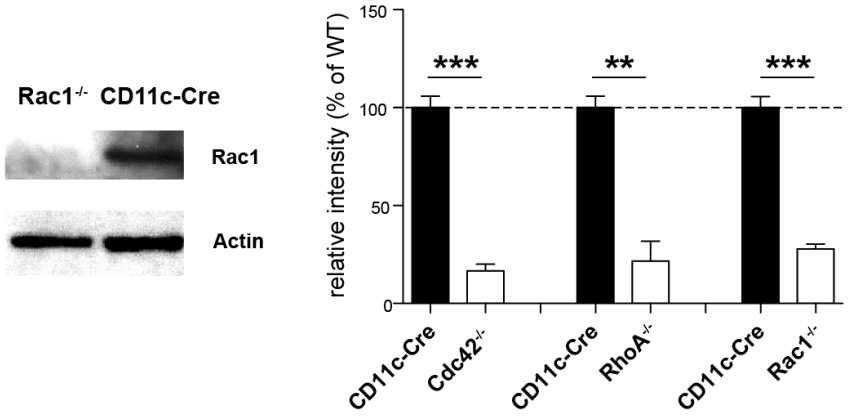

Figure 26: Expression of total Cdc42, RhoA and Rac1 proteins in the respective KO mice
CD11c$^+$ cells were isolated from spleen and lysed. Protein lysates were blotted and Rac1 quantity was measured compared to actin. Rac1 data are representative of 3 independent experiments. Western blots of Cdc42$^{-/-}$ and RhoA$^{-/-}$ spleen CD11c$^+$ cells were obtained from Nancy Luckashenak (Cdc42$^{-/-}$ data are available in (Luckashenak et al., 2013)). Groups were compared by unpaired *t* test: not significant $p>0.05$; * $0.01>p>0.05$; ** $0.001>p>0.01$; *** $p<0.001$.

V.3.2 Spleen CD8$^+$ DC population

Next, we investigated whether the KO mice have decreased CD8$^+$ spleen DCs, similarly to what was published for Rac1N17 mice (Kerksiek et al., 2005). It was indeed the case for RhoA$^{-/-}$ and Rac1$^{-/-}$ mice but not for Cdc42$^{-/-}$ mice (**Figure 27**), reflecting a role of Rac1 and RhoA in the homeostasis of CD8$^+$ spleen DCs.

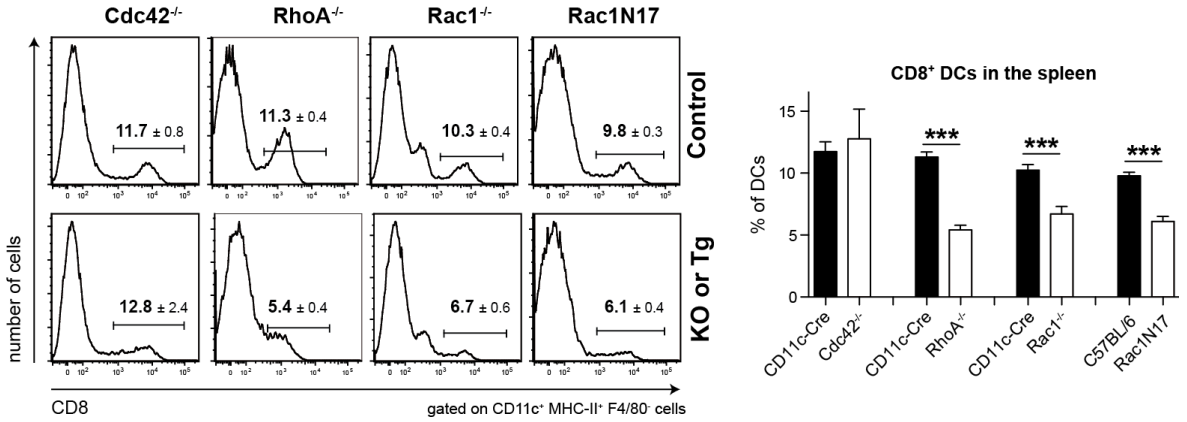

Figure 27: CD8$^+$ DCs in spleens of the three KO mice and Rac1N17 mice
Spleens were isolated, enzymatically digested and further stained for CD11c, MHC-II, F4/80 and CD8. The percentages indicated on the graphs and statistics represent the proportions of CD8$^+$ DCs in the DC population. Data are representative of 3 independent experiments; groups were compared by unpaired *t* test: not significant $p>0.05$; * $0.01>p>0.05$; ** $0.001>p>0.01$; *** $p<0.001$. Tg: transgenic Rac1N17; KO: Knockout.

V.3.3 Uptake of apoptotic material

The uptake of apoptotic material by spleen CD8$^+$ DCs was reduced in Rac1N17 mice (Kerksiek et al., 2005). It was measured by the *in vivo* uptake of CFSE-labeled B cells obtained from BALB/cJ mice, which results in MHC-I mismatch leading to opsonization and cell death. We repeated this experiment with the three KO mice. As expected, almost no uptake was detected for CD8$^-$ DCs (**Figure 28**). However, the uptake by CD8$^+$ DCs was dramatically reduced in the three KO strains, demonstrating a major role of Cdc42, RhoA and Rac1 in the uptake of apoptotic material by CD8$^+$ spleen DCs.

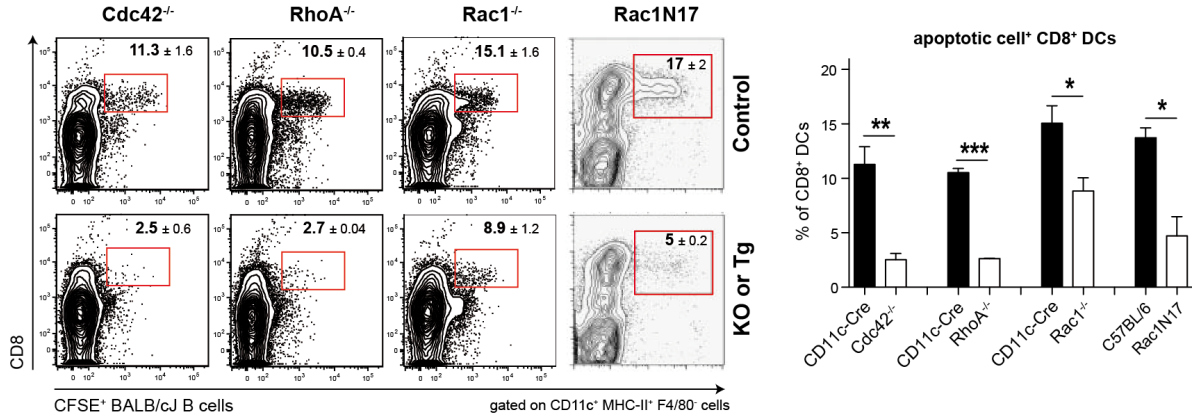

Figure 28: *In vivo* uptake of apoptotic material in the three KO mice
The three KO mice on C57BL/6 background received 10^7 CFSE-labeled B cells from BALB/cJ mice via i.v. injection. Spleens were harvested 14 hours later, enzymatically digested and stained for CD11c, MHC-II, F4/80 and CD8. The percentages indicated on the graphs and statistics represent the proportions of $CFSE^+$ $CD8^+$ DCs in the $CD8^+$ DC population. Rac1N17 dot plots were shown for comparison here again and taken from (Kerksiek et al., 2005). Data are representative of 3 independent experiments; groups were compared by unpaired *t* test: not significant $p>0.05$; * $0.01>p>0.05$; ** $0.001>p>0.01$; *** $p<0.001$. Tg: transgenic Rac1N17; KO: Knockout.

V.3.4 Uptake of soluble protein

Previously, the *in vivo* uptake of OVA by Rac1N17 $CD8^+$ DCs was shown to be impaired (Kerksiek et al., 2005). The $CD8^+$ DC population being reduced in two of the three KO mice, we decided to test the OVA-uptake capacity of these cells *in vitro*. We isolated the spleen $CD8^+$ DCs and incubated them with OVA-AF647 for 40 minutes. There was a significant decrease in the amount of OVA-AF647 taken up by the three KO and Rac1N17 $CD8^+$ DCs (around 50 % OVA^+ cells) as compared to control cells (around 70 % OVA^+ cells), indicating the importance of Cdc42, RhoA and Rac1 for the uptake of OVA (**Figure 29**).

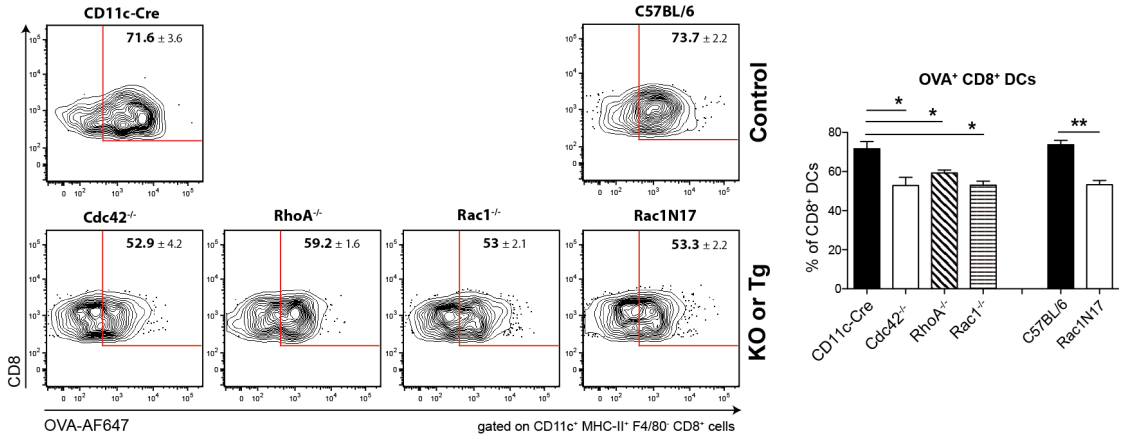

Figure 29: *In vitro* uptake of soluble Ovalbumin by $CD8^+$ DCs
Spleens were isolated, enzymatically digested and $CD8^+$ DCs were purified. Cells were incubated for 40 min at a concentration of $6x10^6$ cells/ml with 5 µg/ml of pH insensitive OVA-AF647. (*Figure legend continues*)

Cells were then intensively washed and stained for CD11c, MHC-II, F4/80 and CD8. The percentages indicated on the graphs and statistics represent the proportions of OVA^+ $CD8^+$ DCs in the $CD8^+$ DC population. Data are representative of 2 independent experiments; groups were compared by unpaired *t* test: not significant p>0.05; * 0.01>p>0.05; ** 0.001>p>0.01. Tg: transgenic Rac1N17; KO: Knockout.

V.3.5 $CD8^+$ T cell response to soluble protein

Rac1N17 spleen DCs have a cross-presentation defect *in vivo* (Kerksiek et al., 2005). To find out to which extent this phenotype was due to the absence of Rac1 activity in $CD8^+$ DCs, we tested the ability of the different KO spleen $CD8^+$ DCs to induce $CD8^+$ T cell proliferation *in vitro*. $CD8^+$ DCs were isolated, incubated with OVA for 40 minutes, washed intensively and co-cultivated with CFSE-labeled OT-I cells. Three days later, T cell proliferation was assessed by measuring CFSE dilution. As shown in **Figure 30**, the $CD8^+$ T cell responses induced by $Cdc42^{-/-}$, $RhoA^{-/-}$ and Rac1N17 $CD8^+$ DCs were reduced as compared to the proliferation induced by control $CD8^+$ DCs. We concluded that Cdc42 and RhoA play a role in the induction of $CD8^+$ T cell responses. In our settings, $Rac1^{-/-}$ $CD8^+$ DCs induced a $CD8^+$ T cell proliferation similar to the one induced by control cells. This result contrasts with what we observed for Rac1N17 $CD8^+$ DCs, demonstrating that the phenotype obtained in Rac1N17 mice regarding T cell priming was not Rac1-specific.

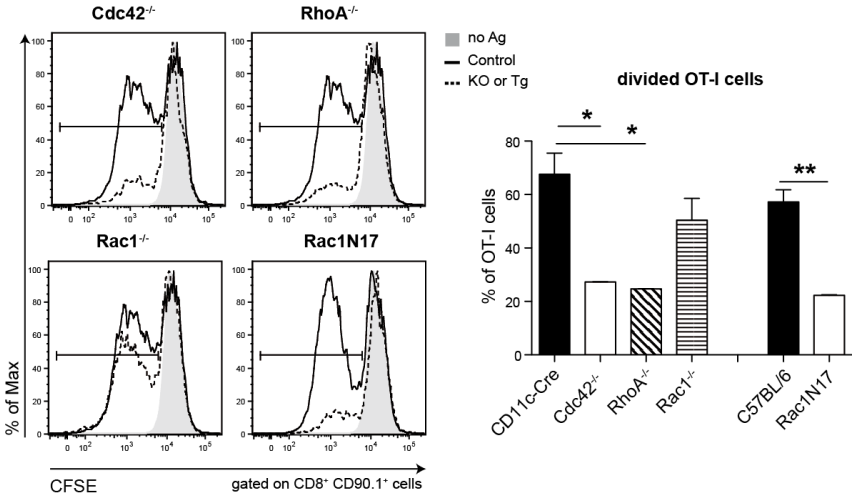

Figure 30: *In vitro* $CD8^+$ T cell response to Ovalbumin
Spleens were isolated, enzymatically digested and $CD8^+$ DCs were purified. Cells were incubated with OVA-AF647 for 40 min. Cells were then intensively washed and stained to know the amount of $CD8^+$ DCs in each sample. Then $CD8^+$ DCs were co-cultivated with CFSE-labeled OT-I cells at a 1:10 DC to T cell ratio for 3 days. The overlays represent OT-I cell proliferation. OT-I cells were identified as $CD8^+$ $CD90.1^+$. Filled line: control; dotted line: KO or Tg; gray filled histogram: no antigen control. Statistics represent the proportions of divided OT-I cells. Data are representative of 2 independent experiments; groups were compared by unpaired *t* test: not significant p>0.05; * 0.01>p>0.05; ** 0.001>p>0.01. Tg: transgenic Rac1N17; KO: Knockout.

V.3.6 CD4$^+$ T cell response to soluble protein

Next, we investigated the ability of spleen CD8$^+$ DCs to prime CD4$^+$ T cells. We used the same protocol as described for the CD8$^+$ T cell priming, expect that we used OT-II cells. The CD4$^+$ T cell responses induced by Cdc42$^{-/-}$ and RhoA$^{-/-}$ CD8$^+$ DCs were dramatically reduced compared to controls (**Figure 31**). In our settings, Rac1$^{-/-}$ and control CD8$^+$ DCs induced a similar CD4$^+$ T cell proliferation, whereas Rac1N17 CD8$^+$ DCs generated a CD4$^+$ T cell response that was decreased compared to control.

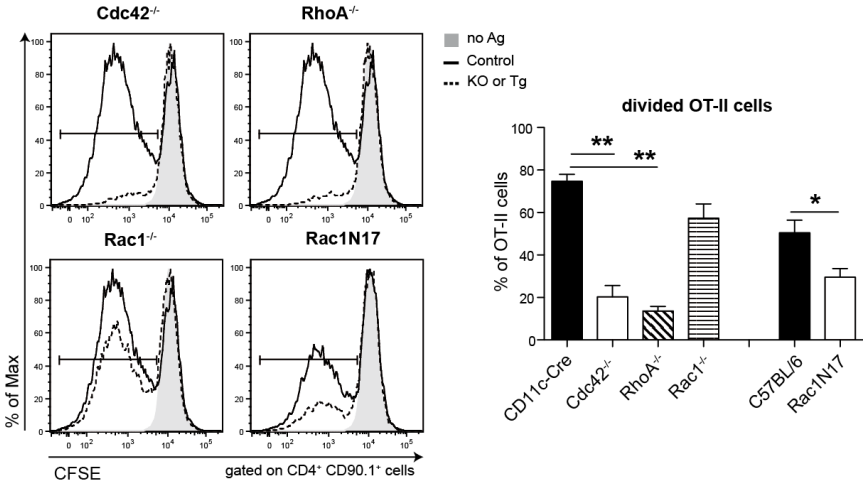

Figure 31: *In vitro* CD4$^+$ T cell response to Ovalbumin
Spleens were isolated, enzymatically digested and CD8$^+$ DCs were purified. Cells were incubated with OVA-AF647 for 40 min. Cells were then intensively washed and stained to know the amount of CD8$^+$ DCs in each sample. Then CD8$^+$ DCs were co-cultivated with CFSE-labeled OT-II cells at a 1:10 DC to T cell ratio for 4 days. The overlays represent OT-II cell proliferation. OT-II cells were identified as CD4$^+$ CD90.1$^+$. Filled line: control; dotted line: KO or Tg; gray filled histogram: no antigen control. Statistics represent the proportions of divided OT-II cells. Data are representative of 2 independent experiments; groups were compared by unpaired *t* test: not significant p>0.05; * 0.01>p>0.05; ** 0.001>p>0.01. Tg: transgenic Rac1N17; KO: Knockout.

In brief, we could demonstrate that Rac1 and RhoA but not Cdc42 Rho-GTPase functions are required for CD8$^+$ DCs homeostasis. We could show the involvement of Cdc42, RhoA and Rac1 in uptake, as well as the importance of Cdc42 and RhoA for MHC-I and MHC-II presentation of antigen by spleen CD8$^+$ DCs. However, in our settings, Rac1 was not involved in T cell responses induced by spleen CD8$^+$ DCs. Moreover, Rac1N17 and Rac1$^{-/-}$ DCs have a similar phenotype in term of antigen uptake, but they behaved differently in term of T cell priming, indicating that the phenotype obtained in Rac1N17 mice was not Rac1-specific.

VI DISCUSSION

VI.1 THE ROLE OF Rac1 IN LCs

VI.1.1 General phenotype of Rac1N17 LCs

Spleen DCs from Rac1N17 mice have an uptake defect and are not able to cross-present antigen properly (Kerksiek et al., 2005; Neuenhahn et al., 2006; Luckashenak et al., 2008; Nopora et al., 2012). However, it has been published that Rac1 has different roles in different cell types. As the DC population is composed of different subsets with specialized functions, we wanted to know if Rac1 is required for similar functions in different DC subsets, and decided to investigate the functional changes in Rac1N17 LCs.

In contrast to $CD8^+$ spleen DCs (Kerksiek et al., 2005), Rac1N17 transgene has no effect on LC homeostasis (**Figure 10**). In our settings, we could not detect any defect in either uptake or cross-presentation of soluble antigen by Rac1N17 LCs (**Figure 12**), which was unexpected regarding our knowledge on spleen DCs from the same mouse model.

Compared to WT mice, we found fewer LCs in the dermis and the sdLNs of the Rac1N17 mice, which reveals a migratory defect of LCs at the steady state (**Figure 10** and **Figure 11**). Both *in vitro* and *in vivo* migration assays under inflammatory conditions revealed a severe impairment of the migratory capacity of Rac1N17 LCs (**Figure 13**). As Rac1N17 LCs are able to mature, this result cannot be due to a disability of the LCs to sense inflammation. This was an unexpected finding, as Rac1N17 spleen DCs do not have any migratory defect (Kerksiek et al., 2005). It is possible that Rac1 is required for the mechanisms involved in the migration of LCs from epidermis to sdLNs, but not for the processes used by spleen DCs to travel from the red pulp to the white pulp.

VI.1.2 The molecular machinery required to exit the epidermis

Given the normal homeostasis of Rac1N17 LCs in the epidermis and their reduced frequency in the dermis (**Figure 10**), we were wondering if LCs could exit the epidermis. Therefore, we performed an *in vitro* migration assay from the epidermis. Here, Rac1N17 LCs leave the epidermis in comparable amounts as WT LCs (**Figure 14**). This leads us to two hypotheses. First, the molecules required for LC migration are not normally regulated. Second, Rac1N17 LCs do not reorganize their cytoskeleton properly to cross the DEBM.

LCs need different surface molecules to exit the epidermis and to pass through the DEBM. The chemokine receptors CCR7 and CXCR4 were normally up-regulated, as well as the adhesion molecule CD44 (**Figure 15.A**). CCR5, which controls DC retention in the skin, was properly down-regulated (**Figure 15.A**). However, we could not detect α6-integrin up-regulation even on control LCs (**Figure 15.A**), in contrast to previous publications on human epidermal cells (Ioffreda et al., 1993). As we are working with murine LCs, a species difference may explain the discrepancy. In 2006, Hamakawa and colleagues showed that α6-integrin level does not change upon maturation on the LC surface, with the same kind of isolation protocol we are using (Hamakawa et al., 2006). However, they have stopped their investigation after 48 hours of stimulation and have cultured the cells in medium and serum only, without inflammatory signals. We also did not detect E-cadherin down-regulation on control LCs (**Figure 15.A**). However, a clear down-regulation of E-cadherin is mainly described in human LCs in case of viral infection (papillomavirus) and during histiocytosis or allergic contact dermatitis. Only few other groups have published E-cadherin down-regulation on murine LCs upon activation, but using stimuli different from those we used (Schwarzenberger and Udey, 1996; Jakob and Udey, 1998; Puttur et al., 2010). Rac1 controls the internalization of CXCR4 (Bartolome et al., 2004; Freret et al., 2011; Ghosh et al., 2012; Zoughlami et al., 2012). Therefore, it was surprising to find CXCR4 normally regulated in Rac1N17 LCs (**Figure 15.A**). It is possible that even if the Rac1N17 transgene is expressed in Rac1N17 LCs, there is still enough endogenous Rac1 activity remaining to mediate this phenotype.

Furthermore, we examined the production of TGF-β and IL1-β by LCs (**Figure 15.B**). As expected, the inflammation-induced IL1-β mRNA was increasing over time, but to the same extent in both Rac1N17 and WT LCs. In 2007, Kaplan and colleagues have shown that the presence of TGF-β retains LCs in the epidermis (Kaplan et al., 2007). However, it is not known whether it needs to be decreased to allow LC migration. As TGF-β mRNA level was found unchanged in epidermal cells upon maturation, we conclude that the absence of TGF-β is sufficient but not necessary to induce LC emigration.

Rac1 inhibition is known to lead to decreased MMP-9 production, at least in macrophages (Skokos et al., 2011). As keratinocytes produce MMP-9 and given the small number of LCs in the epidermis, it would have required a high amount of mice to get enough LCs to measure MMP-9 concentration. Therefore, we used *in vitro* generated BMLCs to investigate the global MMP-9 production. This production was not different between Rac1N17 and WT LCs (**Figure 15.C**). It is possible that the amount of active MMP-9 is different, even if Rac1N17 LCs normally generate the global MMP-9 pool.

MMP-2 and MT1-MMP (alias MMP-14) are also able to degrade the extracellular matrix in the skin (Noirey et al., 2002; Seiki, 2002). It would be interesting to investigate the production of active MMP-9, MMP-2 and MT1-MMP by Rac1N17 LCs.

Furthermore, we used red fluorescence protein reporter Rac1N17 mice to investigate the migratory behaviour of LCs and their polarization on different DEBM components by two photons microscopy. However, this was not successful in our hands so far (data not shown). Another possibility would be to image the Rac1N17 LC cytoskeleton while the cells pass through the pores of the membrane of a Boyden chamber.

All together, it seems that the migratory defect of Rac1N17 LCs is not due to the differential regulation of any of the molecules we have tested, and we have so far no data about how the cytoskeleton is reorganized in Rac1N17 LCs during the exit of the epidermis.

VI.1.3 The role of LCs in T cell priming

As Rac1N17 LCs have a migratory defect and therefore do not arrive properly in the sdLNs, Rac1N17 mice are an excellent tool to study the functions of LCs *in vivo*. LCs are the only radioresistant hematopoietic cells in the skin and the sdLNs. We exploited this property to generate bone marrow chimeras to address the roles of LCs in skin T cell responses (**Figure 17** and **Figure 18**). To prevent soluble protein to migrate passively through the lymph to the sdLNs, we immunized the mice with antigen-coated beads. The beads were small enough to be taken up by DCs (Reis e Sousa et al., 1993; Champion et al., 2008), but remained too big to migrate to the sdLN T cell zone (Gretz et al., 2000).

In the Rac1N17→Rac1N17 chimeras, the priming of $CD8^+$ T cells was impaired compared to Rac1N17→WT control mice (**Figure 17.A**), meaning that functional LCs contribute to the $CD8^+$ T cell response induced by Rac1N17 DCs. However, even if there was a tendency to a decreased $CD8^+$ T cell response in the WT→Rac1N17 mice compared to the WT→WT mice, it was not significant (**Figure 17.C**). It is possible that in the presence of functional dDCs, the fewer numbers of Rac1N17 LCs arriving in the sdLNs do not have enough impact on the $CD8^+$ T cell response to be detected in our settings. We haven't found any contribution of LCs in the $CD4^+$ T cell proliferation or differentiation (**Figure 18**).

This study was the first to investigate the role of LCs upon intradermal immunization with particulate antigen. In 2011, mice with MHC-II KO LCs were immunized subcutaneously with peptide in complete Freund adjuvant (Shklovskaya et al., 2011). This group did not find any influence of LCs on $CD4^+$ T cell priming, which is

consistent with our findings. However, they have shown that these normally primed T cells could not form a memory pool, highlighting a regulatory role for LCs. Another group has performed gene gun immunization in mice expressing the diphtheria toxin receptor under the control of the murine Langerin promotor (Nagao et al., 2009). According to the antibody production detected two and four weeks later, they concluded that LCs promote Th2 responses. However, when studying IFN-γ production by $CD4^+$ T cells at the same time points, they could not see any effect of LCs, similarly to what we found (**Figure 18.B** and **Figure 18.D**). It would be interesting to further investigate the role of LCs for the generation of T cell memory and antibody production in the context of intradermal immunization with particulate antigen.

The implication of LCs in immune responses is tightly linked to the nature of the antigen and to the available inflammatory signals. In case of fungi, LCs bias the response to a Th17 phenotype (Igyarto et al., 2011). In GVHD, they seem not to play a role (Li et al., 2011). LCs negatively control the response to self antigen, to skin graft and to leishmaniasis among others (Romani et al., 2012). In the case of particulate dermal antigen, we showed that LCs contribute to $CD8^+$ T cell responses without affecting the $CD4^+$ T cell priming.

VI.2 DIFFERENT MOUSE MODELS TO INVESTIGATE THE ROLE OF Rac1 IN SKIN DCs

VI.2.1 Absence of Rac1 versus blockade of Rac1 GEF

The dominant negative Rac1N17 protein blocks Rac1-GEFs, preventing the activation of Rac1 and of other Rho-GTPases that require the same GEFs (**Figure 7**). To dissect which part of the transgenic Rac1N17 LC phenotype was due to the inhibition of pathways controlled by Rac1, we compared the phenotype of transgenic LCs to the phenotype of Rac1-KO LCs from CD11c-$Rac1^{-/-}$ mice.

The first discrepancy between both models was the frequency of LCs in the steady state epidermis (**Figure 19**). We found the same proportion of LCs in Rac1N17 and WT epidermis, whereas CD11c-$Rac^{-/-}$ epidermis has decreased amounts of LCs compared to its control. This shows that Rac1 pathways regulate LC homeostasis. The amounts of $Langerin^+$ dDCs in Rac1N17 and CD11c-$Rac1^{-/-}$ dermis were comparable to controls (**Figure 20**), indicating that Rac1 is not required for $Langerin^+$ dDCs homeostasis.

The migratory phenotype however, was similar in both mice: decreased LCs in the steady state dermis and sdLNs (**Figure 20** and **Figure 21**) as well as decreased migratory

capacity of LCs both *in vitro* and *in vivo* (**Figure 22** and **Figure 23**); migratory defect of Langerin$^+$ dDCs both *in vitro* and *in vivo* (**Figure 22** and **Figure 23**). Therefore, pathways controlled by Rac1 control LC and Langerin$^+$ dDC migration.

Finally, we investigated the capacity of these mice to induce T cell responses to dermal antigen. Both mouse strains showed no defect in CD4$^+$ T cell priming (**Figure 25**), meaning that Rac1 is not necessary for the CD4$^+$ T cell response to skin antigen. However, for CD8$^+$ T cell priming we get a second discrepancy: Rac1N17 mice but not CD11c-Rac1$^{-/-}$ mice had a reduced CD8$^+$ T cell proliferation after intradermal immunization (**Figure 24**). Both mice have the same migratory defect for skin DCs. However, their spleen DCs have distinct T cell priming ability. In the third part of this study, we showed that Rac1N17 but not CD11c-Rac$^{-/-}$ spleen CD8$^+$ DCs have an impaired cross-presentation capacity (**Figure 30**). The LN resident CD8$^+$ DCs are the counterparts of the spleen CD8$^+$ DCs and therefore display the same phenotype. These facts can explain the impaired cross-presentation capacity of Rac1N17 mice to skin immunization, compared to CD11c-Rac$^{-/-}$ mice. Another explanation could be that Rac1N17 dDCs also have a T cell priming defect but not the CD11c-Rac$^{-/-}$ dDCs. Addressing the T cell priming capacity of Rac1N17 and CD11c-Rac$^{-/-}$ dDCs would be interesting.

All together, we showed that Rac1 is required for LC homeostasis and for the migration of LCs and Langerin$^+$ dDCs. Regarding T cell priming, Rac1 expression is not required for CD4$^+$ or CD8$^+$ T cell proliferation. The comparison of the KO model with the DN model revealed that the phenotypes can be different, highlighting the advantages to work with a specific deletion of the protein of interest.

VI.2.2 CD11c versus Langerin promotor

To examine the role of Rac1 in LCs and Langerin$^+$ DCs more closely, we used mouse-Lang-Rac1$^{-/-}$ mice, which lacks Rac1 protein in LCs and CD103$^+$ Langerin$^+$ dDCs.

We expected the same phenotype as in CD11c-Rac$^{-/-}$ mice. Indeed, we found the same decreased amounts of LC in epidermis, dermis and sdLNs, as well as the same normal proportion of Langerin$^+$ dDCs in dermis and sdLNs (**Figure 19**, **Figure 20** and **Figure 21**).

Similar to CD11c-Rac$^{-/-}$ LCs, the migratory defect of Lang-Rac1$^{-/-}$ LCs was present in both mice *in vitro* and *in vivo* (**Figure 22** and **Figure 23**). However, even if Lang-Rac1$^{-/-}$ Langerin$^+$ dDCs showed reduced capacity to migrate *in vitro*, they were able to migrate *in vivo*. In the *in vivo* assay, the skin is exposed to inflammation, whereas in the *in vitro* assay

the cells are exposed only to chemokine signal. It is possible that the inflammatory signals produced *in vivo* overcome the chemotaxis defect of Lang-Rac1$^{-/-}$ Langerin^{+} dDCs.

The use of the Langerin promotor to control Rac1 deletion in Langerin^{+} dDCs did not lead to a migration defect *in vivo*, in contrast to what we observed for CD11c-Rac$^{-/-}$ Langerin^{+} dDCs. Whereas LCs are long lived cells and Langerin remains expressed long enough to get a complete deletion of Rac1 in these cells, the life span of Langerin^{+} dDCs and the moment they begin to express Langerin remain unknown. The life span of dermal DCs is about 10 and 13 days, (Kamath et al., 2002; Iijima et al., 2007), but the particular case of Langerin^{+} dDCs was never investigated. Whereas CD11c is already expressed on DC precursors (Naik et al., 2006), the moment Langerin begins to be expressed is not known. A late expression of Langerin would lead to a late disappearance of Rac1 protein in Lang-Rac1$^{-/-}$ Langerin^{+} dDCs. In this case, by the time Lang-Rac1$^{-/-}$ Langerin^{+} dDCs migrate, remaining Rac1 protein would still not be completely degraded, resulting in the absence of phenotype. Moreover, in almost all the different stainings we showed, the Langerin^{+} dDCs had a lower expression of Langerin compared to LCs. Therefore, it is possible that the KO of Rac1 under the control of the Langerin promotor is less complete in Langerin^{+} dDCs than in LCs. Because there are very few LCs and Langerin^{+} dDCs in epidermis and dermis respectively, and because western blot and mRNA quantification require a significant amount of cells, we did not investigate whether Rac1 was absent in Lang-Rac1$^{-/-}$ and CD11c-Rac$^{-/-}$ LCs and Langerin^{+} dDCs. The previous hypotheses could explain the difference observed between Lang-Rac1$^{-/-}$ and CD11c-Rac$^{-/-}$ Langerin^{+} dDCs.

The priming of CD4^{+} and CD8^{+} T cells in Lang-Rac1$^{-/-}$ mice immunized intradermally with particulate antigen was as strong as the priming in control mice (**Figure 25** and **Figure 24**). These mice only have a defect in the migration capacity of LCs, exactly as the bone marrow chimeras generated in the first part of this study. Therefore, obtaining the same results in Lang-Rac1$^{-/-}$ mice as in the WT→Rac1N17 chimeras (**Figure 17.C** and **Figure 18.C**) was expected.

In brief, we showed that Rac1 controls LCs homeostasis as well as LC and Langerin^{+} dDC migration, but not CD8^{+} or CD4^{+} T cell responses to dermal antigen. The blockade of Rac1 GEFs in all the DCs (Rac1N17 mice) but not Rac1 absence (CD11c-Rac1$^{-/-}$ mice) influences the CD8^{+} T cell priming, whereas none of them play a role in CD4^{+} T cell response. Consequently, the use of a DN protein is never as specific as the use of a KO to investigate the role of a particular protein. The additional defects observed in the Rac1N17 mouse are possibly caused by the inhibition of other Rho-GTPases such as Cdc42

or RhoA. Finally, the Langerin promotor may not be the most appropriate promotor to investigate the role of a protein in Langerin$^+$ DCs.

VI.3 ROLE OF Cdc42, RhoA AND Rac1 IN SPLEEN DC FUNCTIONS

VI.3.1 Cdc42, RhoA and Rac1 in spleen DC homeostasis

We compared spleen DCs specifically depleted of Rac1, Cdc42 or RhoA with Rac1N17 spleen DCs, to investigate which Rho-GTPase functions are actually inhibited in Rac1N17 spleen DCs.

In Rac1N17 mice, there is a decrease in CD8$^+$ spleen DC numbers (Kerksiek et al., 2005). A similar reduction could be found in CD11c-Rac1$^{-/-}$ and CD11c-RhoA$^{-/-}$ but not in CD11c-Cdc42$^{-/-}$ mice (**Figure 27**). We conclude that in contrast to Cdc42, Rac1 and RhoA are involved in the homeostasis of CD8$^+$ DCs.

VI.3.2 Roles of Cdc42, RhoA and Rac1 in the control of endocytosis by spleen CD8$^+$ DCs

Next, we have investigated the endocytic capacities of spleen CD8$^+$ DCs from the three KO strains.

We found that the three Rho-GTPases were indispensable to take up dying cells, as this ability was impaired in every mouse strain (**Figure 28**). However, this impairment was less pronounced in the CD11c-Rac1$^{-/-}$ than in the Rac1N17 mice, maybe reflecting the combined block of several Rho-GTPase pathways in the Rac1N17 spleen DCs. Except for the Rac1 *in vivo* data from Kerksiek and colleagues in 2005, nothing is known about the involvement of these different Rho-GTPases in the uptake of apoptotic cells by DCs. In the literature, there are only *in vitro* macrophages data available, performed with DN or CA mutants, showing that Rac1 and Cdc42 are required for the uptake of opsonized cells (Hoppe and Swanson, 2004; Nakaya et al., 2006), whereas RhoA negatively regulates the uptake of apoptotic cells (Leverrier and Ridley, 2001; Nakaya et al., 2006). The cell type difference and the use of DN and CA mutants could explain the discrepancy in RhoA requirement.

Next, we tested whether Rac1, Cdc42 and RhoA were also required for the uptake of soluble protein by spleen CD8$^+$ DCs such as OVA, our model antigen. Cdc42$^{-/-}$, Rac1$^{-/-}$ and

RhoA$^{-/-}$ CD8^{+} DCs have a reduced uptake capacity compared to the control cells (**Figure 29**). Even if from previous studies with DN mutants (West et al., 2000; Shurin et al., 2005; Tourkova et al., 2007), it was expected for Rac1$^{-/-}$ and Cdc42$^{-/-}$ cells, this finding was surprising for RhoA$^{-/-}$ DCs. It was assessed once by drug treatment that RhoA is not required for receptor-mediated uptake of FITC-dextran by DCs derived from splenocytes cultivated for 14 days (West et al., 2000). As these splenocytes were cultivated in the presence of GM-SCF and TGF-β, they do not resemble the CD8^{+} spleen DCs.

Taken together, Rac1, Cdc42 and RhoA proteins are required for the uptake of apoptotic cells and soluble OVA by spleen DCs.

VI.3.3 Control of T cell priming by Cdc42$^{-/-}$, RhoA$^{-/-}$ and Rac1$^{-/-}$ spleen CD8^{+} DCs

In the spleen, CD8^{+} DCs can present antigens to both CD4^{+} and CD8^{+} T cells but they are specialized in cross-presentation. It was published that Rac1N17 mice have a cross-presentation defect (Kerksiek et al., 2005; Neuenhahn et al., 2006; Nopora et al., 2012) but normal CD4^{+} T cell priming capacity (Luckashenak et al., 2008).

Addressing these functions in the KO mice revealed that Cdc42$^{-/-}$ and RhoA$^{-/-}$ spleen CD8^{+} DCs induced reduced *in vitro* proliferation of both CD8^{+} and CD4^{+} T cells compared to control mice (**Figure 30** and **Figure 31**). This demonstrates the role of Cdc42 and RhoA in CD8^{+} and CD4^{+} T cell priming. Shurin and colleagues have shown that BMDCs transfected with RhoA or Cdc42 CA mutants both induced an increased CD4^{+} T cell response to OVA (Shurin et al., 2005), which is in accordance with our results. Cdc42 was shown to be involved in the polarization of MTOC at the immunological synapse with CD8^{+} T cells (Pulecio et al., 2010). This polarization is essential for IL12 production at the immunological synapse as well as for the proper activation of CD8^{+} T cells. Therefore, similar to us, they found a decreased CD8^{+} T cell response in the absence of Cdc42. Our study with Cdc42$^{-/-}$ and RhoA$^{-/-}$ spleen CD8^{+} DCs also provides a direct proof of the role of Cdc42 and RhoA in CD4^{+} T cell priming and cross-presentation.

Rac1$^{-/-}$ spleen CD8^{+} DCs induced the same *in vitro* proliferation of CD4^{+} and CD8^{+} T cells as control cells (**Figure 30** and **Figure 31**), suggesting that Rac1 is neither involved in cross-presentation nor CD4^{+} T cell priming. To the contrary, Rac1N17 CD8^{+} DCs induced reduced CD4^{+} and CD8^{+} T cell proliferation (**Figure 30** and **Figure 31**). The two studies investigating the role of Rac1 in cross-presentation used a dominant negative form

of Rac1 (Jaksits et al., 2004; Kerksiek et al., 2005). Therefore, there is no direct data in the literature to discuss the differences between the cross-presentation capacities of $Rac1^{-/-}$ and Rac1N17 $CD8^+$ DCs. Benvenuti and colleagues have demonstrated that a single KO of Rac1 or Rac2 was insufficient to get a decreased $CD4^+$ T cell priming in response to peptide presentation (Benvenuti et al., 2004). Solely the cumulative KO of both Rac1 and Rac2 was resulting in reduced $CD4^+$ T cell response. It is most likely that the GEFs activating Rac1 are the same as the ones activating Rac2, which would lead to a cumulative inhibition of endogenous Rac1 and Rac2 activities in Rac1N17 cells. It could explain the discrepancy between the $CD4^+$ T cell priming and the cross-presentation capacities of $Rac1^{-/-}$ and Rac1N17 $CD8^+$ DCs. It was intriguing that $Rac1^{-/-}$ $CD8^+$ DCs perform reduced antigen uptake but normal T cell priming. It is possible that peptide generation for cross-presentation and MHC-II presentation is better in absence of Rac1. One should also investigate whether peptide presentation itself is increased in $Rac1^{-/-}$ $CD8^+$ DCs.

In brief, spleen $CD8^+$ DC homeostasis is controlled by RhoA and Rac1; Cdc42, RhoA and Rac1 are involved in the uptake of apoptotic cells and soluble protein; and RhoA and Cdc42 are essential for both $CD8^+$ and $CD4^+$ T cell priming whereas Rac1 is not. Finally, the phenotype of Rac1N17 mice does not reflect Rac1 inhibition only.

VII CONCLUSION

This project investigates the role of Rho-GTPases in LC and spleen DC functions by the use of different mouse models.

We first hypothesized that the Rho-GTPase Rac1 could be required for different functions in different DC subsets. Our investigation of Rac1N17 LC functions confirms this hypothesis. Rac1N17 LCs mature, take up antigen and present it to $CD8^+$ and $CD4^+$ T cells normally. However, their migratory capacity is impaired. The examined molecules required for migration were normally regulated. It is possible that this migration defect is due to a more general problem in the cytoskeleton coordination. Using these mice with migration defective LCs, we generated bone marrow chimeras to investigate the role of LCs in skin T cell response. It appears that LCs contribute to $CD8^+$ T cell response to particulate dermal antigen, without affecting T cell differentiation. However, LCs play no role in the $CD4^+$ T cell response in the same settings.

Second, we examine skin DCs from Rac1N17, CD11c-$Rac^{-/-}$ and Lang-$Rac1^{-/-}$ mice to determine which mouse model would be the most appropriate for the study of Rac1 functions in LCs and $Langerin^+$ dDCs. This study showed that Rac1 is implicated in the homeostasis of LCs but not of $Langerin^+$ dDCs. LCs and $Langerin^+$ dDCs display a migration defect, highlighting a crucial role of Rac1 in this process. The CD11c-$Rac^{-/-}$ mouse phenotype indicates that Rac1 is dispensable for T cell responses against dermal antigens, in contrast to Rac1N17 mice. The comparison of CD11c-$Rac^{-/-}$ to Lang-$Rac1^{-/-}$ mice revealed that the Langerin promotor might not be ideal to investigate the role of a protein in $Langerin^+$ dDCs.

Finally, we examined whether only the Rac1 pathway was inhibited in Rac1N17 spleen DCs. To do so, we compared Rac1N17 spleen $CD8^+$ DCs with CD11c-$Rac1^{-/-}$, CD11c-$Cdc42^{-/-}$ and CD11c-$RhoA^{-/-}$ spleen $CD8^+$ DCs. Rac1 and RhoA but not Cdc42 are required for $CD8^+$ spleen DC homeostasis. The three Rho-GTPases control the phagocytosis of apoptotic cells and the uptake of soluble protein by spleen $CD8^+$ DCs, which was surprising for RhoA. The resulting $CD4^+$ and $CD8^+$ T cell responses were dramatically impaired when induced by Cdc42 and RhoA spleen $CD8^+$ DCs. For the first time a direct proof of RhoA involvement in T cell priming by DCs is provided. The normal T cell responses induced by CD11c-$Rac1^{-/-}$ $CD8^+$ DCs were unexpected and argue for the fact that Rac1 is not required for cross-presentation and that the phenotype observed in Rac1N17 mice is not due to Rac1 inhibition only.

In brief, we provided evidences that the Rac1N17 model is not entirely specific for Rac1. We could show the involvement of Rac1 in LC homeostasis and migration, as well as its role in the uptake of apoptotic cells and soluble antigen by spleen DCs. Surprisingly Rac1 is not implicated in cross-presentation. We demonstrated the indispensable role of Cdc42 and RhoA in spleen $CD8^+$ DCs for both antigen uptake and T cell priming. Finally, we showed that LCs contribute to $CD8^+$ T cell response to dermal antigen.

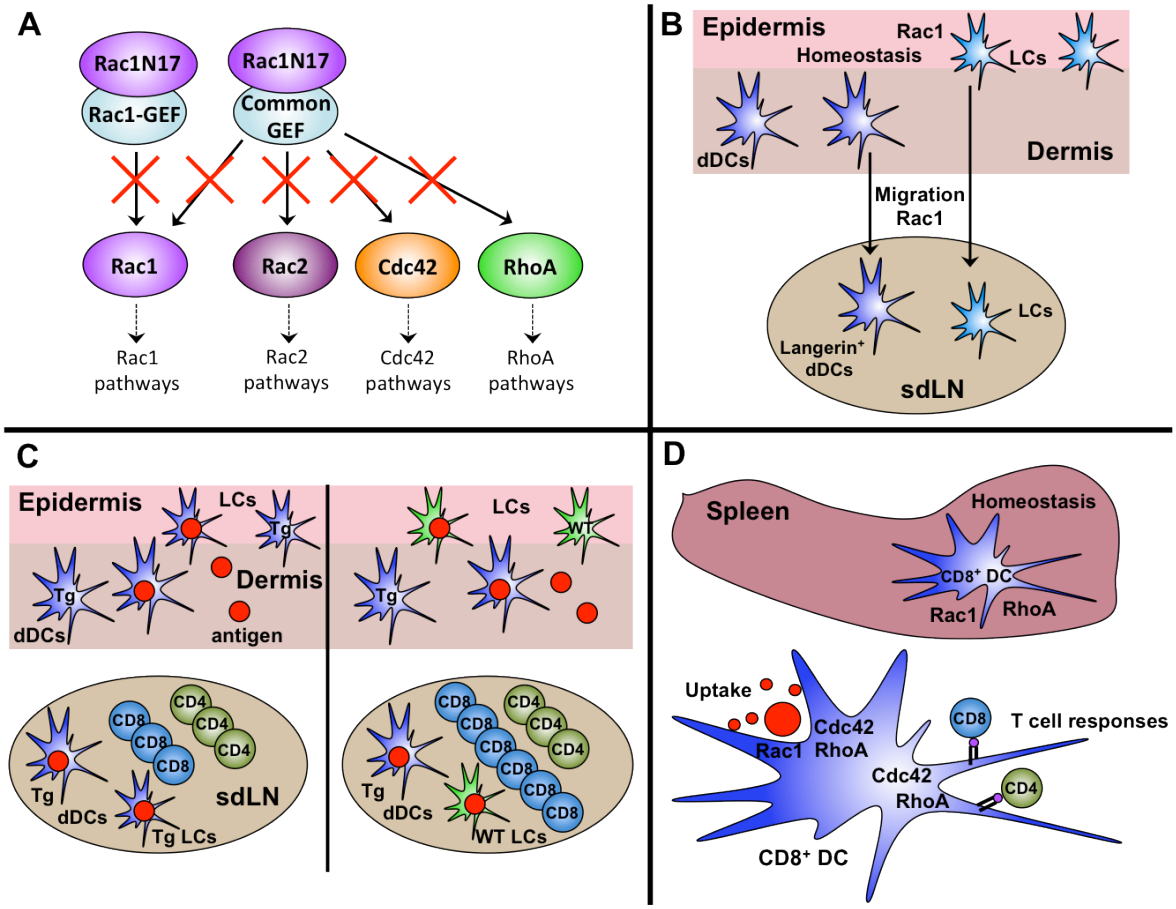

Graphical abstract

A: The Rac1N17 model is not specific for Rac1. The dominant negative Rac1N17 protein remains bound to GEFs able to activate Rac1. These GEFs are Rac1-specific only or activate other Rho-GTPases such as Rac2, Cdc42 or RhoA. Therefore, Rac1N17 phenotype is the result of the blockade of several Rho-GTPases. **B**: Rac1 functions in Langerin$^+$ skin DCs. Rac1 is implicated in the homeostasis of LCs but not of Langerin$^+$ dDCs. The migration capacity of both LCs and Langerin$^+$ dDCs requires Rac1 activity. **C**: LCs contribute to $CD8^+$ T cell responses to dermal antigens. Rac1N17 DCs induce $CD4^+$ and $CD8^+$ T cell priming (left, purple cells), but the presence of functional LCs (right, green cells) leads to increased $CD8^+$ T cell proliferation (as shown in bone marrow chimeras). Tg: transgenic Rac1N17; WT: control; sdLN: skin draining lymph node. **D**: The role of Rac1, Cdc42 and RhoA in spleen $CD8^+$ DCs. Rac1 and RhoA are required for proper $CD8^+$ DC homeostasis. Rac1, Cdc42 and RhoA control the uptake of both soluble protein and dying cells by spleen $CD8^+$ DCs. The $CD8^+$ and $CD4^+$ T cell priming by spleen $CD8^+$ DCs is dependent on Cdc42 and RhoA but not on Rac1.

VIII REFERENCES

Alberts, A.S., and R. Treisman. 1998. **Activation of RhoA and SAPK/JNK signalling pathways by the RhoA-specific exchange factor mNET1**. *Embo J* 17:4075-85.

Alvarez, D., E.H. Vollmann, and U.H. von Andrian. 2008. **Mechanisms and consequences of dendritic cell migration**. *Immunity* 29:325-42.

Ansel, J., P. Perry, J. Brown, D. Damm, T. Phan, C. Hart, T. Luger, and S. Hefeneider. 1990. **Cytokine modulation of keratinocyte cytokines**. *J Invest Dermatol* 94:101S-07S.

Arthur, W.T., S.M. Ellerbroek, C.J. Der, K. Burridge, and K. Wennerberg. 2002. **XPLN, a guanine nucleotide exchange factor for RhoA and RhoB, but not RhoC**. *J Biol Chem* 277:42964-72.

Balamatsias, D., A.M. Kong, J.E. Waters, A. Sriratana, R. Gurung, C.G. Bailey, J.E. Rasko, T. Tiganis, S.L. Macaulay, and C.A. Mitchell. 2011. **Identification of P-Rex1 as a novel Rac1-guanine nucleotide exchange factor (GEF) that promotes actin remodeling and GLUT4 protein trafficking in adipocytes**. *J Biol Chem* 286:43229-40.

Bartolome, R.A., B.G. Galvez, N. Longo, F. Baleux, G.N. Van Muijen, P. Sanchez-Mateos, A.G. Arroyo, and J. Teixido. 2004. **Stromal cell-derived factor-1alpha promotes melanoma cell invasion across basement membranes involving stimulation of membrane-type 1 matrix metalloproteinase and Rho GTPase activities**. *Cancer Res* 64:2534-43.

Bedoui, S., S. Prato, J. Mintern, T. Gebhardt, Y. Zhan, A.M. Lew, W.R. Heath, J.A. Villadangos, and E. Segura. 2009. **Characterization of an immediate splenic precursor of CD8+ dendritic cells capable of inducing antiviral T cell responses**. *J Immunol* 182:4200-7.

Behrens, D.T., D. Villone, M. Koch, G. Brunner, L. Sorokin, H. Robenek, L. Bruckner-Tuderman, P. Bruckner, and U. Hansen. 2012. **The epidermal basement membrane is a composite of separate laminin- or collagen IV-containing networks connected by aggregated perlecan, but not by nidogens**. *J Biol Chem* 287:18700-9.

Bellanger, J.M., S. Estrach, S. Schmidt, A. Briancon-Marjollet, O. Zugasti, S. Fromont, and A. Debant. 2003. **Different regulation of the Trio Dbl-Homology domains by their associated PH domains**. *Biol Cell* 95:625-34.

Benninger, Y., T. Thurnherr, J.A. Pereira, S. Krause, X. Wu, A. Chrostek-Grashoff, D. Herzog, K.A. Nave, R.J. Franklin, D. Meijer, C. Brakebusch, U. Suter, and J.B. Relvas. 2007. **Essential and distinct roles for cdc42 and rac1 in the regulation of Schwann cell biology during peripheral nervous system development**. *J Cell Biol* 177:1051-61.

Benvenuti, F., S. Hugues, M. Walmsley, S. Ruf, L. Fetler, M. Popoff, V.L. Tybulewicz, and S. Amigorena. 2004. **Requirement of Rac1 and Rac2 expression by mature dendritic cells for T cell priming**. *Science* 305:1150-3.

Bi, Y., and R. Yang. 2012. **Direct and indirect regulatory mechanisms in TH17 cell differentiation and functions**. *Scand J Immunol* 75:543-52.

Birbeck, M.S., A.S. Breathnach, and J.D. Everall. 1961. **An electron microscope study of basal melanocytes and high-Level clear cells (Langerhans cells) in Vitiligo.** *journal of investigative dermatology* 37:

Bos, J.L., H. Rehmann, and A. Wittinghofer. 2007. **GEFs and GAPs: critical elements in the control of small G proteins**. *Cell* 129:865-77.

Boulter, E., R. Garcia-Mata, C. Guilluy, A. Dubash, G. Rossi, P.J. Brennwald, and K. Burridge. 2010. **Regulation of Rho GTPase crosstalk, degradation and activity by RhoGDI1**. *Nat Cell Biol* 12:477-83.

Brewig, N., A. Kissenpfennig, B. Malissen, A. Veit, T. Bickert, B. Fleischer, S. Mostbock, and U. Ritter. 2009. **Priming of CD8+ and CD4+ T cells in experimental leishmaniasis is initiated by different dendritic cell subtypes**. *J Immunol* 182:774-83.

Bristow, J.M., M.H. Sellers, D. Majumdar, B. Anderson, L. Hu, and D.J. Webb. 2009. **The Rho-family GEF Asef2 activates Rac to modulate adhesion and actin dynamics and thereby regulate cell migration**. *J Cell Sci* 122:4535-46.

Brugnera, E., L. Haney, C. Grimsley, M. Lu, S.F. Walk, A.C. Tosello-Trampont, I.G. Macara, H. Madhani, G.R. Fink, and K.S. Ravichandran. 2002. **Unconventional Rac-GEF activity is mediated through the Dock180-ELMO complex**. *Nat Cell Biol* 4:574-82.

Buchsbaum, R.J. 2007. **Rho activation at a glance**. *J Cell Sci* 120:1149-52.

Burgeson, R.E., and A.M. Christiano. 1997. **The dermal-epidermal junction**. *Curr Opin Cell Biol* 9:651-8.

Bursch, L.S., L. Wang, B. Igyarto, A. Kissenpfennig, B. Malissen, D.H. Kaplan, and K.A. Hogquist. 2007. **Identification of a novel population of Langerin+ dendritic cells**. *J Exp Med* 204:3147-56.

Caton, M.L., M.R. Smith-Raska, and B. Reizis. 2007. **Notch-RBP-J signaling controls the homeostasis of CD8- dendritic cells in the spleen**. *J Exp Med* 204:1653-64.

Champion, J.A., A. Walker, and S. Mitragotri. 2008. **Role of particle size in phagocytosis of polymeric microspheres**. *Pharm Res* 25:1815-21.

Chavrier, P., M. Vingron, C. Sander, K. Simons, and M. Zerial. 1990. **Molecular cloning of YPT1/SEC4-related cDNAs from an epithelial cell line**. *Mol Cell Biol* 10:6578-85.

Chen, F., L. Ma, M.C. Parrini, X. Mao, M. Lopez, C. Wu, P.W. Marks, L. Davidson, D.J. Kwiatkowski, T. Kirchhausen, S.H. Orkin, F.S. Rosen, B.J. Mayer, M.W. Kirschner, and F.W. Alt. 2000. **Cdc42 is required for PIP(2)-induced actin polymerization and early development but not for cell viability**. *Curr Biol* 10:758-65.

Chorro, L., A. Sarde, M. Li, K.J. Woollard, P. Chambon, B. Malissen, A. Kissenpfennig, J.B. Barbaroux, R. Groves, and F. Geissmann. 2009. **Langerhans cell (LC) proliferation mediates neonatal development, homeostasis, and inflammation-associated expansion of the epidermal LC network**. *J Exp Med* 206:3089-100.

Coso, O.A., M. Chiariello, J.C. Yu, H. Teramoto, P. Crespo, N. Xu, T. Miki, and J.S. Gutkind. 1995. **The small GTP-binding proteins Rac1 and Cdc42 regulate the activity of the JNK/SAPK signaling pathway**. *Cell* 81:1137-46.

Cox, A.D., and C.J. Der. 1992. **Protein prenylation: more than just glue?** *Curr Opin Cell Biol* 4:1008-16.

Cumberbatch, M., R.J. Dearman, C.E. Griffiths, and I. Kimber. 2000. **Langerhans cell migration**. *Clin Exp Dermatol* 25:413-8.

Cumberbatch, M., R.J. Dearman, and I. Kimber. 1997. **Langerhans cells require signals from both tumour necrosis factor-alpha and interleukin-1 beta for migration**. *Immunology* 92:388-95.

Das, B., X. Shu, G.J. Day, J. Han, U.M. Krishna, J.R. Falck, and D. Broek. 2000. **Control of intramolecular interactions between the pleckstrin homology and Dbl homology domains of Vav and Sos1 regulates Rac binding**. *J Biol Chem* 275:15074-81.

den Haan, J.M., S.M. Lehar, and M.J. Bevan. 2000. **CD8(+) but not CD8(-) dendritic cells cross-prime cytotoxic T cells in vivo**. *J Exp Med* 192:1685-96.

Ding, W., L.L. Stohl, J.A. Wagner, and R.D. Granstein. 2008. **Calcitonin gene-related peptide biases Langerhans cells toward Th2-type immunity**. *J Immunol* 181:6020-6.

Donald, S., K. Hill, C. Lecureuil, R. Barnouin, S. Krugmann, W. John Coadwell, S.R. Andrews, S.A. Walker, P.T. Hawkins, L.R. Stephens, and H.C. Welch. 2004. **P-Rex2, a new guanine-nucleotide exchange factor for Rac**. *FEBS Lett* 572:172-6.

Dubash, A.D., C. Guilluy, M.C. Srougi, E. Boulter, K. Burridge, and R. Garcia-Mata. 2011. **The small GTPase RhoA localizes to the nucleus and is activated by Net1 and DNA damage signals**. *PLoS One* 6:e17380.

Dudziak, D., A.O. Kamphorst, G.F. Heidkamp, V.R. Buchholz, C. Trumpfheller, S. Yamazaki, C. Cheong, K. Liu, H.W. Lee, C.G. Park, R.M. Steinman, and M.C. Nussenzweig. 2007. **Differential antigen processing by dendritic cell subsets in vivo**. *Science* 315:107-11.

Dutartre, H., J. Davoust, J.P. Gorvel, and P. Chavrier. 1996. **Cytokinesis arrest and redistribution of actin-cytoskeleton regulatory components in cells expressing the Rho GTPase CDC42Hs**. *J Cell Sci* 109 (Pt 2):367-77.

Edelson, B.T., W. Kc, R. Juang, M. Kohyama, L.A. Benoit, P.A. Klekotka, C. Moon, J.C. Albring, W. Ise, D.G. Michael, D. Bhattacharya, T.S. Stappenbeck, M.J. Holtzman, S.S. Sung, T.L. Murphy, K. Hildner, and K.M. Murphy. 2010. **Peripheral CD103+ dendritic cells form a unified subset developmentally related to CD8alpha+ conventional dendritic cells**. *J Exp Med* 207:823-36.

Feig, L.A. 1999. **Tools of the trade: use of dominant-inhibitory mutants of Ras-family GTPases**. *Nat Cell Biol* 1:E25-7.

Feng, Q., J.G. Albeck, R.A. Cerione, and W. Yang. 2002. **Regulation of the Cool/Pix proteins: key binding partners of the Cdc42/Rac targets, the p21-activated kinases**. *J Biol Chem* 277:5644-50.

Forster, R., A. Schubel, D. Breitfeld, E. Kremmer, I. Renner-Muller, E. Wolf, and M. Lipp. 1999. **CCR7 coordinates the primary immune response by establishing functional microenvironments in secondary lymphoid organs**. *Cell* 99:23-33.

Franco, M., P.J. Peters, J. Boretto, E. van Donselaar, A. Neri, C. D'Souza-Schorey, and P. Chavrier. 1999. **EFA6, a sec7 domain-containing exchange factor for ARF6, coordinates membrane recycling and actin cytoskeleton organization**. *Embo J* 18:1480-91.

Freret, M., F. Gouel, C. Buquet, E. Legrand, J.P. Vannier, M. Vasse, and I. Dubus. 2011. **Rac-1 GTPase controls the capacity of human leukaemic lymphoblasts to migrate on fibronectin in response to SDF-1alpha (CXCL12)**. *Leuk Res* 35:971-3.

Furuta, S., K. Miura, T. Copeland, W.H. Shang, A. Oshima, and T. Kamata. 2002. **Light Chain 3 associates with a Sos1 guanine nucleotide exchange factor: its significance in the Sos1-mediated Rac1 signaling leading to membrane ruffling**. *Oncogene* 21:7060-6.

Garcia-Mata, R., E. Boulter, and K. Burridge. 2011. **The 'invisible hand': regulation of RHO GTPases by RHOGDIs**. *Nat Rev Mol Cell Biol* 12:493-504.

Ghosh, M.C., P.S. Makena, V. Gorantla, S.E. Sinclair, and C.M. Waters. 2012. **CXCR4 regulates migration of lung alveolar epithelial cells through activation of Rac1 and matrix metalloproteinase-2**. *Am J Physiol Lung Cell Mol Physiol* 302:L846-56.

Ginhoux, F., M.P. Collin, M. Bogunovic, M. Abel, M. Leboeuf, J. Helft, J. Ochando, A. Kissenpfennig, B. Malissen, M. Grisotto, H. Snoeck, G. Randolph, and M. Merad. 2007. **Blood-derived dermal langerin+ dendritic cells survey the skin in the steady state**. *J Exp Med* 204:3133-46.

Ginhoux, F., K. Liu, J. Helft, M. Bogunovic, M. Greter, D. Hashimoto, J. Price, N. Yin, J. Bromberg, S.A. Lira, E.R. Stanley, M. Nussenzweig, and M. Merad. 2009. **The origin and development of nonlymphoid tissue CD103+ DCs**. *J Exp Med* 206:3115-30.

Ginhoux, F., F. Tacke, V. Angeli, M. Bogunovic, M. Loubeau, X.M. Dai, E.R. Stanley, G.J. Randolph, and M. Merad. 2006. **Langerhans cells arise from monocytes in vivo**. *Nat Immunol* 7:265-73.

Glaven, J.A., I. Whitehead, S. Bagrodia, R. Kay, and R.A. Cerione. 1999. **The Dbl-related protein, Lfc, localizes to microtubules and mediates the activation of Rac signaling pathways in cells**. *J Biol Chem* 274:2279-85.

Glaven, J.A., I.P. Whitehead, T. Nomanbhoy, R. Kay, and R.A. Cerione. 1996. **Lfc and Lsc oncoproteins represent two new guanine nucleotide exchange factors for the Rho GTP-binding protein**. *J Biol Chem* 271:27374-81.

Gotthardt, K., and M.R. Ahmadian. 2007. **Asef is a Cdc42-specific guanine nucleotide exchange factor**. *Biol Chem* 388:67-71.

Granucci, F., E. Ferrero, M. Foti, D. Aggujaro, K. Vettoretto, and P. Ricciardi-Castagnoli. 1999. **Early events in dendritic cell maturation induced by LPS**. *Microbes Infect* 1:1079-84.

Gretz, J.E., C.C. Norbury, A.O. Anderson, A.E. Proudfoot, and S. Shaw. 2000. **Lymph-borne chemokines and other low molecular weight molecules reach high endothelial venules via specialized conduits while a functional barrier limits access to the lymphocyte microenvironments in lymph node cortex**. *J Exp Med* 192:1425-40.

Guillemot, J.C., P. Montcourrier, E. Vivier, J. Davoust, and P. Chavrier. 1997. **Selective control of membrane ruffling and actin plaque assembly by the Rho GTPases Rac1 and CDC42 in FcepsilonRI-activated rat basophilic leukemia (RBL-2H3) cells**. *J Cell Sci* 110 (Pt 18):2215-25.

Guilliams, M., S. Henri, S. Tamoutounour, L. Ardouin, I. Schwartz-Cornil, M. Dalod, and B. Malissen. 2010. **From skin dendritic cells to a simplified classification of human and mouse dendritic cell subsets**. *Eur J Immunol* 40:2089-94.

Guilluy, C., R. Garcia-Mata, and K. Burridge. 2011. **Rho protein crosstalk: another social network?** *Trends Cell Biol* 21:718-26.

Habets, G.G., E.H. Scholtes, D. Zuydgeest, R.A. van der Kammen, J.C. Stam, A. Berns, and J.G. Collard. 1994. **Identification of an invasion-inducing gene, Tiam-1, that encodes a protein with homology to GDP-GTP exchangers for Rho-like proteins**. *Cell* 77:537-49.

Haley, K., B.Z. Igyarto, D. Ortner, A. Bobr, S. Kashem, D. Schenten, and D.H. Kaplan. 2012. **Langerhans cells require MyD88-dependent signals for Candida albicans response but not for contact hypersensitivity or migration**. *J Immunol* 188:4334-9.

Hamakawa, M., A. Sugihara, H. Okamoto, and T. Horio. 2006. **Ultraviolet B radiation suppresses Langerhans cell migration in the dermis by down-regulation of alpha4 integrin**. *Photodermatol Photoimmunol Photomed* 22:116-23.

Hart, M.J., A. Eva, D. Zangrilli, S.A. Aaronson, T. Evans, R.A. Cerione, and Y. Zheng. 1994. **Cellular transformation and guanine nucleotide exchange activity are catalyzed by a common domain on the dbl oncogene product**. *J Biol Chem* 269:62-5.

Hayakawa, M., H. Kitagawa, K. Miyazawa, M. Kitagawa, and K. Kikugawa. 2005. **The FWD1/beta-TrCP-mediated degradation pathway establishes a 'turning off switch' of a Cdc42 guanine nucleotide exchange factor, FGD1**. *Genes Cells* 10:241-51.

Heasman, S.J., and A.J. Ridley. 2008. **Mammalian Rho GTPases: new insights into their functions from in vivo studies**. *Nat Rev Mol Cell Biol* 9:690-701.

Henri, S., L.F. Poulin, S. Tamoutounour, L. Ardouin, M. Guilliams, B. de Bovis, E. Devilard, C. Viret, H. Azukizawa, A. Kissenpfennig, and B. Malissen. 2010. **CD207+ CD103+ dermal dendritic cells cross-present keratinocyte-derived antigens irrespective of the presence of Langerhans cells**. *J Exp Med* 207:189-206.

Henri, S., D. Vremec, A. Kamath, J. Waithman, S. Williams, C. Benoist, K. Burnham, S. Saeland, E. Handman, and K. Shortman. 2001. **The dendritic cell populations of mouse lymph nodes**. *J Immunol* 167:741-8.

Hervouet, C., C. Luci, N. Rol, D. Rousseau, A. Kissenpfennig, B. Malissen, C. Czerkinsky, and F. Anjuere. 2010. **Langerhans cells prime IL-17-producing T cells and dampen genital cytotoxic responses following mucosal immunization**. *J Immunol* 184:4842-51.

Heufler, C., G. Topar, F. Koch, B. Trockenbacher, E. Kampgen, N. Romani, and G. Schuler. 1992. **Cytokine gene expression in murine epidermal cell suspensions: interleukin 1 beta and macrophage inflammatory protein 1 alpha are selectively expressed in Langerhans cells but are differentially regulated in culture**. *J Exp Med* 176:1221-6.

Hirahara, K., G. Vahedi, K. Ghoreschi, X.P. Yang, S. Nakayamada, Y. Kanno, J.J. O'Shea, and A. Laurence. 2011. **Helper T-cell differentiation and plasticity: insights from epigenetics**. *Immunology* 134:235-45.

Hogquist, K.A., S.C. Jameson, W.R. Heath, J.L. Howard, M.J. Bevan, and F.R. Carbone. 1994. **T cell receptor antagonist peptides induce positive selection**. *Cell* 76:17-27.

Holcmann, M., P. Stoitzner, B. Drobits, P. Luehrs, G. Stingl, N. Romani, D. Maurer, and M. Sibilia. 2009. **Skin inflammation is not sufficient to break tolerance induced against a novel antigen**. *J Immunol* 183:1133-43.

Hoppe, A.D., and J.A. Swanson. 2004. **Cdc42, Rac1, and Rac2 display distinct patterns of activation during phagocytosis**. *Mol Biol Cell* 15:3509-19.

Horii, Y., J.F. Beeler, K. Sakaguchi, M. Tachibana, and T. Miki. 1994. **A novel oncogene, ost, encodes a guanine nucleotide exchange factor that potentially links Rho and Rac signaling pathways**. *Embo J* 13:4776-86.

Huber, C., A. Martensson, G.M. Bokoch, D. Nemazee, and A.L. Gavin. 2008. **FGD2, a CDC42-specific exchange factor expressed by antigen-presenting cells, localizes to early endosomes and active membrane ruffles**. *J Biol Chem* 283:34002-12.

Igyarto, B.Z., K. Haley, D. Ortner, A. Bobr, M. Gerami-Nejad, B.T. Edelson, S.M. Zurawski, B. Malissen, G. Zurawski, J. Berman, and D.H. Kaplan. 2011. **Skin-resident murine dendritic cell subsets promote distinct and opposing antigen-specific T helper cell responses**. *Immunity* 35:260-72.

Iijima, N., M.M. Linehan, S. Saeland, and A. Iwasaki. 2007. **Vaginal epithelial dendritic cells renew from bone marrow precursors**. *Proc Natl Acad Sci U S A* 104:19061-6.

Ioffreda, M.D., D. Whitaker, and G.F. Murphy. 1993. **Mast cell degranulation upregulates alpha 6 integrins on epidermal Langerhans cells**. *J Invest Dermatol* 101:150-4.

Jaffe, A.B., and A. Hall. 2005. **Rho GTPases: biochemistry and biology**. *Annu Rev Cell Dev Biol* 21:247-69.

Jaiswal, M., L. Gremer, R. Dvorsky, L.C. Haeusler, I.C. Cirstea, K. Uhlenbrock, and M.R. Ahmadian. 2011. **Mechanistic insights into specificity, activity, and regulatory elements of the regulator of G-protein signaling (RGS)-containing Rho-specific guanine nucleotide exchange factors (GEFs) p115, PDZ-RhoGEF (PRG), and leukemia-associated RhoGEF (LARG)**. *J Biol Chem* 286:18202-12.

Jakob, T., and M.C. Udey. 1998. **Regulation of E-cadherin-mediated adhesion in Langerhans cell-like dendritic cells by inflammatory mediators that mobilize Langerhans cells in vivo**. *J Immunol* 160:4067-73.

Jaksits, S., W. Bauer, E. Kriehuber, M. Zeyda, T.M. Stulnig, G. Stingl, E. Fiebiger, and D. Maurer. 2004. **Lipid raft-associated GTPase signaling controls morphology and CD8+ T cell stimulatory capacity of human dendritic cells**. *J Immunol* 173:1628-39.

Joachim, R.A., B. Handjiski, S.M. Blois, E. Hagen, R. Paus, and P.C. Arck. 2008. **Stress-induced neurogenic inflammation in murine skin skews dendritic cells towards maturation and migration: key role of intercellular adhesion molecule-1/leukocyte function-associated antigen interactions**. *Am J Pathol* 173:1379-88.

Josefowicz, S.Z., R.E. Niec, H.Y. Kim, P. Treuting, T. Chinen, Y. Zheng, D.T. Umetsu, and A.Y. Rudensky. 2012. **Extrathymically generated regulatory T cells control mucosal TH2 inflammation**. *Nature* 482:395-9.

Joseph, R.E., and F.A. Norris. 2005. **Substrate specificity and recognition is conferred by the pleckstrin homology domain of the Dbl family guanine nucleotide exchange factor P-Rex2**. *J Biol Chem* 280:27508-12.

Kabashima, K., N. Shiraishi, K. Sugita, T. Mori, A. Onoue, M. Kobayashi, J. Sakabe, R. Yoshiki, H. Tamamura, N. Fujii, K. Inaba, and Y. Tokura. 2007. **CXCL12-CXCR4 engagement is required for migration of cutaneous dendritic cells**. *Am J Pathol* 171:1249-57.

Kamath, A.T., S. Henri, F. Battye, D.F. Tough, and K. Shortman. 2002. **Developmental kinetics and lifespan of dendritic cells in mouse lymphoid organs**. *Blood* 100:1734-41.

Kaplan, D.H. 2010. **In vivo function of Langerhans cells and dermal dendritic cells**. *Trends Immunol* 31:446-51.

Kaplan, D.H., M.O. Li, M.C. Jenison, W.D. Shlomchik, R.A. Flavell, and M.J. Shlomchik. 2007. **Autocrine/paracrine TGFbeta1 is required for the development of epidermal Langerhans cells**. *J Exp Med* 204:2545-52.

Kautz-Neu, K., M. Noordegraaf, S. Dinges, C.L. Bennett, D. John, B.E. Clausen, and E. von Stebut. 2011. **Langerhans cells are negative regulators of the anti-Leishmania response**. *J Exp Med* 208:885-91.

Kawai, T., and S. Akira. 2009. **The roles of TLRs, RLRs and NLRs in pathogen recognition**. *Int Immunol* 21:317-37.

Kawasaki, Y., M. Sagara, Y. Shibata, M. Shirouzu, S. Yokoyama, and T. Akiyama. 2007. **Identification and characterization of Asef2, a guanine-nucleotide exchange factor specific for Rac1 and Cdc42**. *Oncogene* 26:7620-267.

Kel, J.M., M.J. Girard-Madoux, B. Reizis, and B.E. Clausen. 2010. **TGF-beta is required to maintain the pool of immature Langerhans cells in the epidermis**. *J Immunol* 185:3248-55.

Kerksiek, K.M., F. Niedergang, P. Chavrier, D.H. Busch, and T. Brocker. 2005. **Selective Rac1 inhibition in dendritic cells diminishes apoptotic cell uptake and cross-presentation in vivo**. *Blood* 105:742-9.

Kissenpfennig, A., S. Henri, B. Dubois, C. Laplace-Builhe, P. Perrin, N. Romani, C.H. Tripp, P. Douillard, L. Leserman, D. Kaiserlian, S. Saeland, J. Davoust, and B. Malissen.

2005. **Dynamics and function of Langerhans cells in vivo: dermal dendritic cells colonize lymph node areas distinct from slower migrating Langerhans cells**. *Immunity* 22:643-54.

Kulkarni, K., J. Yang, Z. Zhang, and D. Barford. 2011. **Multiple factors confer specific Cdc42 and Rac protein activation by dedicator of cytokinesis (DOCK) nucleotide exchange factors**. *J Biol Chem* 286:25341-51.

Lammermann, T., J. Renkawitz, X. Wu, K. Hirsch, C. Brakebusch, and M. Sixt. 2009. **Cdc42-dependent leading edge coordination is essential for interstitial dendritic cell migration**. *Blood* 113:5703-10.

Langerhans, P. 1868. **Ueber die Nerven der menschlichen Haut.** *Virchows Arch* 44:

Lanning, C.C., R. Ruiz-Velasco, and C.L. Williams. 2003. **Novel mechanism of the co-regulation of nuclear transport of SmgGDS and Rac1**. *J Biol Chem* 278:12495-506.

Leverrier, Y., and A.J. Ridley. 2001. **Requirement for Rho GTPases and PI 3-kinases during apoptotic cell phagocytosis by macrophages**. *Curr Biol* 11:195-9.

Li, H., D.H. Kaplan, C. Matte-Martone, H.S. Tan, S. Venkatesan, K. Johnson, A.J. Demetris, J. McNiff, M.J. Shlomchik, and W.D. Shlomchik. 2011. **Langerhans cells are not required for graft-versus-host disease**. *Blood* 117:697-707.

Ligeti, E., S. Welti, and K. Scheffzek. 2012. **Inhibition and termination of physiological responses by GTPase activating proteins**. *Physiol Rev* 92:237-72.

Lin, Q., W. Yang, D. Baird, Q. Feng, and R.A. Cerione. 2006. **Identification of a DOCK180-related guanine nucleotide exchange factor that is capable of mediating a positive feedback activation of Cdc42**. *J Biol Chem* 281:35253-62.

Liu, B.P., and K. Burridge. 2000. **Vav2 activates Rac1, Cdc42, and RhoA downstream from growth factor receptors but not beta1 integrins**. *Mol Cell Biol* 20:7160-9.

Livak, K.J., and T.D. Schmittgen. 2001. **Analysis of relative gene expression data using real-time quantitative PCR and the 2(-Delta Delta C(T)) Method**. *Methods* 25:402-8.

Luckashenak, N., S. Schroeder, K. Endt, D. Schmidt, K. Mahnke, M.F. Bachmann, P. Marconi, C.A. Deeg, and T. Brocker. 2008. **Constitutive crosspresentation of tissue antigens by dendritic cells controls CD8+ T cell tolerance in vivo**. *Immunity* 28:521-32.

Luckashenak, N., A. Wähe, K. Breit, C. Brakebusch, and T. Brocker. 2013. **Rho-Family GTPase Cdc42 controls migration of Langerhans cells in vivo**. *J Immunol* 190:

Macatonia, S.E., A.J. Edwards, and S.C. Knight. 1986. **Dendritic cells and the initiation of contact sensitivity to fluorescein isothiocyanate**. *Immunology* 59:509-14.

Madaule, P., and R. Axel. 1985. **A novel ras-related gene family**. *Cell* 41:31-40.

Maeda, Y., H. Matsuyuki, K. Shimano, H. Kataoka, K. Sugahara, and K. Chiba. 2007. **Migration of CD4 T cells and dendritic cells toward sphingosine 1-phosphate (S1P) is mediated by different receptor subtypes: S1P regulates the functions of murine mature dendritic cells via S1P receptor type 3**. *J Immunol* 178:3437-46.

Mao, J., H. Yuan, W. Xie, and D. Wu. 1998. **Guanine nucleotide exchange factor GEF115 specifically mediates activation of Rho and serum response factor by the G protein alpha subunit Galpha13**. *Proc Natl Acad Sci U S A* 95:12973-6.

Mauviel, A., N. Temime, D. Charron, G. Loyau, and J.P. Pujol. 1991. **Induction of interleukin-1 beta production in human dermal fibroblasts by interleukin-1 alpha and tumor necrosis factor-alpha. Involvement of protein kinase-dependent and adenylate cyclase-dependent regulatory pathways**. *J Cell Biochem* 47:174-83.

Mavrakis, K.J., K.J. McKinlay, P. Jones, and F. Sablitzky. 2004. **DEF6, a novel PH-DH-like domain protein, is an upstream activator of the Rho GTPases Rac1, Cdc42, and RhoA**. *Exp Cell Res* 294:335-44.

Merad, M., L. Fong, J. Bogenberger, and E.G. Engleman. 2000. **Differentiation of myeloid dendritic cells into CD8alpha-positive dendritic cells in vivo**. *Blood* 96:1865-72.

Merad, M., M.G. Manz, H. Karsunky, A. Wagers, W. Peters, I. Charo, I.L. Weissman, J.G. Cyster, and E.G. Engleman. 2002. **Langerhans cells renew in the skin throughout life under steady-state conditions**. *Nat Immunol* 3:1135-41.

Miller, N.L., C. Lawson, X.L. Chen, S.T. Lim, and D.D. Schlaepfer. 2012. **Rgnef (p190RhoGEF) knockout inhibits RhoA activity, focal adhesion establishment, and cell motility downstream of integrins**. *PLoS One* 7:e37830.

Minden, A., A. Lin, F.X. Claret, A. Abo, and M. Karin. 1995. **Selective activation of the JNK signaling cascade and c-Jun transcriptional activity by the small GTPases Rac and Cdc42Hs**. *Cell* 81:1147-57.

Miyamoto, Y., J. Yamauchi, A. Sanbe, and A. Tanoue. 2007. **Dock6, a Dock-C subfamily guanine nucleotide exchanger, has the dual specificity for Rac1 and Cdc42 and regulates neurite outgrowth**. *Exp Cell Res* 313:791-804.

Movilla, N., and X.R. Bustelo. 1999. **Biological and regulatory properties of Vav-3, a new member of the Vav family of oncoproteins**. *Mol Cell Biol* 19:7870-85.

Nagao, K., F. Ginhoux, W.W. Leitner, S. Motegi, C.L. Bennett, B.E. Clausen, M. Merad, and M.C. Udey. 2009. **Murine epidermal Langerhans cells and langerin-expressing dermal dendritic cells are unrelated and exhibit distinct functions**. *Proc Natl Acad Sci U S A* 106:3312-7.

Nagao, K., T. Kobayashi, K. Moro, M. Ohyama, T. Adachi, D.Y. Kitashima, S. Ueha, K. Horiuchi, H. Tanizaki, K. Kabashima, A. Kubo, Y.H. Cho, B.E. Clausen, K. Matsushima, M. Suematsu, G.C. Furtado, S.A. Lira, J.M. Farber, M.C. Udey, and M. Amagai. 2012. **Stress-induced production of chemokines by hair follicles regulates the trafficking of dendritic cells in skin**. *Nat Immunol* 13:744-52.

Naik, S.H., D. Metcalf, A. van Nieuwenhuijze, I. Wicks, L. Wu, M. O'Keeffe, and K. Shortman. 2006. **Intrasplenic steady-state dendritic cell precursors that are distinct from monocytes**. *Nat Immunol* 7:663-71.

Nakaya, M., M. Tanaka, Y. Okabe, R. Hanayama, and S. Nagata. 2006. **Opposite effects of rho family GTPases on engulfment of apoptotic cells by macrophages**. *J Biol Chem* 281:8836-42.

Nethe, M., and P.L. Hordijk. 2010. **The role of ubiquitylation and degradation in RhoGTPase signalling**. *J Cell Sci* 123:4011-8.

Neuenhahn, M., K.M. Kerksiek, M. Nauerth, M.H. Suhre, M. Schiemann, F.E. Gebhardt, C. Stemberger, K. Panthel, S. Schroder, T. Chakraborty, S. Jung, H. Hochrein, H. Russmann, T. Brocker, and D.H. Busch. 2006. **CD8alpha+ dendritic cells are required for efficient entry of Listeria monocytogenes into the spleen**. *Immunity* 25:619-30.

Niu, J., J. Profirovic, H. Pan, R. Vaiskunaite, and T. Voyno-Yasenetskaya. 2003. **G Protein betagamma subunits stimulate p114RhoGEF, a guanine nucleotide exchange factor for RhoA and Rac1: regulation of cell shape and reactive oxygen species production**. *Circ Res* 93:848-56.

Noirey, N., M.J. Staquet, M.J. Gariazzo, M. Serres, C. Andre, D. Schmitt, and C. Vincent. 2002. **Relationship between expression of matrix metalloproteinases and migration of epidermal and in vitro generated Langerhans cells**. *Eur J Cell Biol* 81:383-9.

Noordegraaf, M., V. Flacher, P. Stoitzner, and B.E. Clausen. 2010. **Functional redundancy of Langerhans cells and Langerin+ dermal dendritic cells in contact hypersensitivity**. *J Invest Dermatol* 130:2752-9.

Nopora, K., C.A. Bernhard, C. Ried, A.A. Castello, K.M. Murphy, P. Marconi, U. Koszinowski, and T. Brocker. 2012. **MHC class I cross-presentation by dendritic cells counteracts viral immune evasion**. *Front Immunol* 3:348.

Oakford, M.E., S.V. Dixon, S. August, C. Pickard, M. Ardern-Jones, P. Lackie, P.S. Friedmann, and E. Healy. 2011. **Migration of immunocytes across the basement membrane in skin: the role of basement membrane pores**. *J Invest Dermatol* 131:1950-3.

Obhrai, J.S., M. Oberbarnscheidt, N. Zhang, D.L. Mueller, W.D. Shlomchik, F.G. Lakkis, M.J. Shlomchik, and D.H. Kaplan. 2008. **Langerhans cells are not required for efficient skin graft rejection**. *J Invest Dermatol* 128:1950-5.

Ocana-Morgner, C., P. Reichardt, M. Chopin, S. Braungart, C. Wahren, M. Gunzer, and R. Jessberger. 2011. **Sphingosine 1-phosphate-induced motility and endocytosis of dendritic cells is regulated by SWAP-70 through RhoA**. *J Immunol* 186:5345-55.

Ocana-Morgner, C., C. Wahren, and R. Jessberger. 2009. **SWAP-70 regulates RhoA/RhoB-dependent MHCII surface localization in dendritic cells**. *Blood* 113:1474-82.

Oestreich, K.J., and A.S. Weinmann. 2012. **Transcriptional mechanisms that regulate T helper 1 cell differentiation**. *Curr Opin Immunol* 24:191-5.

Okoye, I.S., and M.S. Wilson. 2011. **CD4+ T helper 2 cells--microbial triggers, differentiation requirements and effector functions**. *Immunology* 134:368-77.

Olson, M.F., A. Ashworth, and A. Hall. 1995. **An essential role for Rho, Rac, and Cdc42 GTPases in cell cycle progression through G1**. *Science* 269:1270-2.

Onai, N., A. Obata-Onai, M.A. Schmid, and M.G. Manz. 2007. **Flt3 in regulation of type I interferon-producing cell and dendritic cell development**. *Ann N Y Acad Sci* 1106:253-61.

Ono, Y., H. Nakanishi, M. Nishimura, M. Kakizaki, K. Takahashi, M. Miyahara, K. Satoh-Horikawa, K. Mandai, and Y. Takai. 2000. **Two actions of frabin: direct activation of Cdc42 and indirect activation of Rac**. *Oncogene* 19:3050-8.

Ouwehand, K., S.J. Santegoets, D.P. Bruynzeel, R.J. Scheper, T.D. de Gruijl, and S. Gibbs. 2008. **CXCL12 is essential for migration of activated Langerhans cells from epidermis to dermis**. *Eur J Immunol* 38:3050-9.

Pedersen, E., A. Basse, T. Lefever, K. Peyrollier, and C. Brakebusch. 2012. **Rho GTPase knockout induction in primary keratinocytes from adult mice**. *Methods Mol Biol* 827:157-66.

Pedersen, E., and C. Brakebusch. 2012. **Rho GTPase function in development: how in vivo models change our view**. *Exp Cell Res* 318:1779-87.

Penzes, P., R.C. Johnson, V. Kambampati, R.E. Mains, and B.A. Eipper. 2001. **Distinct roles for the two Rho GDP/GTP exchange factor domains of kalirin in regulation of neurite growth and neuronal morphology**. *J Neurosci* 21:8426-34.

Pflicke, H., and M. Sixt. 2009. **Preformed portals facilitate dendritic cell entry into afferent lymphatic vessels**. *J Exp Med* 206:2925-35.

Pooley, J.L., W.R. Heath, and K. Shortman. 2001. **Cutting edge: intravenous soluble antigen is presented to CD4 T cells by CD8- dendritic cells, but cross-presented to CD8 T cells by CD8+ dendritic cells**. *J Immunol* 166:5327-30.

Poulin, L.F., S. Henri, B. de Bovis, E. Devilard, A. Kissenpfennig, and B. Malissen. 2007. **The dermis contains langerin+ dendritic cells that develop and function independently of epidermal Langerhans cells**. *J Exp Med* 204:3119-31.

Price, A.A., M. Cumberbatch, I. Kimber, and A. Ager. 1997. **Alpha 6 integrins are required for Langerhans cell migration from the epidermis**. *J Exp Med* 186:1725-35.

Pulecio, J., J. Petrovic, F. Prete, G. Chiaruttini, A.M. Lennon-Dumenil, C. Desdouets, S. Gasman, O.R. Burrone, and F. Benvenuti. 2010. **Cdc42-mediated MTOC polarization in dendritic cells controls targeted delivery of cytokines at the immune synapse**. *J Exp Med* 207:2719-32.

Puttur, F.K., M.A. Fernandez, R. White, B. Roediger, A.L. Cunningham, W. Weninger, and C.A. Jones. 2010. **Herpes simplex virus infects skin gamma delta T cells before Langerhans cells and impedes migration of infected Langerhans cells by inducing apoptosis and blocking E-cadherin downregulation**. *J Immunol* 185:477-87.

Quast, T., B. Tappertzhofen, C. Schild, J. Grell, N. Czeloth, R. Forster, R. Alon, L. Fraemohs, K. Dreck, C. Weber, T. Lammermann, M. Sixt, and W. Kolanus. 2009. **Cytohesin-1 controls the activation of RhoA and modulates integrin-dependent adhesion and migration of dendritic cells**. *Blood* 113:5801-10.

Ratzinger, G., P. Stoitzner, S. Ebner, M.B. Lutz, G.T. Layton, C. Rainer, R.M. Senior, J.M. Shipley, P. Fritsch, G. Schuler, and N. Romani. 2002. **Matrix metalloproteinases 9 and 2 are necessary for the migration of Langerhans cells and dermal dendritic cells from human and murine skin**. *J Immunol* 168:4361-71.

Reis e Sousa, C. 2006. **Dendritic cells in a mature age**. *Nat Rev Immunol* 6:476-83.

Reis e Sousa, C., P.D. Stahl, and J.M. Austyn. 1993. **Phagocytosis of antigens by Langerhans cells in vitro**. *J Exp Med* 178:509-19.

Ren, Y., R. Li, Y. Zheng, and H. Busch. 1998. **Cloning and characterization of GEF-H1, a microtubule-associated guanine nucleotide exchange factor for Rac and Rho GTPases**. *J Biol Chem* 273:34954-60.

Robbe, K., A. Otto-Bruc, P. Chardin, and B. Antonny. 2003. **Dissociation of GDP dissociation inhibitor and membrane translocation are required for efficient activation of Rac by the Dbl homology-pleckstrin homology region of Tiam**. *J Biol Chem* 278:4756-62.

Robbins, S.H., T. Walzer, D. Dembele, C. Thibault, A. Defays, G. Bessou, H. Xu, E. Vivier, M. Sellars, P. Pierre, F.R. Sharp, S. Chan, P. Kastner, and M. Dalod. 2008. **Novel insights into the relationships between dendritic cell subsets in human and mouse revealed by genome-wide expression profiling**. *Genome Biol* 9:R17.

Robertson, J.M., P.E. Jensen, and B.D. Evavold. 2000. **DO11.10 and OT-II T cells recognize a C-terminal ovalbumin 323-339 epitope**. *J Immunol* 164:4706-12.

Romani, N., P.M. Brunner, and G. Stingl. 2012. **Changing views of the role of Langerhans cells**. *J Invest Dermatol* 132:872-81.

Rossman, K.L., C.J. Der, and J. Sondek. 2005. **GEF means go: turning on RHO GTPases with guanine nucleotide-exchange factors**. *Nat Rev Mol Cell Biol* 6:167-80.

Rouzaut, A., S. Garasa, A. Teijeira, I. Gonzalez, I. Martinez-Forero, N. Suarez, E. Larrea, C. Alfaro, A. Palazon, J. Dubrot, S. Hervas-Stubbs, and I. Melero. 2010. **Dendritic cells adhere to and transmigrate across lymphatic endothelium in response to IFN-alpha**. *Eur J Immunol* 40:3054-63.

Ruusala, A., and P. Aspenstrom. 2004. **Isolation and characterisation of DOCK8, a member of the DOCK180-related regulators of cell morphology**. *FEBS Lett* 572:159-66.

Sallusto, F., P. Schaerli, P. Loetscher, C. Schaniel, D. Lenig, C.R. Mackay, S. Qin, and A. Lanzavecchia. 1998. **Rapid and coordinated switch in chemokine receptor expression during dendritic cell maturation**. *Eur J Immunol* 28:2760-9.

Salomon, B., J.L. Cohen, C. Masurier, and D. Klatzmann. 1998. **Three populations of mouse lymph node dendritic cells with different origins and dynamics**. *J Immunol* 160:708-17.

Sarfstein, R., Y. Gorzalczany, A. Mizrahi, Y. Berdichevsky, S. Molshanski-Mor, C. Weinbaum, M. Hirshberg, M.C. Dagher, and E. Pick. 2004. **Dual role of Rac in the assembly of NADPH oxidase, tethering to the membrane and activation of p67phox: a study based on mutagenesis of p67phox-Rac1 chimeras**. *J Biol Chem* 279:16007-16.

Schiller, M.R. 2006. **Coupling receptor tyrosine kinases to Rho GTPases--GEFs what's the link**. *Cell Signal* 18:1834-43.

Schuler, G., and R.M. Steinman. 1985. **Murine epidermal Langerhans cells mature into potent immunostimulatory dendritic cells in vitro**. *J Exp Med* 161:526-46.

Schumann, K., T. Lammermann, M. Bruckner, D.F. Legler, J. Polleux, J.P. Spatz, G. Schuler, R. Forster, M.B. Lutz, L. Sorokin, and M. Sixt. 2010. **Immobilized chemokine fields and soluble chemokine gradients cooperatively shape migration patterns of dendritic cells**. *Immunity* 32:703-13.

Schwarzenberger, K., and M.C. Udey. 1996. **Contact allergens and epidermal proinflammatory cytokines modulate Langerhans cell E-cadherin expression in situ**. *J Invest Dermatol* 106:553-8.

Seiki, M. 2002. **The cell surface: the stage for matrix metalloproteinase regulation of migration**. *Curr Opin Cell Biol* 14:624-32.

Seneschal, J., R.A. Clark, A. Gehad, C.M. Baecher-Allan, and T.S. Kupper. 2012. **Human epidermal Langerhans cells maintain immune homeostasis in skin by activating skin resident regulatory T cells**. *Immunity* 36:873-84.

Sere, K., J.H. Baek, J. Ober-Blobaum, G. Muller-Newen, F. Tacke, Y. Yokota, M. Zenke, and T. Hieronymus. 2012. **Two Distinct Types of Langerhans Cells Populate the Skin during Steady State and Inflammation**. *Immunity* 37:905-16.

Shamah, S.M., M.Z. Lin, J.L. Goldberg, S. Estrach, M. Sahin, L. Hu, M. Bazalakova, R.L. Neve, G. Corfas, A. Debant, and M.E. Greenberg. 2001. **EphA receptors regulate growth cone dynamics through the novel guanine nucleotide exchange factor ephexin**. *Cell* 105:233-44.

Shinohara, M., Y. Terada, A. Iwamatsu, A. Shinohara, N. Mochizuki, M. Higuchi, Y. Gotoh, S. Ihara, S. Nagata, H. Itoh, Y. Fukui, and R. Jessberger. 2002. **SWAP-70 is a guanine-nucleotide-exchange factor that mediates signalling of membrane ruffling**. *Nature* 416:759-63.

Shklovskaya, E., B.J. O'Sullivan, L.G. Ng, B. Roediger, R. Thomas, W. Weninger, and B. Fazekas de St Groth. 2011. **Langerhans cells are precommitted to immune tolerance induction**. *Proc Natl Acad Sci U S A* 108:18049-54.

Shurin, G.V., I.L. Tourkova, G.S. Chatta, G. Schmidt, S. Wei, J.Y. Djeu, and M.R. Shurin. 2005. **Small rho GTPases regulate antigen presentation in dendritic cells**. *J Immunol* 174:3394-400.

Skokos, E.A., A. Charokopos, K. Khan, J. Wanjala, and T.R. Kyriakides. 2011. **Lack of TNF-alpha-induced MMP-9 production and abnormal E-cadherin redistribution associated with compromised fusion in MCP-1-null macrophages**. *Am J Pathol* 178:2311-21.

Spurrell, D.R., N.A. Luckashenak, D.C. Minney, A. Chaplin, J.M. Penninger, R.S. Liwski, J.L. Clements, and K.A. West. 2009. **Vav1 regulates the migration and adhesion of dendritic cells**. *J Immunol* 183:310-8.

Steinman, R.M., and Z.A. Cohn. 1973. **Identification of a novel cell type in peripheral lymphoid organs of mice. I. Morphology, quantitation, tissue distribution**. *J Exp Med* 137:1142-62.

Stoitzner, P., S. Holzmann, A.D. McLellan, L. Ivarsson, H. Stossel, M. Kapp, U. Kammerer, P. Douillard, E. Kampgen, F. Koch, S. Saeland, and N. Romani. 2003. **Visualization and characterization of migratory Langerhans cells in murine skin**

and lymph nodes by antibodies against Langerin/CD207. *J Invest Dermatol* 120:266-74.

Stoitzner, P., C.H. Tripp, A. Eberhart, K.M. Price, J.Y. Jung, L. Bursch, F. Ronchese, and N. Romani. 2006. **Langerhans cells cross-present antigen derived from skin**. *Proc Natl Acad Sci U S A* 103:7783-8.

Stutte, S., T. Quast, N. Gerbitzki, T. Savinko, N. Novak, J. Reifenberger, B. Homey, W. Kolanus, H. Alenius, and I. Forster. 2010. **Requirement of CCL17 for CCR7- and CXCR4-dependent migration of cutaneous dendritic cells**. *Proc Natl Acad Sci U S A* 107:8736-41.

Sugihara, K., N. Nakatsuji, K. Nakamura, K. Nakao, R. Hashimoto, H. Otani, H. Sakagami, H. Kondo, S. Nozawa, A. Aiba, and M. Katsuki. 1998. **Rac1 is required for the formation of three germ layers during gastrulation**. *Oncogene* 17:3427-33.

Swetman, C.A., Y. Leverrier, R. Garg, C.H. Gan, A.J. Ridley, D.R. Katz, and B.M. Chain. 2002. **Extension, retraction and contraction in the formation of a dendritic cell dendrite: distinct roles for Rho GTPases**. *Eur J Immunol* 32:2074-83.

Tal, O., H.Y. Lim, I. Gurevich, I. Milo, Z. Shipony, L.G. Ng, V. Angeli, and G. Shakhar. 2011. **DC mobilization from the skin requires docking to immobilized CCL21 on lymphatic endothelium and intralymphatic crawling**. *J Exp Med* 208:2141-53.

Tatsumoto, T., X. Xie, R. Blumenthal, I. Okamoto, and T. Miki. 1999. **Human ECT2 is an exchange factor for Rho GTPases, phosphorylated in G2/M phases, and involved in cytokinesis**. *J Cell Biol* 147:921-8.

Taya, S., N. Inagaki, H. Sengiku, H. Makino, A. Iwamatsu, I. Urakawa, K. Nagao, S. Kataoka, and K. Kaibuchi. 2001. **Direct interaction of insulin-like growth factor-1 receptor with leukemia-associated RhoGEF**. *J Cell Biol* 155:809-20.

Thacker, R.I., and E.M. Janssen. 2012. **Cross-presentation of cell-associated antigens by mouse splenic dendritic cell populations**. *Front Immunol* 3:41.

Tourkova, I.L., G.V. Shurin, S. Wei, and M.R. Shurin. 2007. **Small rho GTPases mediate tumor-induced inhibition of endocytic activity of dendritic cells**. *J Immunol* 178:7787-93.

Ugolev, Y., Y. Berdichevsky, C. Weinbaum, and E. Pick. 2008. **Dissociation of Rac1(GDP).RhoGDI complexes by the cooperative action of anionic liposomes containing phosphatidylinositol 3,4,5-trisphosphate, Rac guanine nucleotide exchange factor, and GTP**. *J Biol Chem* 283:22257-71.

van Helden, S.F., and P.L. Hordijk. 2011. **Podosome regulation by Rho GTPases in myeloid cells**. *Eur J Cell Biol* 90:189-97.

van Helden, S.F., M.M. Oud, B. Joosten, N. Peterse, C.G. Figdor, and F.N. van Leeuwen. 2008. **PGE2-mediated podosome loss in dendritic cells is dependent on actomyosin contraction downstream of the RhoA-Rho-kinase axis**. *J Cell Sci* 121:1096-106.

Vega, F.M., and A.J. Ridley. 2008. **Rho GTPases in cancer cell biology**. *FEBS Lett* 582:2093-101.

Villablanca, E.J., and J.R. Mora. 2008. **A two-step model for Langerhans cell migration to skin-draining LN**. *Eur J Immunol* 38:2975-80.

Villadangos, J.A., and P. Schnorrer. 2007. **Intrinsic and cooperative antigen-presenting functions of dendritic-cell subsets in vivo**. *Nat Rev Immunol* 7:543-55.

Vishwanath, M., A. Nishibu, S. Saeland, B.R. Ward, N. Mizumoto, H.L. Ploegh, M. Boes, and A. Takashima. 2006. **Development of intravital intermittent confocal imaging system for studying Langerhans cell turnover**. *J Invest Dermatol* 126:2452-7.

Wang, B., P. Amerio, and D.N. Sauder. 1999. **Role of cytokines in epidermal Langerhans cell migration**. *J Leukoc Biol* 66:33-9.

Wang, Y., K.J. Szretter, W. Vermi, S. Gilfillan, C. Rossini, M. Cella, A.D. Barrow, M.S. Diamond, and M. Colonna. 2012. **IL-34 is a tissue-restricted ligand of CSF1R required for the development of Langerhans cells and microglia**. *Nat Immunol* 13:753-60.

Weiss, J.M., J. Sleeman, A.C. Renkl, H. Dittmar, C.C. Termeer, S. Taxis, N. Howells, M. Hofmann, G. Kohler, E. Schopf, H. Ponta, P. Herrlich, and J.C. Simon. 1997. **An essential role for CD44 variant isoforms in epidermal Langerhans cell and blood dendritic cell function**. *J Cell Biol* 137:1137-47.

Welch, H.C., W.J. Coadwell, C.D. Ellson, G.J. Ferguson, S.R. Andrews, H. Erdjument-Bromage, P. Tempst, P.T. Hawkins, and L.R. Stephens. 2002. **P-Rex1, a PtdIns(3,4,5)P3- and Gbetagamma-regulated guanine-nucleotide exchange factor for Rac**. *Cell* 108:809-21.

West, M.A., A.R. Prescott, E.L. Eskelinen, A.J. Ridley, and C. Watts. 2000. **Rac is required for constitutive macropinocytosis by dendritic cells but does not control its downregulation**. *Curr Biol* 10:839-48.

Williams, M.A., and M.J. Bevan. 2007. **Effector and memory CTL differentiation**. *Annu Rev Immunol* 25:171-92.

Wu, W., Y.M. Hsu, L. Bi, Z. Songyang, and X. Lin. 2009. **CARD9 facilitates microbe-elicited production of reactive oxygen species by regulating the LyGDI-Rac1 complex**. *Nat Immunol* 10:1208-14.

Wu, X., F. Quondamatteo, T. Lefever, A. Czuchra, H. Meyer, A. Chrostek, R. Paus, L. Langbein, and C. Brakebusch. 2006. **Cdc42 controls progenitor cell differentiation and beta-catenin turnover in skin**. *Genes Dev* 20:571-85.

Yaku, H., T. Sasaki, and Y. Takai. 1994. **The Dbl oncogene product as a GDP/GTP exchange protein for the Rho family: its properties in comparison with those of Smg GDS**. *Biochem Biophys Res Commun* 198:811-7.

Yen, J.H., T. Khayrullina, and D. Ganea. 2008. **PGE2-induced metalloproteinase-9 is essential for dendritic cell migration**. *Blood* 111:260-70.

Zahner, S.P., J.M. Kel, C.A. Martina, I. Brouwers-Haspels, M.A. van Roon, and B.E. Clausen. 2011. **Conditional deletion of TGF-betaR1 using Langerin-Cre mice results in Langerhans cell deficiency and reduced contact hypersensitivity**. *J Immunol* 187:5069-76.

Zhang, S., H. Zhang, and J. Zhao. 2009. **The role of CD4 T cell help for CD8 CTL activation**. *Biochem Biophys Res Commun* 384:405-8.

Zheng, Y. 2001. **Dbl family guanine nucleotide exchange factors**. *Trends Biochem Sci* 26:724-32.

Zheng, Y., D.J. Fischer, M.F. Santos, G. Tigyi, N.G. Pasteris, J.L. Gorski, and Y. Xu. 1996. **The faciogenital dysplasia gene product FGD1 functions as a Cdc42Hs-specific guanine-nucleotide exchange factor**. *J Biol Chem* 271:33169-72.

Zoughlami, Y., C. Voermans, K. Brussen, K.A. van Dort, N.A. Kootstra, D. Maussang, M.J. Smit, P.L. Hordijk, and P.B. van Hennik. 2012. **Regulation of CXCR4 conformation by the small GTPase Rac1: implications for HIV infection**. *Blood* 119:2024-32.

IX CURRICULUM VITAE

Personal data

Name	Céline Leroy
Date of birth	9 April 1983
Place of birth	Lannion, France
Nationality	French
E-mail	leroy.celine2@yahoo.fr

Education

Since 09/2008	**PhD in Immonology** Prof. Dr. Thomas Brocker, Institut for Immunology, LMU, Munich, Germany Thesis title: "The role of Rho-GTPases in dendritic cell functions"
09/2006 - 07/2007	Post-graduate degree following the **Master in Infectious Diseases and Immunology** Dr. Silvie Guerder, Inserm U1043 / CNRS UMR 5282, Toulouse, France Thesis title: "Study of the anti-tumoral immune response of CD4 and CD8 T cells according to the tumor degree with a mouse model"
09/2003 - 09/2006	**Engineer in Biotechnology** Ecole Supérieure de Biotechnologie de Strasbourg, France Dr. Stefan Stevanovic, Institut for cell biology, Tübingen, Germany Thesis title: "Stimulation of CTL with Adipophiline peptide, in order to see the ability of this peptide to induce an immune response"

09/2001 - 06/2003	Two-years of competitive exam preparation to allow the entry to engineer school Prépa TB, Lycée Ozenne, Toulouse, France
07/2001	**High School Diploma in STL-BGB** (Baccalauréat "Lab Techniques and Sciences, speciality Biochemistry-Biological Engineering") Lycée Chaptal, Quimper, France

Conferences and awards

02/2012	SFB914 retreat, *St Johann, Austria*
11/2011	12th International Workshop on Langerhans Cells, *Innsbruck, Austria*
11/2011	Travel grant from the 12th International Workshop on Langerhans Cells
09/2010	SFB571 international symposium, *Munich, Germany*
10/2009	SFB571 retreat, *Venicia, Italy*
09/2006	1st European Congress of Immunology (ECI 2006), *Paris, France*
03/2001	Prize for feminine technical and scientific vocation

Self-development courses

01-02/2013	"Good Scientific Practice", soft skill course from SFB914
01/2013	"Presentation Skills", LMU Graduate Center
11/2012	"Communication and Teams", soft skill course from SFB914
04-02/2012	Summer and winter semesters 2012 of the SFB914 courses
06/2012	"Job application in English", LMU Graduate Center
06/2012	"Work-life Balance", LMU Center of Leadership and People Management
01/2012	"Leading with Excellence", LMU Center of Leadership and People Management
05/2011	6th ENII Spring/Summer School / 2011 Event in Advanced Immunology
03/2010	FlowJo application seminar, Max-Planck-Gesellschaft